Characterization of *Arabidopsis thaliana* CPR5 via the Elucidation of Interacting Protein Partners

A thesis presented in partial fulfilment of the requirements for the degree of

Masters of Science in Biochemistry

At Massey University, Palmerston North, New Zealand

Fiona (Shane) Chiem 2015

Abstract

The *Arabidopsis thaliana* Constitutive expresser of pathogenesis related genes5 (*CPR5*) has previously been suggested to play a role in the regulation of disease resistance, plant and cell proliferation, development and death. Analysis of *cpr5* mutant alterations to hormone and hormone-like signalling mechanisms have provided evidence that abolishment of *CPR5* involvement within these hormone signalling pathways, results in many of the stunted growth, early senescence and constitutive expression of pathogen defense phenotypes observed. Despite the pleiotropic effect that *cpr5* mutants have on the plant system, it is unclear whether *CPR5*-dependent pathways are due to a direct interaction with *CPR5* or due to a more indirect association. *CPR5* has been proposed to be a regulator of a multitude of different pathways, including reactive oxygen species (ROS), cell wall biosynthesis, and transcription but evidence of these proposals are limited to the effects that *cpr5* mutants have on downstream targets.

In an attempt to address the involvement of CPR5 in *Arabidopsis* plant processes, a series of studies were conducted to determine the protein interacting partners of CPR5. Proteins were identified via 2 independent yeast 2 hybrid (Y2H) screening of an *Arabidopsis* transcriptome library. Ten proteins of interest were identified via two independent screenings using two truncated forms of CPR5. Functional involvement of CPR5 with the identified proteins was further explored using the Y2H pairwise interaction system. CPR5 was found to interact with 3 full length proteins identified.

To explore the possibility that CPR5 interacts with multiple protein partners in different locations within the cell, Bifluorescence molecular complementation assays were performed to determine the localization and interaction of CPR5 with the ten identified genes as well as 3 previously identified genes. Several novel interactions were identified that occur within the nucleus and outside of the nucleus. Not only was CPR5 confirmed to have an interaction with KRP2 within the nucleus, CPR5 exhibited interaction with FSD1, CRK4, PATL3, PATL5, and PATL6, outside of the nucleus.

In the final set of experiments, several double mutant lines were produced that did not yield any observable phenotypes that differ from *cpr5-2* single mutant plants. In order to determine the effects these double mutants have on various plant processes affected by *cpr5-2* single mutant; qRT-PCR was performed to determine the expression pattern of pathogen related genes (*PR1* and *PDF1.2*) known to be significantly upregulated in *cpr5-2* plants. qRT-PCR analysis revealed that *cpr5-2 fsd1* exhibits a down-regulation of *PDF1.2*.

PR1 regulation was found to be down-regulation in *cpr5-2 bzip61* and up-regulated in *cpr5-2 patl3* compared to *cpr5-2.*

Sugar and dark treatment of the *cpr5-2* double mutant lines yielded several alterations to hypocotyl length, root length, and apical hook curvature by several of the double mutant lines, indicating a connection between CPR5 and the knocked out gene of interest. None of the double mutants were able to completely rescue the sugar-induced morphological phenotypes exhibited by *cpr5-2*, and some double mutant lines exhibited more pronounced effects indicating an additive effect by sugar treatment.

Together this data suggests that CPR5 interacts with various proteins involved in different plant processes in various locations throughout the cell. Further research of these proteins and a more direct analysis of the interaction that may occur between CPR5 and these proteins will be required to provide a foundation for more direct characterization the *CPR5* molecular function; and ultimately to determine the role that CPR5 plays within the hormone and hormone like signalling pathway and their effects on major plant processes.

Acknowledgements

I would like to thank my supervisor Dr. Paul Dijkwel for giving me this opportunity and for helping me complete my Masters degree. Paul has been an exemplary supervisor providing me with the guidance I required when help was asked and for challenging me. I thank you for the patience you have shown me and for providing me with the independence I required to succeed. Thank you especially for your confidence in my abilities to successfully accomplish the goals we set forth and for allowing me to carry out these goals in my own unorthodox fashion.

I would like to thank Elizabeth Jennens for always believing in me and for giving me the love, space, and time to complete my degree. Without you I would not have started my Masters and I would not be where I am in my life without you.

I would like to thank Prof. Michael McManus and all of my C5.19 lab mates for their critiques and insights and for listening when I needed help with my research. In particular, I would like to thank my family away from home, Jay Jayaraman and Srishti Joshi, for their continual help academically and personally. I cannot imagine my time at Massey without your unwavering friendships, and willingness and dedication to helping me in all aspects of my life.

To my parents, family, and friends, I am forever grateful for your unending encouragement as I continued my studies around the world, and for your understanding as I concentrated on finishing my thesis. Knowing that you are all waiting for me to come home gave me the motivation I needed to return to you having successfully completed another chapter of my life.

I would most especially like to thank my mother, Sandy Chiem, for allowing me to be my independent self despite how much it hurt to let me travel in distance and on my own path of life. You have shown me such unrelenting selfless love and support regardless the decisions I make, and it is for you and because of you that I am inspired to be the best version of myself.

Abbreviations

‘	minutes
"	seconds
Ade	Adenine
aa	amino acids
amp	Ampicillin
BiFC	BiFluorescence Molecular Complementation
BLAST	Basic logical alignment search tool
bp	Base-pair
cDNA	DNA synthesized from an mRNA template
C-terminus (terminal)	(at the) carboxy-terminal end of a polypeptide chain
CPR5	*CPR5* wild-type gene
CPR5	CPR5 wild-type protein
cpr5	CPR5 mutant gene
cpr5	CPR5 mutant protein
cpr5-2	*cpr5* mutant line with mutation at aa420 (W->stop)
DAPI	A DNA binding fluorescent stain ((4',6-diamidino-2-phenylindole)
DNA	Deoxyribonucleic acid
DNase	Deoxyribonuclease
dNTP	2´-deoxynucleotide 5´ triphosphate
dH2O	distilled water
ddH2O	double distilled water
E. coli	*Escherichia coli*
EDTA	Ethylenediaminetetraacetic acid
FW	Fresh weight
g	Gram
gDNA	Genomic DNA
Gen	Gentamycin
h	Hour
His	Histidine
IPTG	Isopropyl-β-D-thiogalactopyranoside
kan	kanamycin
kb	Kilo base-pair
kD(a)	Kilo daltons
L	Litre
LB	Luria-Bertani (media or broth)
Leu	Leucine
M	Molarity (moles per litre)
MCS	Multiple cloning site
mg	Miligram
Milli-Q-water	Water purified by Milli-Q-ion exchange chromatography

ml	Milliters
mol	Mole (Avagadro's number)
mRNA	Messenger RNA
MS	Murashige & Skoog Media
NCBI	National Centre for Biotechnology Information
ng	Nanogram
OD600	optical density at 600nm (measured in a spectrophotometer)
°C	Degree celsius
PAGE	Polyacrylamide gel electrophoresis
PBS	Phosphate buffer saline
PCR	Polymerase chain reaction
pH	-Log (H+)
psi	a unit of pressure (pounds per square inch)
qRT-PCR	Reverse transcriptase-polymerase chain reaction
RE	Restriction Enzyme
Rnase	Riboxynuclease
RO	Reverse osmosis
rpm	revolutions per minute
SALK	Arabidopsis T-DNA insertion lines from the SALK Institute, a non-profit research organization
SD	Synthetic Defined (media)
SDS	Sodium Dodecyl Sulfate
SEM	Standard error mean
TAE	Tris base, acetic acid, and EDTA buffer
TAIR	The Arabidopsis Information Resource
TE	Tris base, EDTA buffer
Tet	Tetracycline
Tm	Melting temperature at which DNA strands separate prior to annealing
Tris	Tris (hydroxymethyl) aminomethane
Trp	Trpytophan
Tween-20	Polyoxyethylenesorbitan monolaurate
U	Unit (based on enzyme activity)
µg	Microgram
µl	Microlitre
µM	Micromolar
V	Volt
v/v	Volume per volume
w/v	Weight per volume
w/w	Weight per weight
X-α-Gal	X-α-Gal is a chromogenic substrate used to detect α-galactosidase activity
Y2H	Yeast-2-hybrid
YFP	Yellow fluorescent protein
YPDA	yeast peptone dextrose adenine (media/agar)

List of Figures

List of Tables

Table of Contents

Chapter 1: Introduction

1.1 General Introduction to CPR5

Plants have numerous enemies including animals, insects, and pathogens such as viruses and bacteria. Many of these pathogens can have devastating long-term effects on plants that are unable to defend themselves. Plants respond to the presence of pathogens through a series of defense and resistance mechanisms (Boch, Verbsky, Robertson, Larkin, & Kunkel, 1998). These pathogen resistance pathways are triggered by pathogen attacks, and often result in sacrificing cells in order to limit the spread of infection (Fesik, 2000; Gilchrist, 1998). Pathogen related 1 (*PR1*) gene from *Arabidopsis thaliana* is required for the induced defense response against various pathogens. Expression of *PR1* is a marker of an activated defense mechanism (Bowling, Clarke, Liu, Klessig, & Dong, 1997; Penninckx et al., 1996). Identification of mutants displaying constitutive expression of pathogen defense response and resistance, yielded several mutants that exhibited a constitutive expression of *PR1* gene (*cpr)* (Bowling, et al., 1997). One mutant in particular revealed a gene, *CPR5* (Bowling, et al., 1997) with unexpected links to growth regulation, development and senescence in addition to pathogen resistance in *Arabidopsis thaliana* (Boch, et al., 1998; Kirik et al., 2001).

CPR5 gene involvement within these crucial plant processes is highlighted by the pleiotropic phenotypes that *cpr5* mutant plants possess. *cpr5* mutant lines were first identified by their altered resistance phenotype and abnormal formation of necrotic lesions that mimic the programmed cell death of pathogen response despite the lack of a pathogen attack (Bowling, et al., 1997). *cpr5* mutant plants are much smaller than wild-type plants with thinner cell walls, smaller cells and premature growth arrest at an early age (Kirik, et al., 2001). Trichome development is significantly altered with *cpr5* plants producing smaller trichomes with reduced branching, cell size, nuclear DNA content and cell wall cellulose content(Brininstool et al., 2008). *cpr5* mutant plants also display an early senescence phenotype characterized by early yellowing in leaves, as well as decreased soluble protein content, chlorophyll content, and Photosystem II efficiency associated with senescence (H.-C. Jing, Anderson, Sturre, Hille, & Dijkwel, 2007; Yoshida, Ito, Nishida, & Watanabe, 2002).

More specifically, *cpr5* mutants exhibit constitutive expression of resistance related PR genes, elevated levels of salicylic acid (SA) (Kirik, et al., 2001) and jasmonic acid (JA)

(Clarke, Volko, Ledford, Ausubel, & Dong, 2000) hormones, and hypersensitivity phenotypes related to sugar, and stress related hormones abscisic acid (ABA)(Gao et al., 2011; Zhao et al., 2010), ethylene (ET)(H.-C. Jing, et al., 2007; H. C. Jing, Sturre, Hille, & Dijkwel, 2002), and JA(Clarke, et al., 2000). In fact, hormone and sugar signalling pathways are involved in all the seemingly independent processes altered in *cpr5* mutants, including plant growth, development, senescence, and pathogen resistance.

In *cpr5* mutants, the alterations to the major phenotypes exhibited are due to misregulation of *CPR5*-dependent pathways. The molecular mechanism by which *CPR5* is involved and controls these pathways is yet to be determined. There have been many suggestions on the mechanism by which *CPR5* is involved in various pathways throughout the plant systems. What is currently known from the data is that *CPR5* is somehow involved upstream of multiple pathways and that abolishing *CPR5* function effectively alters crucial processes required for normal plant function. It is unknown from the current research whether *CPR5* gene involvement within its associated pathways is due to direct or indirect interactions with one pathway or several. Due to the pleiotropic nature of *cpr5* mutant alterations, there are several possible molecular mechanisms to explain *CPR5* gene function. *CPR5* has been suggested as a master regulatory protein of a general signal transduction pathway supported by the multitude of alterations caused by mutations in the *CPR5* gene(Kirik, et al., 2001). Work has been done involving cell development that suggests the effects exhibited by *cpr5* mutants on multiple pathways may be due to a molecular function directly involved with cell wall interaction. In support of this are genes involved in cell expansion that have been identified to affect multiple hormone signalling pathways and cell morphology when mutated (Brininstool, et al., 2008). Study of pre-symptomatic *cpr5* mutant plants have revealed that many reactive oxygen species (ROS) related gene expression profiles are affected in early plant development (H. C. Jing et al., 2008). The misregulation of ROS-related pathways suggest that *CPR5* acts as a master regulator of ROS cellular status and signalling that subsequently interacts with the predicted *CPR5* associated signalling pathways (H.-C. Jing & Dijkwel, 2008; H. C. Jing, et al., 2008). A recent study identifying a set of transcription factors that independently regulate a subset of *CPR5*-dependent gene targets suggests *CPR5* may function in the regulation of transcriptional activity (Daniel Perazza et al., 2011).

As shown in figure 1.1, all previously proposed *CPR5* molecular mechanisms are unified in *CPR5* action upstream of all associated signalling pathways, but the direct interactions involving *CPR5* are unclear. Without this more direct characterization, we can only speculate on the specific molecular function of *CPR5*.

1.2 Phytohormones Signalling

The plant system is controlled by various molecules that are able to relay and receive signals in response to external stimuli, and are required for normal plant growth and development. One such class of molecules, called phytohormones, is involved in and affects all major regulatory plant processes from growth and development to age-related senescence and pathogen resistance. (Larrieu & Vernoux, 2015; McSteen & Zhao, 2008; Robert-Seilaniantz, Grant, & Jones, 2011). The hormone signalling mechanism consists of two steps involving recognizing the target and transmitting the signal towards its final target to affect the necessary changes to properly regulate the plant (Larrieu & Vernoux, 2015; McSteen & Zhao, 2008). These hormones play various roles in germination, growth, development, senescence, resistance, stress and metabolism (De Vleesschauwer, Xu, & Höfte, 2014; Gururani, Mohanta, & Bae, 2015; Iqbal, Trivellini, Masood, Ferrante, & Khan, 2013; Kim, Chang, & Tucker, 2015; Larrieu & Vernoux, 2015; McSteen & Zhao, 2008; Robert-Seilaniantz, et al., 2011; Swamy & Smith, 1999). There are 9 families of phytohormones, many of which CPR5 has been associated with (McSteen & Zhao, 2008) and knockout of the *CPR5* gene results in hypersensitivity to the phytohormones ABA, JA, SA, and ET (Aki et al., 2007; Boch, et al., 1998; Bowling, et al., 1997; Gao, et al., 2011; H.-C. Jing, et al., 2007; H. C. Jing, et al., 2008; Kirik, et al., 2001; Yoshida, et al., 2002).

The hormone signalling pathways are involved in all major plant processes and are crucial for the proper regulation and maintenance of all plant systems. As *cpr5* mutants display hypersensitivity to numerous phytohormones, it appears that *CPR5* controls normal seedling growth and development through the mediation of signals from multiple hormone response pathways. These hormone pathways do not work exclusively, but as an overlapping network to help regulate plant processes, and CPR5 involvement in these processes is further discussed below. (Figure 1.1)

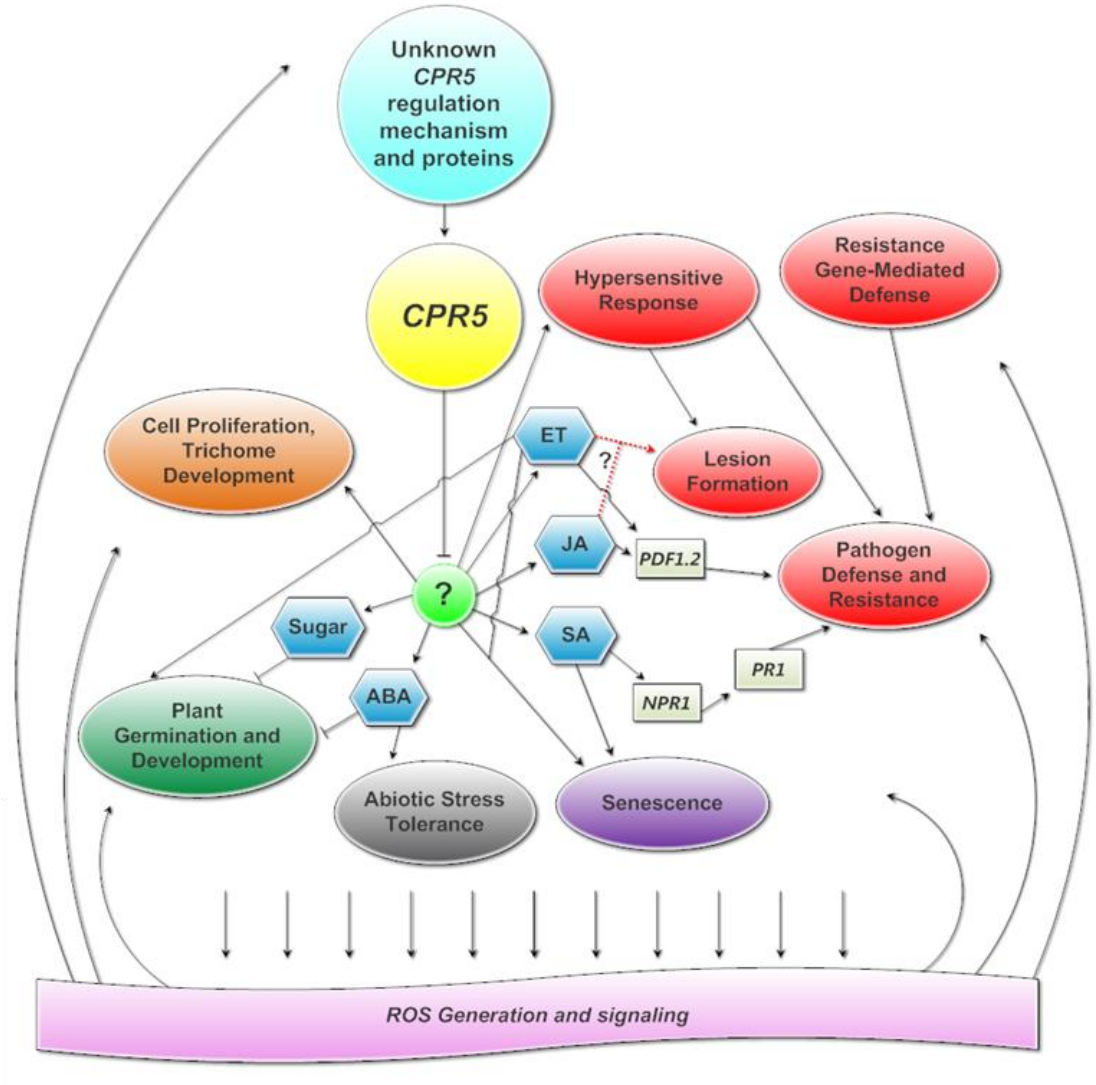

Figure 1.1: Predicted CPR5 Involvement in Plant Processes.
Outlining CPR5 dependent hormone signalling induced plant processes via an unknown molecular mechanism. CPR5 is placed downstream of unknown regulators of CPR5 (LIGHT BLUE) and upstream of an unknown CPR5 dependent molecular mechanism (NEON GREEN) that regulates the hormones and sugar (DARK BLUE) induced plant processes related to Pathogen defense (RED), Senescence (PURPLE), Abiotic Stresses (GREY), Plant Development (GREEN), and Cell Proliferation and trichome development (ORANGE). Genes known to be involved in particular mechanisms are mentioned to provide specific characterization pertaining to that pathway (RECTANGLES). ROS generation and signalling (PINK RIBBON) is shown as a general signalling and response mechanism involved in all major plant processes. Indicated also are known CPR5-independent pathways and putative CPR5-dependent pathway interactions

1.3 Plant Germination and Development

Plant germination and development are complex processes that have been suggested to involve the interaction of several hormones including ABA, gibberellic acid (GA), and ET (Dekkers & Bentsink, 2015; Kepczynski & Kepczynska, 1997; Kucera, Cohn, & Leubner-Metzger, 2005; McSteen & Zhao, 2008; Rodriguez-Gacio, Matilla-Vazquez, & Matilla, 2009). In wild-type plants, seed dormancy as well as the transition from embryonic to germination growth is maintained by ABA (Finkelstein & Gibson, 2001; Kucera, et al., 2005). ABA also elicits numerous physiological responses, from the inhibition of seedling growth, to the closing of stomatal openings to restrict water loss and to regulate responses to changes in temperature (Dekkers & Bentsink, 2015; Kucera, et al., 2005; Swamy & Smith, 1999). Antagonistic to ABA is GA, which is a positive regulator of embryo to germination growth (Rodriguez-Gacio, et al., 2009). Ethylene has also been shown to promote seed germination and to counter ABA effects on seed germination (Figure 1.1).

Exogenous application of ABA inhibits seedling germination in both *cpr5* and Col-0 wild-type plants. However, *cpr5* mutants exhibited lower germination rate, less greening of the cotyledons and shorter root lengths at lower concentrations of applied ABA as compared to wild-type plants (Gao, et al., 2011). In contrast, *CPR5* overexpression plants were insensitive to ABA treatment (Gao, et al., 2011) suggesting that *CPR5* may act as a repressor of ABA signalling. Exogenous addition of NDGA, an ABA biosynthesis inhibitor (Gao, et al., 2011), resulted in inhibited germination and seedling development in cpr5 mutants. This observation indicates that *CPR5* is involved in ABA signalling rather than ABA biosynthesis.

These observations suggest that the morphological phenotype of *cpr5* mutants is due to hypersensitivities to ABA signalling (Aki, et al., 2007; Gao, et al., 2011; Yoshida, et al., 2002) which is a known regulator of plant proliferation and development. Thus, *CPR5* appears to coordinate plant proliferation and development through the regulation of the ABA signalling pathway. *Arabidopsis thaliana* plant proliferation and development appears to be dependent on the proper regulation of these pathways by *CPR5*. However, the exact mechanism of this regulation remains to be elucidated.

In addition, sugar signalling pathways have been associated with ABA-regulated plant germination and dormancy as well (Finkelstein & Gibson, 2001). Physiological studies have shown that high concentrations of exogenously added sugar resulted in an inhibition of seed germination and overall seedling development (Dekkers, Schuurmans, & Smeekens, 2008). Studies have shown that there is cross-talk between ABA and sugar

signalling pathways and that these two molecules can act antagonistically, or additively depending on the affected processes (Dekkers, et al., 2008).

Abolishing glucose-HXK dependent signalling in a *cpr5 hxk5* double mutant rescued the *cpr5* mutant hypersensitivity to sugar but not to ABA, JA, ET, or SA (Aki, et al., 2007; Yoshida, et al., 2002). This observation indicates that the hypersensitivity of *cpr5* plants to sugar is not due to increased sugar levels but rather due to deregulation of sugar sensing and signalling (Aki, et al., 2007; Yoshida, et al., 2002). These results suggest that *CPR5* is involved in the regulation of sugar signalling response and acts as a negative regulator of sugar-induced inhibition of plant development by suppressing, at least in part, the glucose dependent HXK signalling pathway. Hypersensitivity to sugar is due to misregulation of HXK-mediated sugar response but the altered plant growth and development phenotypes displayed in *cpr5* plants are not only due to a hypersensitivy to sugar. The inability of an insensitive HXK pathway within a *cpr5* mutant background to rescue the *cpr5* inhibited plant growth phenotype, suggests the involvement of *CPR5*-dependent ABA pathways in the regulation plant growth, as illustrated in figure 1.1.

Taken together, the hypersensitivities exhibited by *cpr5* mutants can be uncoupled through the knockout of components specific to each hormone's regulatory pathway. This uncoupling however does not provide the direct interaction that causes the altered regulation of all the hormone regulatory pathways affected in *cpr5*.

Several hormone response mutants, such as mutation of *Arabidopsis AXR2* gene, have been shown to have altered sensitivities to more than one hormone. Mutation of *AXR2* was able to confer resistance to ABA, ethylene, and auxin in roots (Wilson, Pickett, Turner, & Estelle, 1990). CPR5 hypersensitivity to ABA, sugar and other hormones could be due to the cross interaction and regulation between hormone pathways and could potentially be caused by the misregulation of just one pathway. More recently, the ethylene-insensitive2 (*EIN2*) gene has been shown to be involved in multiple hormone responses including ABA. More specifically however, *EIN2* loss of function mutant was able to separate *EIN2* ethylene-related responses and JA-regulated responses showing that JA and ET as well as ABA are likely regulated by the ethylene related *EIN2* regulatory pathway (Alonso, Hirayama, Roman, Nourizadeh, & Ecker, 1999). More precisely, ET, has been shown to negatively regulate ABA signalling during germination but positively regulate ABA action during root growth (Ghassemian et al., 2000).

1.4 Plant Senescence

Plant senescence is a genetically programmed final stage of development in plant leaves regulated by age-related signals (BuchananWollaston, 1997). ET is a hormone involved in numerous regulatory pathways that are involved in different stages of plant development including germination and age-induced senescence. Although ET is not necessary for inducing senescence, it provides a signalling mechanism by which senescence can be induced within a specific age range (H. C. Jing, Schippers, Hille, & Dijkwei, 2005; H. C. Jing, et al., 2002). During senescence, nutrient and molecules are processed and transported from dying parts of the plant to growing parts, including newly emerging leaves and flowers (BuchananWollaston, 1997). This program is necessary to ensure the fitness of the overall plant by ensuring that optimal growth and reproduction occurs. When senescence occurs in plants growing under normal growth conditions, it is considered age-induced senescence and is regulated by the interaction of various hormonal and environmental influences (Kim, et al., 2015). The hormone ethylene has been implicated to play a key role in age-related senescence, which is also influenced by light/dark conditions (Figure 1.1) (H. C. Jing, et al., 2005; Kim, et al., 2015).

Plants with mutations in the *CPR5* gene were identified to have an early senescence phenotype that exhibited a hypersensitivy to ET (H. C. Jing, et al., 2005; H. C. Jing, et al., 2002). Upon exogenous application of ET, *cpr5* mutants displayed an accelerated and enhanced early senescence phenotype (Fujiki et al., 2005; H. C. Jing, et al., 2002). ET is known to promote senescence, but only within a specific age range and the exacerbated senescence phenotype implicates a disruption in the age-dependent mediation of ET signal-induced senescence. The inability of *cpr5* plants to suppress ET-induced senescence implicates a misregulation of the interaction between ET and age-related factors that are likely facilitated by *CPR5*.

Evidence of this conclusion is provided by Jing et al. (2007), showing that overexpression of *CPR5* accelerated senescence during later development but had no effect on early plant development. *cpr5* plants exhibited early senescence before reproduction whereas *CPR5* overexpression mutants only senesced after reproduction similar to wild type plants(H.-C. Jing, et al., 2007). The unaffected development of *CPR5* overexpression plants and the enhanced late senescence phenotype exhibited, support that *CPR5* negatively regulates responses that induce senescence in young plants in order to provide normal early growth development but may conversely also play a role in promoting senescence in later stages of development (H.-C. Jing, et al., 2007). The mechanism by which *CPR5* promotes late-life

senescence has not yet been studied, but it is clear that *CPR5* involvement in senescence is age-dependent and that the late-life senescence may be due to a relief of repression of ET and other senescence triggering signals.

Furthermore, the early senescence phenotype in *cpr5* plants can be enhanced by ET but ET is not responsible for the early senescence in untreated plants. Interestingly, the same study by Jing et al. (2002) reported that *cpr5* mutants with abolished ET, JA, SA, ABA, or sugar signalling did not alter the *cpr5* early senescence phenotype, characterized by premature leaf senescence and cell death (H.-C. Jing, et al., 2007).

Plant senescence involves the interaction of many complex mechanisms, a large number of which have yet to be characterized. Although only ET involvement in *cpr5* early senescence has been analyzed, normal plant senescence has also been observed to be accelerated by JA, ABA, and SA, but delayed by auxin (Buchanan-Wollaston, 1997; Buchanan-Wollaston et al., 2005; Khan, Rozhon, & Poppenberger, 2014; Kim, et al., 2015). Although CPR5 involvement in age-induced senescence has generally been associated with ET regulation, it is also possible that CPR5 regulation of other hormone regulatory pathways is involved in the early senescence phenotype exhibited by *cpr5* mutants. Alternatively, CPR5 involvement in germination could be due to ET regulation of ABA and sugar rather than direct regulation of ABA and sugar regulatory pathways (Figure 1.1). *CPR5* involvement in the hormone and sugar signalling pathways does not necessarily explain *CPR5* involvement in the regulation of senescence. Abolishment of one type of hormone signalling pathway in a *cpr5-2* background did not result in any observable alterations to the early senescence phenotype or in the hypersensitive responses to other hormones independent of the abolished pathway. Analysis of transcriptome data for *cpr5* plants has shown early increases in senescence associated genes, some of which are associated with resistance and stress response, thus providing a putative link to *CPR5* involvement in stress-related senescence (Brininstool, et al., 2008; H.-C. Jing, et al., 2007; H. C. Jing, et al., 2008; H. C. Jing, et al., 2005; Yoshida, et al., 2002).

1.5 Resistance and Hypersensitive Response-Mediated PCD

Programmed cell death (PCD) in plants is a genetically directed process that is involved in maintaining healthy cell states (Collazo, Chacón, & Borrás, 2006; Gilchrist, 1998). PCD is a process that involves the action of both senescence and stress regulatory pathways. Plant PCD

has similarities in mechanism and chemical components to the mammalian PCD mechanism (Ausubel, 2005; Collazo, et al., 2006). PCD is triggered by various internal and external cues and is a natural process that occurs in plant development and ageing (Fesik, 2000; Gilchrist, 1998; Khurana, Pandey, Sarkar, & Chanemougasoundharam, 2005). In the case of biotic stresses, PCD is often triggered by the presence or effect of a pathogen-produced 'effector protein' and the plant exhibits an effector triggered immunity (ETI) with an accompanying hypersensitive response (HR) phenotype yielding necrotic lesions (J. D. G. Jones & Dangl, 2006). Within the plant genome, there are potentially hundreds of *R*-genes that recognize pathogen effectors and trigger ETI (Ausubel, 2005). Many of these *R*-genes encode nucleotide-binding leucine-rich repeat (NB-LRR) proteins which are very similar to components in mammals that can be activated and trigger apoptosis, a form of PCD (Ausubel, 2005).

The *CPR5* gene has been of interest in the study of plant pathogen resistance and senescence since its discovery in 1997; and the *cpr5* mutant exhibits increased resistance to biotrophic pathogens as well as a spontaneous lesion phenotype that mimics the HR lesion phenotype (Boch, et al., 1998; Bowling, et al., 1997). In addition, *cpr5* mutants exhibit constitutive expression of resistance-related PR genes, elevated levels of the resistance hormones SA (Kirik, et al., 2001) and JA (Clarke, et al., 2000). Pathogen resistance is a complex process that involves several different regulatory pathways, including a SA-dependent resistance pathway and a JA-dependent pathway (Figure 1.1). These pathways however are not completely independent and can act antagonistically.

In order to assess *CPR5* involvement in the plant pathogen defense pathways, *cpr5* mutants were used to determine which pathways were being constitutively expressed. *cpr5* plants have known induced resistance to *Pseudomona syringae* pv maculicola and *Peronospora parasitica*. Abolishing the Salicylic acid-dependent resistance pathway, effectively suppressed induced resistance to *P.s.* maculicola but not *P. parasitica,* indicating that the constitutive expression of pathogen resistance in *cpr5* plants is only in part due to the constitutive expression of the SA-dependent resistance pathway (Boch, et al., 1998; Bowling, et al., 1997) and suggests that *CPR5* acts upstream of SA-mediated resistance (Figure 1.1). The inability to completely suppress *cpr5*-induced resistance through the abolishment of the SA-dependent resistance pathway, suggests that this continuous expression of resistance is also dependent on a SA-independent resistance pathway. Evidence of this is the constitutive expression of defensin *PDF1.2*, a component of a resistance pathway dependent on JA/ET hormone signalling (Figure 1.1) (Boch, et al., 1998; Bowling, et al., 1997; Clarke, et al., 2000). Furthermore, this constitutive expression

of resistance is independent of resistance gene-mediated pathways and appears to induce the constant activity of more general resistance pathways (Boch, et al., 1998; Chen, Kloek, Boch, Katagiri, & Kunkel, 2000).

Lesion formation is a known attribute of an early hypersensitive response (HR) pathogen defense mechanism that sacrifices infected cells and surrounding tissue in order to limit the spread of infection(Gilchrist, 1998; Heath, 2000). A positive correlation between the size and number of lesions and *PR-1* gene expression is observed in *cpr5* plants (Boch, et al., 1998). The formations of these random necrotic lesions are identified to be independent of humidity, day length, and nutrient conditions (Bowling, et al., 1997; Heidel, Clarke, Antonovics, & Dong, 2004). Lesion formation occurs first on cotyledons only after true leaves have emerged, and only on true leaves in an age-dependent manner (Boch, et al., 1998; Bowling, et al., 1997). High levels of SA and *PR-1* have been observed around lesions independent of pathogen attacks suggesting that these lesions are phenocopies of HR-induced lesions (Boch, et al., 1998; Bowling, et al., 1997; H. C. Jing, et al., 2005). Contrary to this evidence, the cause of the observed lesion formation in *cpr5* mutants may be the result of the JA/ET-dependent 'systemic resistance response' (SAR) that is independent of SA-dependent resistance response, as shown in figure 1.1. Inhibition of JA or ET signalling pathways was found to reduce the lesion forming phenotype of *cpr5* mutants which suggests that random lesion formation may be dependent on several resistance pathways (Clarke, et al., 2000).

The formation of random necrotic lesions by *cpr5* mutants indicates that *CPR5* is involved in plant resistance and is not only specific to the SA-defense pathway but may include HR, JA/ET and perhaps other resistance pathways(Boch, et al., 1998; Bowling, et al., 1997; H. C. Jing, et al., 2008; Kirik, et al., 2001). From current findings, it can be seen that *CPR5* involvement in the plant pathogen response is not localized to a single pathway, but rather involves the negative regulation of multiple hormone signalling pathways that are responsible for various plant resistance responses.

Examination of constitutive expression of plant resistance pathways in *cpr5* mutants suggests a link between *CPR5* and these pathways, but studies do not characterize the role of *CPR5* within these pathways. The research indicates that *CPR5* plays a repressive role upstream of such defense and resistance pathways (Figure 1.1). Whole genome microarray data analysis indicate that CPR5 may act as negative and positive regulators of effector triggered immunity. More specifically, SA-induced genes were identified to be upregulated in the *cpr5* mutant but expression levels of SA and SA induced genes were found to be at WT levels in the *cpr5 sim smr1* triple mutant (S. Wang et al., 2014). These

findings however do not provide a direct physical interaction between CPR5 and SIM/SMR1. CPR5 appears to play a direct role in effector triggered immunity and is hypothesized to play a role as a nuclear envelope protein that binds directly to SIM/SMR1 complex; and under normal conditions would inhibit SIM/SMR1 activation of effector triggered programmed cell death and resistance (S. Wang, et al., 2014).

This body of work requires a more in-depth look in order to determine the extent of *CPR5* involvement in the regulation of resistance. Further study needs to be done to examine the interacting partners with which *CPR5* coordinates to mediate resistance pathways, and to distinguish if *CPR5* involvement is based on interaction with components specific to respective pathways, and how it may selectively activate this pathway alone.

1.6 Reactive Oxygen Species (ROS)

Reactive oxygen species (ROS) are generated as a product of numerous biochemical reactions and are normally generated molecules. The generation of ROS is essential for normal plant processes, but an imbalance in the detoxification of these molecules can lead to the accumulation of ROS, which can lead to oxidative stress that is harmful to plants (Apel & Hirt, 2004; Pallavi, Jha, Dubey, & Pessarakli, 2012; Tripathy & Oelmüller, 2014). Environmental stresses such as drought, pathogen attacks, and UV-B radiation can lead to enhanced ROS generation which can cause the oxidation of proteins, damage to nucleic acids, and activation of PCD (Fesik, 2000; Gilchrist, 1998; Pallavi, et al., 2012). Despite being potentially harmful to plants, ROS serves as a signalling molecule (Apel & Hirt, 2004). Evidence suggests that ROS molecules may act as messengers in the abscisic acid (ABA) transduction pathway in guard cells (Neill, Desikan, & Hancock, 2002). Alternatively, ROS-mediated induction of defense genes in tomatoes appears to be regulated by SA in plants undergoing HR (Nanda, Andrio, Marino, Pauly, & Dunand, 2010).

Transcriptome data analysis of *cpr5* plants showed increased accumulation of senescence-associated gene (*SAG)*, notably *SAG13* which is also induced by oxidative stress (H.-C. Jing, et al., 2007). Further analysis of the gene expression profile of *cpr5* plants related to signalling pathways highlighted several stress-related genes involved in the hormone signalling pathways that were upregulated (H.-C. Jing, et al., 2007). An increase in many ROS-dependent putative transcription factors was also exhibited (Aki, et al., 2007). The alterations to the genetic expression profile of these genes indicate that *cpr5* experiences high levels of oxidative stress. Concurrent with this, an increase in gene and protein levels

of glutathione (GSH) detoxifying enzymes were exhibited in *cpr5* mutants (Aki, et al., 2007). Taking into account that misregulation of ROS generation and scavenging are some of the earliest altered processes in *cpr5* mutants; Jing et al. (2002) propose that *CPR5* may act as a master regulator of ROS-related signalling and balance which may subsequently interact with other signalling pathways to regulate *CPR5*-dependent pathways (Figure 1.1) (H.-C. Jing & Dijkwel, 2008; H. C. Jing, et al., 2008).

1.7 *CPR5* Molecular Function: Protein Localization and Structural Analysis

CPR5 is constitutively expressed within all plant tissues with equal expression levels in leaves and root tissue (Borghi, Rus, & Salt, 2011). This is interesting as a majority of the annotated phenotypes observed in *cpr5* mutants do not concern the root system. CPR5 is a predicted 564 amino acid Type IIIa membrane protein with 5 putative transmembrane domains located within the C-terminus and a putative bipartite nuclear localization signal located in the N-terminal region (Figure. 1.2) (Kirik, et al., 2001). Beyond the identification of a putative structure, little study has been done to elucidate the importance of the structural components of CPR5 or the localization pattern of the CPR5 protein. A study by Gao et al. (2011) using *CPR5*-GFP-fusion transgenic plants concluded that CPR5 protein is localized to the cytosol based on the observed GFP signal emanating from the cytoplasm. Similar assays performed by Perazza et al. (2011) indicated that CPR5-GFP fusion construct signal was present in plant cell nuclei. The *CPR5*-GFP fusion constructs from both studies were found to rescue *cpr5* mutant phenotypes when expressed in the mutant background confirming the functionality of the fusion proteins. A recent study by Wang et al, (2014), using Bimolecular Fluorescence complementation (BiFC), found that YFP signal could be detected in the nucleus in the presence of C-terminal nYFP tagged-SIM and N-terminal cYFP tagged-CPR5 indicative of an interaction occurring within the nucleus between the two proteins. This recent study coupled with the resolves observed by Gao et al. (2011) provides strong evidence that the N-terminus of CPR5 is localized and functions in the nucleus. However, the localization and functionality of the C-terminus of CPR5 remain unclear.

There is compelling evidence that the transmembrane domain is crucial for proper *CPR5* function as many of the *cpr5* mutants possess point mutations within the transmembrane

domain, as shown in Figure 1.2. However, it is unclear if the importance of these regions is to provide proper anchoring of the protein, or if there is a yet unidentified interaction that occurs between the putative transmembrane domain and other proteins. A study of CPR5 function lacking the ambiguous first transmembrane domain and the 4 commonly predicted transmembrane domains produced plants exhibiting *cpr5* mutant phenotypes (Gao, et al., 2011), indicating that this structural component is necessary for the functionality of the protein. It is still unclear whether the CPR5 protein is localized within the cell wall, the cytoplasm, or the nucleus; or what membrane is associated with the predicted transmembrane domains. Although study has been done to characterize the putative transmembrane domains of *CPR5*, there has been no reported study on the functionality or properties of the putative bipartite localization signal. Due to the lack of homology between *CPR5* and other genes, it is difficult to assess the importance of the structural components of the CPR5 protein, namely the transmembrane domains and the nuclear localization signal.

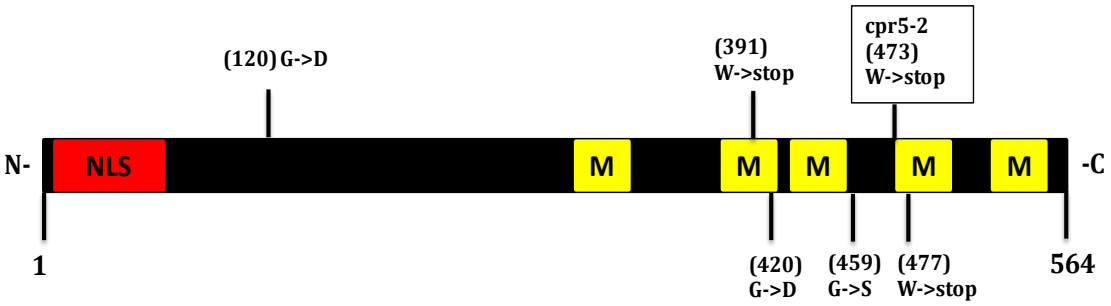

Figure 1.2: Diagram of CPR5 putative protein structure and location of several identified cpr mutant alleles.
CPR5 predicted 564 amino acid protein structure and location of the bipartite nuclear localization signal (NLS-red), 5 transmembrane domains (M-Yellow) relative to the N- and C- terminus. Several cpr5 mutant alleles are listed and identified by location of their single mutation relative to the protein structure. cpr5-2 mutation is highlighted.

1.7 *CPR5* and Cell Cycle Involvement

Cell cycle regulation is a highly complex and fundamentally conserved mechanism among eukaryotes. Plants, however, have deviated from the conserved mechanism in several aspects. Like mammals, plants contain cell cycle-related genes (CKIs) that are known to inhibit cyclin-dependent kinase (CDK) activity. These CKIs help coordinate the balance between cell cycle progression and cell growth (De Veylder, Beeckman, & Inze, 2007).

Cell cycle regulation involves the regulation of several checkpoints to facilitate the progression of the cell cycle. However these checkpoints are not concrete and can be uncoupled in some cell types. One alternate cell cycle pathway, called endoreduplication, involves cell differentiation and often includes DNA replication to increase the DNA content. In cells such as trichomes, endoreduplication occurs wherein DNA continues to replicate in the nucleus after mitosis and cytokinesis have terminated resulting in greater than 2C DNA content (Inze & De Veylder, 2006; Larkins et al., 2001). *cpr5* mutants exhibit lower endoreplication rates than wild-type plants resulting in lower DNA content as well as trichomes developing with less branching (Bao & Hua, 2014; Brininstool, et al., 2008; Kirik, et al., 2001).

Cell cycle regulation is not only essential for plant growth and development but has also been suggested to be involved in stress and resistance responses. Studies support that defects in cell cycle progression could result in autoimmune responses and PCD (Parker, 2014; S. Wang, et al., 2014). *cpr5* mutants not only exhibit perturbed endoreduplication and subsequent altered trichome development, but also increased stress and resistance (Brininstool, et al., 2008; Kirik, et al., 2001). The interlinking of cell cycle with innate immunity in Arabidopsis suggests that *cpr5*-altered cell cycle and stress and resistance responses could be due to interaction of CPR5 in the cell cycle pathway that indirectly affects the resistance and stress regulatory pathways, and abolishment of CPR5 would affect all related pathways.

Until recently, no proteins had been identified to interact directly with CPR5. However, new evidence suggests that there may be a direct link between CPR5 and cell cycle-related genes (CKIs). The double mutant *sim smr1* was observed to not only to suppress *cpr5*-enhanced resistance but also restored observable morphological phenotypes (S. Wang, et al., 2014). Interaction between CPR5, SIM and SMR1 was defined using BiFC and split luciferase assays, the findings of these assays provide strong evidence that CPR5 is not only genetically linked to CKIs, but may also be direct interacting partners of CPR5. This is the first evidence of CPR5 direct interaction with known proteins in a specific pathway.

1.8 Concluding Remarks

Evidence suggests that *CPR5* plays a role in multiple hormones and sugar sensing response pathways that are crucial to all major plant processes and these pathways are drastically altered when *CPR5* function is abolished. *CPR5* has been shown to act as a negative regulator of (1) JA, ET, and SA dependent pathogen response pathways (Clarke, et al., 2000), (2) ABA, and sugar-induced inhibition of proliferation (Aki, et al., 2007; Gao, et al., 2011; Yoshida, et al., 2002), and (3) early senescence induced by ET (H. C. Jing, et al., 2005) (Figure 1.1).

What is unclear, however, is the mechanism by which CPR5 acts on these pathways. Several suggestions have been provided by researchers of the *CPR5* gene, some of which involve CPR5 acting as a cell wall synthesis protein (Brininstool, et al., 2008), as a mediator of ROS (H.-C. Jing & Dijkwel, 2008), or as a transcription factor interacting protein (Daniel Perazza, et al., 2011). Studies characterizing *CPR5* based on observations of phenotype changes, downstream effects to hormone, and sugar sensitivities and levels, can only speculate on the primary function of CPR5 due to the lack of research on the specific partners CPR5 interacts with within the cellular system. Until recently, there has been no study involving CPR5 specific targets or what proteins target *CPR5* upstream of dependent pathways, which would provide answers to the mechanism by which *CPR5* controls multiple cellular processes. However, the identification of SIM/SMR1 as direct interacting partners of CPR5 may provide the first step towards uncovering how CPR5 is involved in so many pathways. Despite the findings that the *cpr5 sim smr1* triple mutant is able to effectively abolish morphological and resistance cpr5 mutant phenotypes, this interaction does not provide all the pieces of the CPR5 story as morphological phenotypes are not the only altered characteristics of *cpr5* mutants. SIM/SMR1 may provide the first direct downstream link to CPR5, but there are likely to be more interacting partners to be identified upstream of this interaction and perhaps downstream as well (Figure 1.1).

A large reason for the lack of direct interaction and localization studies involving CPR5 is due to the insoluble nature of transmembrane domain proteins. Although widely accepted as transmembrane-containing protein whose membrane regions are crucial for CPR5 function by Gao et al. (2011), it is unclear if these 4 or 5 putative domains are in fact all true transmembrane domains. Sequence analysis shows the possibility of a beta-strand in the transmembrane domain closest to the N-terminal region, which could indicate that this domain may be part of the non-membrane bound peptide and required for proper protein

folding (Faisal, 2015). Current methods do not provide many options for analysis of the full length protein; and limit study to characterizing CPR5 interacting partners using truncated CPR5 proteins whose localization and interactions may be affected.

Confirming the localization and the structure of CPR5 is a crucial next step in the characterization of CPR5. This, in addition to identifying CPR5 interacting partners, will help elucidate the mechanisms by which CPR5 controls the various pathways it is involved in, to regulate central plant processes in *Arabidopsis thaliana*. Without new advances in the characterization of insoluble proteins, determination of CPR5 molecular function will prove to be a difficult task.

The purpose of this thesis it to use current methods such as Yeast-two-Hybrid (Y2H), Bimolecular fluorescence complementation (BiFC), qRT-PCR and physiological plant assays to ascertain potential protein partners that may interact with CPR5 and to provide further evidence of their physical link with CPR5.

Chapter 2: Materials and Methods

Chemicals used

Unless otherwise stated, the chemicals used in this study were obtained from Sigma-Aldrich Corporation (St. Louis, Mo., US), Duchefa Biochemie BV (Madison, Wi, USA), Qiagen GmbH (Hilden, Germany). Life Technologies Corp. (Grand Island, NY, USA). Roche Applied Sciences (Roche Diagnostics GmbH, Manheim, Germany) and Bio-Rad Laboratories (Hercules, CA, USA).

2.1 General Use Protocols:

2.1.1 Bacterial Propagation

All bacteria cells were cultured in Luria broth (LB) containing 1% (w/v) bacto-tryptone (DIFCO Laboratories, Detroit, MI, USA), 0.5% (w/v) bacto-yeast extract (DIFCO Laboratories), 1% (w/v) NaCl, and adjusted to pH 7.5. For LB agar, add agar to a final concentration of 1.5%. (w/v). LB media and LB agar were sterilized by autoclaving at 121°C at 15psi for 20'. In a sterilized laminar flow hood, antibiotics were added to LB agar media after cooling to ~50-60°C and subsequently ~25mL was poured into round 100x15mm petri plates. Once solidified (at least 15' cooling period), plates were sealed with Parafilm and placed upside-down in 4°C until ready to use. Antibiotics were added to LB media prior to use.

DH5α *E. coli* cells were used for general lab manipulations including cloning and plasmid amplification. The DH5α was cultured in LB media and on LB agar plates with appropriate antibiotics (Table 2.1). During incubation, cultures were shaken at 250 x rpm at 37° and grown overnight.

Antibiotics	Concentration
Ampicillin	100mg/ml
Kanamycin	50mg/ml
Gentamycin	25mg/ml
Tetracycline	10mg/ml

Table 2.1 Concentration of Antibiotics used for positive bacterial selection

2.1.2 Preparation of Plasmid DNA (Alkaline Lysis Miniprep)

Cells were collected from 3mL overnight LB media cultures (with appropriate antibiotic) by centrifugation at 13,000 x rpm at room temperature (Table 2.1). The cell pellet was resuspended in 200µl ice cold Solution I (50mM glucose, 25mM Tris pH8.0, 10mM EDTA, 4mg/ml lysozyme), immediately lysed with the addition of 300µl Solution II (200mM NaOH, 1%SDS) and mixed gently by inversion. Lysed cells were neutralized after 5' of incubation at room temperature by adding 300µl of Solution III (3.0M Sodium Acetate, pH 4.8). The cellular debris was removed by centrifugation at 13,000 x rpm for 10' at RT and the supernatant transferred to a fresh tube and treated with 10µl RNase A (100µg/ml) and incubated at 37°C for 30'. Proteins were removed using 400µl chloroform:isoamyl alcohol (24:1) and the new aqueous layer was transferred to a fresh tube The plasmid DNA was precipitated by addition of isopropanol (0.7xthe volume of the transferred aqueous layer) and incubated for 5' at room temperature. The DNA pellet was collected by centrifugation at 13,000 x rpm for 15' and washed twice with 70% ethanol and centrifuged at 13,000 x rpm for 2' before removing the ethanol and air-drying and subsequent resuspension with sterile MillQ water.

2.1.3 Agarose Gel Electrophoresis

Nucleic acid fragments were separated and visualized using agarose gel electrophoresis. A 1% (w/v) gel was prepared by heating and dissolving 1g of agarose (UltraPURE™ agarose, Life Technologies) in 100ml of 1 x TAE buffer (40 mM Tris base, 1% glacial acetic acid, 1 mM EDTA, pH 7.8) (Sigma-Aldrich Corporation). A sample well forming comb was inserted and after the solidification of the gel, the comb was removed and running buffer (1 x TAE) was added to the tray until the gel was submerged. DNA samples were loaded onto the gel

mixed with 1µ of 10x DNA loading dye per 9µl of sample to a final concentration of x1 [(0.1M EDTA, pH 8.0, 50% (v/v) Glycerol, 1% (w/v) SDS, 0.025% (w/v) bromophenol blue)]. HyperLadder™ kb 1DNA ladder (5µl) (Bioline, London, UK) was added to an empty well. The gel was run at 100 V until resolved (~60'). After electrophoresis, the gel was stained with 0.1 µg/ml ethidium bromide for 10' and then de-stained with water for 5'. The fragments were visualized using a Gel Doc 2000 Gel Documentation System from Bio-rad Laboratories, CA, USA.

2.1.4 Preparation of Chemically Competent Bacterial Strains

Chemically competent cells for transformation were prepared using the DH5α (GIBCO BRL) strain of *E. coli* according to the method of Inoue et al., (1990) with some modifications. An aliquot of previously made chemically competent bacterial cells were cultured in LB media (3ml) at 37°C overnight with shaking (250 x rpm). The following day, 2x200µl of culture were used to inoculate 2x100ml of freshly autoclaved and cooled LB media in 500ml flasks. Cell cultures were grown at 18°C and 200 x rpm until an optical density of 0.6 at 600nm was reached. After this, cells were transferred to centrifuge tubes, chilled on ice for 20' and subsequently pelleted at 5,000 x rpm for 5' at 4°C. The supernatant was then decanted and the pellet re-suspended in 20ml of SEM buffer (10mM PIPES, 55mM $MnCl_24H_2O$, 15mM $CaCl_2$ $2H_2O$ and 25mM KCl, pH 6.7), transferred to smaller centrifuge tubes and chilled on ice for 10' before pelleting again at 4°C for 5'. Once the supernatant was decanted, the cells were re-suspended in a total of 12ml of SEM buffer and 920µl of DMSO (final concentration 7%). Aliquots of 100µl of the cells were prepared in 1.7ml microcentrifuge tubes and stored at -80° C until further use. Note that no antibiotics were used in the preparation of competent cells.

2.2 Cloning

2.2.1 PCR Amplification of cDNA

Gene sequences were isolated from *Arabidopsis thaliana* cDNA synthesized from plant material from six 21-day-old *Col-0* plants via PCR amplification using Phusion High Fidelity PCR System (New England Biolabs, MA, USA) as per the supplier recommended standard protocol. Gene specific primers used are listed in the tables' specific for each experimental section.

2.2.2 Restriction Digestion and DNA Ligation

DNA, typically up to 1µg was digested with 1U of selected restriction enzyme in the appropriate buffer specific to each restriction enzyme, for a total volume of 50µl. Digestion was carried out overnight at 37°C. Double restriction digests were carried out under identical conditions with 0.5U of each restriction enzyme and a compatible buffer as per manufacturer's recommendation. Restriction enzymes from Roche Applied Sciences (Roche Diagnostics GmbH, Manheim, Germany) and New England Biolabs (MA, USA)

PCR amplified DNA products and plasmids were digested using the appropriate restriction enzymes (Appendix 3 & 6) (New England Biolabs, MA, USA) and compatible buffer as per manufacturer's recommendation, and subsequently purified via agarose gel electrophoresis (section 2.1.3). The gel areas containing the DNA products of interest were excised under UV light using a sterile scalpel blade and the DNA was recovered using the Zymoclean Gel DNA Recovery kit (Zymo research Corporation, Irvine CA. USA) following the manufacturer's protocol. The concentrations of purified DNA fragments were measured using Nanodrop 1000 spectrophotometer (Thermo Fisher Scientific, Wilmington DE. USA) and agarose gel electrophoresis.

Target DNA fragments and vectors were ligated in a 3 (insert copies):1 (vector copies) ratio up to 100ng of DNA using 1µl T4 DNA Ligase (Roche), 2µl of T4 DNA Ligase Reaction Buffer, and MillQ water (up to 20µl). Samples were incubated overnight at 16°C and subsequently transformed into DH5α *E. coli* competent cells (2.2.3) and plated on LB agar plates with the appropriate antibiotics (section 2.1.1) (Table 2.1).

2.2.3 Bacterial Chemical Transformation

Chemically competent cells were thawed on ice, for 15'-20, mixed with 1-10ng of DNA (dependent on the DNA being transformed) by gently swirling with the pipet tip several times, and incubated on ice for 30'. The cell mixture was then subjected to a heat shock at 42°C for 1' and subsequently placed on ice for at least 2'. Once chilled, in a sterile laminar flow hood 500µl of LB media was added to the cell mixture and shaken at 250 x rpm for 1h at 37°C. The bacteria suspension was then plated out on an LB plate containing the appropriate antibiotics in a sterile laminar flow hood (Table 2.1).

2.2.4 Bacterial Colony PCR

The presence of the proper insert in vector was confirmed by Colony PCR amplification with samples containing Bacterial cells isolated from single colonies were picked up using a sterile toothpick or pipet tip and added to a standard PCR reaction of 10µl of 2x Promega Master Mix, 1µl gene specific forward primer, 1µl of gene specific reverse primer, and 8µl sterile PCR water up to a final volume of 20µl (Promega BioSciences, LLC, CA, USA). The annealing temperature and extension times vary for each primer set and gene length and were chosen based on manufacturer's recommendation. *Note-Annealing time varies between primer sets

Pre-incubation		95°C	5'	
Amplification	Denaturation	95°C	30"	|
	Annealing	50°C*	30"	| x35 cycles
	Extension	72°C	5'	|
	Cooling	4°C		

2.2.5 DNA Sequencing

DNA Sequencing analysis was performed by Macrogen Inc., Korea using their EZ-Seq service. Sample preparation as per the EZ-Seq direct protocol included 5µl of template DNA of either 50ng/µl of PCR product (250ng total DNA) or 100ng/µl of plasmid DNA as well as 5µl of 5pmol/µl of the appropriate primer. Two samples for each DNA sample were prepared, one with the forward primer, and one with the reverse primer.

The sequence results obtained were analyzed and edited using Geneious software (http://geneious.com).

2.3 SDS PAGE and Western Blot Analysis

2.3.1 Protein Extraction and Sodium Dodecyl Sulfate (SDS) Polyacrylamide Gel Electrophoresis (PAGE)

2.3.1.1 Yeast Protein Extraction

Overnight yeast cultures were prepared by inoculating a single 2-3mm colony from freshly grown yeast, grown for 3-5 days, into 5mL of SD/-Trp (or selective media specific to the plasmid construct present in the yeast) and shaken overnight at 250 x rpm at 30°C. Cultures were vortexed vigorously for 1'-2' to disperse any clumped yeast cells. 50mL of sterile YPDA media (20g Difco peptone, 10g yeast extract, 15mL of 0.2% stock adenine hemisulfate solution, MillQ H2O up to 1L, pH 6.5, and 20g agar solid media) was inoculated with the full overnight culture and shaken at 220 x rpm at 30°C until an OD600 of 0.5 was reached (~4-8hours). The 50mL culture was quickly poured into a prechilled 100ml centrifuge tube and spun in a prechilled 4°C centrifuge at 3200 x rpm for 5'. The supernatant was removed and the cell pellet was washed in 50ml of ice-cold H2O and the pellet was recovered by centrifugation at 3200 x rpm for 5' at 4°C.The cell pellet samples were immediately frozen by placing samples in liquid nitrogen. Cells can be stored at this stage in -70°C until ready to use. Once frozen, the cells were transferred to a mortar and ground into a powder using a mortar and pestle to break the cell wall and subsequently placed into a microcentrifuge tube and resuspended in 100µl of ice-cold TCA buffer (20mM Tris-HCl (pH 8), 50mM Ammonium acetate, 2mM EDTA, 50µl/ml prechilled Clontech Protease inhibitor solution, x1 PMSF combined with Deionized H2O, per 7.5 OD600 unit of cells(Clontech Laboratories, 2009). OD units were calculated by multiplying the OD by the number of ml of culture (50). The tubes were placed on ice and ground for 1' using a pestle. The homogenate was centrifuged at 12,000 x rpm for 10' and the supernatant was collected and precipitated with 50% TCA to a final concentration of 10% TCA for 1 hour at 20°C. The protein pellet was recovered via centrifugation at 12,000 x rpm for 10' at 4*C and washed 3 times with ice cold acetone and centrifuged at 12,000 x rpm for 2'. After the last acetone wash, samples were placed in a heatblock at 37°C to remove any residual acetone, and can be stored for further use at -70°C or immediately used for SDS-PAGE gel electrophoresis. Gel electrophoresis was performed using Bio-rad Mini-PROTEAN® II Electrophoresis Cell as per manufacturers protocol (Bio-rad Laboratories, Inc. CA, USA)

2.3.1.2 SDS-PAGE Protein Sample Preparation

The protein pellet was dissolved in TCA-Laemmli loading buffer (10µl loading buffer per OD600 unit of cells) (for 1ml, combine 480µl SDS/glycerol stock solution, 400µl Tris (200mM)/EDTA (20mM), 5µl β-mercaptoethanol, 20µl (x100)PMSF stock solution, 20µl prechilled protease inhibitor, 30µl deionized H2O). Note, if the sample turns yellow, this is indicative of too much acid remaining in the sample, but should not affect the results of SDS-PAGE electrophoresis. The tubes re then incubated at 100°C in a boiling water bath for 10' and subsequently centrifuged at 14,000 x rpm for 10' at 20-22°C before loading 5-10µl of protein samples onto an SDS PAGE gel. Additionally, 5µl PageRuler™ Prestained Protein Ladder (ThermoFisher Scientific, MA, USA) protein ladder was loaded into an empty well for quantification and size comparison of the protein samples.

2.3.1.3 Gel Preparation and gel electrophoresis

Proteins were separated as per their molecular mass as has been described by Laemmli (1970). The proteins were resolved in 12% resolving gel (0.18M Tris-HCL [pH8.8], 0.1% SDS, 12% acrylamide [37:5:1], 0.1% ammonium persulfate and 5 µl of tetramethylethylenediamine). The gel was submerged in running buffer (0.025 M Tris-HCL, 0.1% SDS, 0.192 M glycine, pH 8.3) and electrophoresis was run at 150 V for 75 min.

2.3.2 Transfer of Protein onto PVDF Membrane

Proteins were separated by SDS-PAGE (section 2.3.1) and transferred onto a PVDF membrane (PVDF transfer membranes, PerkinElmer Life Sciences Inc., Boston, MA, USA) as described by Towbin et al, 1979 using the Trans-Blot® Electrophoretic transfer cell (Bio-Rad). The membrane was cut to the size of the gel, and first activated by dipping in MeOH before placing into transfer buffer (25 mM Tris, 190 mM glycine, pH 8.3 containing 10% (v/v) MeOH) and chilled at 4°C prior to use. The transfer cassette was assembled as per the diagram below:

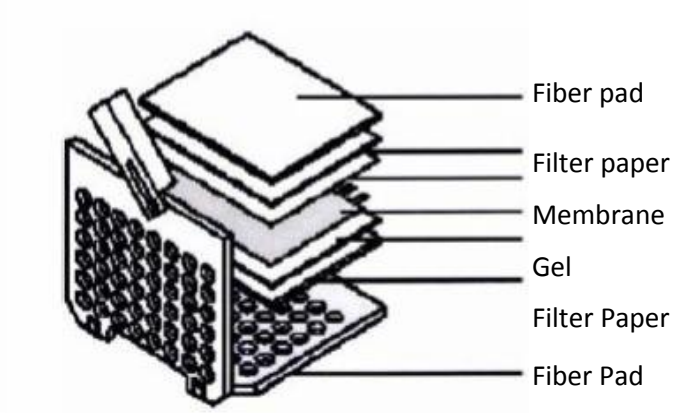

Figure 2.1: Cassette Set Up For Western Blotting Adapted From Mini Trans-Blot Electrophoretic Transfer Cell, Instruction Manual (Bio-Rad Laboratories, Hercules, CA, USA)

The cassette was then transferred to the holder and enough transfer buffer was added to cover the top of the cassette and the Bio-Ice™ cooling unit was inserted. A rotating magnet was added to the holder and the whole unit was placed on top of a magnetic stirrer. The transfer was conducted at 100 V for 60' on constant stirring.

2.4 Yeast-Two-Hybrid (Y2H)

All solutions were prepared according to the Yeast Protocols Handbook (Clontech Laboratories, 2009). For every 1L of SD media, 6.7g Yeast nitrogen base without amino acids, 2% dextrose, and 10% x 10 Dropout Solution and 200mL of H2O was combined, the pH adjusted to 5.8 and filter sterilized using a 0.2µm filter. 20g of agar was combined with

655ml of MillQ H2O, autoclaved at 121° at 15 psi for 20' and cooled to ~50-60*C before combining with SD/dropout media. The pH was adjusted to pH 5.8 if necessary. 40µl 100mM IPTG and 120µl X-α-gal (20mg/ml in DMF stored in dark at -208C) was spread directly onto solid media and allowed to dry for ~30' in a sterile laminar flow hood prior to use. (2% agar added for solid media only)

2.4.1 Generating Bait Plasmids for Y2H "Mate and Plate" Library Screening

Plasmids containing the 2 different truncated CPR5 cDNAs were obtained from PhD colleague Muhammad Faisal. Direct subcloning of CPR5TM0 and CPR5TM1 (Figure 2.2) (Appendix 1) into the multiple cloning site (MCS) of the GAL4-BD containing Y2H vector pGBKT7 (Appendix 2A) was performed using NdeI and BamHI restriction enzymes after confirmation that the DNA fragments would be in frame with the specific GAL4-BD domain (Appendix 3). Restriction digestion (section 2.2.2), ligation (section 2.2.2), and transformations into chemically competent *E. coli* strain DH5α were performed using heat shock transformation (section 2.2.3). Confirmation of successful cloning was done initially via colony PCR using gene and plasmid specific primers. Plasmid DNA miniprep from bacteria was performed using the alkaline lysis method (section 2.1.2). All constructs were fully sequenced by Macrogen Inc. (Korea) prior to Y2H analysis using the sequencing primers shown in with T7/ BD primers listed in Table 2.2. Confirmed plasmids were then transformed into yeast strain AH109.

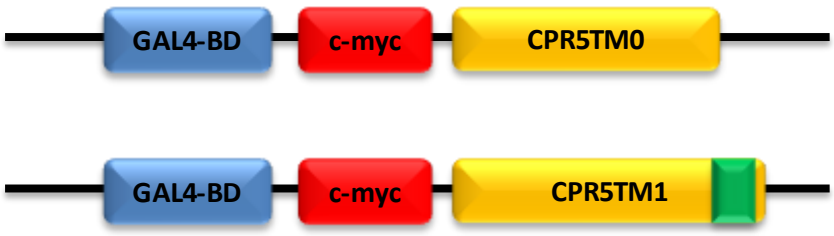

Figure 2.2: Bait Protein Plasmid Constructions.
CPR5TM0 and CPR5TM1 were cloned into GAL4-BD containing plasmid pGBKT7 via the MCS flanking the c-Myc tag.

Y2H Colony PCR and Sequencing Primers

T7 Sequencing	TAATACGACTCACTATAGGGC
3' AD Sequencing	AGATGGTGCACGATGCACAG
3' BD Sequencing	TTTTCGTTTTAAAACCTAAGAGTC

Table 2.2: List of Primers used for colony PCR and sequencing of genes cloned into Y2H AD- and BD- plasmid

2.4.2 Yeast Transformation

Freshly grown yeast cells were transformed with a pGBKT7 plasmid containing a GAL4-BD and the appropriate cDNA insert. For each transformation, 60µl of fresh AH109 yeast cells were placed into a 1.5ml microcentrifuge tube, rinsed with sterile MillQ water and mixed with 34µl of pGBKT7 plasmid (1µg of total plasmid DNA), 240µl of PEG4000, 36µl of 1.0M LiAC, and 50µl of denatured herring sperm carrier DNA (10mg/ml). Herring sperm carrier DNA was denatured by boiling for 5' and immediately placed on ice until adding to transformation mix. After vigorous vortexing, the cells were incubated at 42°C for 2 hours. The cells were then pelleted, and washed with sterile water and resuspended in 1ml of sterile MillQ water. 100µl of the transformation mixture was spread on selective SD plates lacking tryptophan (-Trp). Plates were sealed with Parafilm and incubated for 3-5 days at 30°C until colonies appeared.

2.4.3 Y2H Transcriptome Library Mating Assay

Transformation positive clones were restreaked on selective SD plates (SD/-Trp) and incubated for 3 days at 30°C. Liquid cultures were prepared by resuspending one 2-3mm colony in 50ml of SD/-Trp following by incubation at 30°C 250-300 x rpm until an OD600 of 0.8 was reached. The cells were then pelleted at 3200x rpm for 5' and resuspended in SD/-Trp to an OD of 1x10^8 cells per ml of SD/-Trp media. The resuspended cells were then combined with the commercial *Arabidopsis thaliana Col-0* normalized cDNA library (Clontech Laboratories, USA) in a sterile 2L flask containing 45ml of 2xYDPA and 50µg/ml kanamycin. The cDNA library was expressed in GAL4-AD containing expression vector pGADT7 RecAB (Appendix 2B). The cell mixture was then incubated at 30°C at 30-50 x rpm for 20-24 hours until the presence of yeast zygotes (3-lobed structures) were

confirmed. One drop of mating culture was observed under a phase contrast microscope (40X). Dilutions of mating culture were made as needed to ensure visible individual cells. Following the confirmation of zygote formation, the cells were pelleted at 3200x rpm for 10; and rinsed and centrifuged at 3200x rpm for 5', twice with 0.5 YPDA/kanamycin (50µg/ml). The cells were then resuspended in 10ml of 0.5 YPDA/kanamycin (50µg/ml). 250ml of the cell suspension was plated onto 100mmx15mm plates containing medium stringency SD triple knockout media lacking histidine, leucine, and tryptophan (SD/-His/-Trp/-Leu). The plates were incubated at 30°C for 3-5 days until colony formation. Large colonies (+3mm) and subsequently medium sized (>1.5mm) colonies were restreaked onto high stringency selection SD media additionally lacking adenine and including X-α-galactosidase (X-α-gal). Plates were sealed with Parafilm, wrapped in foil and incubated for 3 days at 30°C. Colonies showing positive growth and exhibiting a blue color were restreaked onto fresh high stringency SD/-Ade/-His/-Trp/-Leu/X-α-gal plates to obtain individual colonies. Positive colonies were restreaked on high stringency media 2-3 consecutive times to allow for the segregation of individual clones that were able to maintain the same phenotype.

2.4.4 Yeast Colony PCR Analysis

Yeast Colony PCR was conducted in order to eliminate duplicate clones. For each potential positive, a fresh colony was added to a tube containing 2µl of lyticase (500units/ml) and 15µl of 0.1M potassium phosphate-buffer (P-buffer) and incubated at room temperature for 2 hours. The samples were diluted with 34µl of MillQ water and 5µl was used in a yeast colony PCR reaction containing 10µl of 2x Promega Master Mix, 1µl of T7 primer, 1µl of AD primer, and 5µl sterile PCR water up to 20µl.

Pre-incubation		95°C	3'	
Amplification	Denaturation	95°C	30"	|
	Annealing	50°C	30"	| x35 cycles
	Extension	72°C	5'	|
	Cooling	4°C		

5µl of PCR samples were then digested with a high frequency cutter restriction enzyme *Hae*III (1U) in 50µl reactions including 5µl of the appropriate buffer and MillQ water up to 50µl. Uncut PCR samples as well as digested samples were analyzed via gel electrophoresis to confirm that each PCR sample consists of one band, indicative of only

one library plasmid present in the yeast sample, as well to analyze the digestion pattern of selected clones to determine duplicate gene containing constructs.

10µl of the PCR samples of selected clones were treated with 2µl of ExoSAP-IT (Affymetrix) for 15' at 37°C then 15' at 85°C to remove unconsumed dNTPs and primers remaining in the PCR product mixture before samples were sent to Macrogen Inc. (Korea) for sequencing with T7/ AD primers listed in Table 2.2.

Sequencing results obtained from the DNA Analysis from Macrogen Inc. were analyzed and edited using Geneious. The sequenced cDNA inserts from the GAL4-AD containing plasmid pGADT7-RecAB was analyzed using the BLAST database to determine the identity of the gene insert. The sequences were then analyzed for duplicate genes as well as proper frame shifts.

2.4.5 Yeast Plasmid Extraction and Rescue

For yeast plasmid extraction, 3ml of overnight yeast culture was prepared in the appropriate SD media (SD/-Leu for selection of library plasmids) shaking at 250 x rpm at 30°C. Yeast plasmid extraction was performed as per section 2.1.2 using alkaline lysis miniprep with some modification. Firstly, 0.5ml of culture was pelleted via centrifugation (top speed x 30"), resuspended in 200µl lyticase solution (made fresh from stock instead of using Solution I, and incubated at room temperature for 2h. The cell solution was then subjected to standard alkaline lysis miniprep starting with the addition of Solution II. (section 2.1.2) Once alkaline lysis miniprep was performed, the DNA was resuspended in 30µl of 10mM Tris-HCl (pH 8.0)

The library plasmids of selected clones were rescued via transformation of DH5α *E. coli* plated on LB agar media with ampicillin (Table 2.1) for selection of the GAL4 AD containing plasmid as per the manufacturer's protocol (Clontech Laboratories, 2009). Isolated plasmids were retransformed into yeast strain Y187 and mated with pGBKT7 plasmid constructs to confirm interaction.

Yeast two hybrid mating assays were performed with yeast strain AH109 and Y187.

2.4.6 Generating "Prey" Plasmids for Y2H Protein Pair Assays

To enable the cloning of selected cDNAs into the Y2H vector pGADT7 (Clontech Laboratories, USA) in frame with the vector specific GAL4-AD domain, PCR reactions were

performed to add appropriate restriction sites and extra nucleotides required to maintain the proper reading frame to the cDNA coding regions (Appendix 2C & 3). Primers used for cloning PCR fragments into the appropriate vectors are shown in Table 2.3. For cloning of all constructs, Phusion Hi-Fidelity DNA Polymerase was used as per manufacturer's protocol. 50µl PCR reactions were set up on ice containing 5x HF fusion buffer (10µl), dNTPs (1µl of 10mM stock), forward and reverse primers (2.5µl each of 10uM stock), cDNA (1µl), Phusion Hot-start DNA polymerase (0.5µl of 2U/µl stock), and PCR grade H2O (32.5µl), PCR reactions were loaded on 1% TAE agarose gels and get purified using Zymogen™ Gel DNA recovery Kit according to manufacturer's manual. Following this the fragments were digested (section 2.2.2), ligated (section 2.2.2) and transformed into chemically competent DH5α (section 2.2.3). Positive clones were identified via colony PCR (section 2.4.4) and plasmid DNA was purified using alkaline lysis miniprep method (section 2.1.2). All constructs were fully sequenced by Macrogen Inc. (Korea) prior to Y2H analysis using the T7/AD sequencing primers shown in Table 2.2. Plasmids containing the previously identified genes of interest (GOI) were then used in Y2H transformation assays.

TAIR Ascension	Gene	Size (bp)	Primer	Sequence
AT3G01090	AKIN10	1608	Akin10FXmaI	GCCCGGG**ATG**TTCAAACGAGTAGATGAGT
			Akin10RSacI	AACGAGCTCTCAGAGGACTCGGAGCTG
AT4G25100	FSD1	639	Fsd1FXmaI	ACCCGGGA**ATG**GCTGCTTCAAGTGCT
			Fsd1RSacI	GACGAGCTCTTAAGCAGAAGCAGCCTT
AT1G22640	MYB3	774	Myb3FNdeI	TAACAT**ATG**GGAAGATCACCATGCT
			Myb3RXmaI	ACCCGGGCTAATGAGTTCTAACATCAGAAA
AT1G72160	PATL3	1473	Patl3FNdeI	GACCAT**ATG**GCTGAAGAACCTACTACT
			Patl3RXmaI	TCCCGGGTTAGAGAGGTTTGACATTGAA
AT2G22360	DNAJ	1329	DnaJFXmaI	ACCCGGG**ATG**GCT ATAATACAACTTGGA GT
			DnaJRSacI	TAAGAGCTCTCATCTACTGGTGCTATTAGC
AT3G59770	SAC9	4941	Sac9FNdeI	AGACAT**ATG**GATCTGCATCCACCAG
			Sac9RXmaI	ACCCGGGTCAGACACTTGAAAGGCTAG
AT3G58120	BZIP61	990	Bzip61FNde1	GCGCAT**ATG**GCACAACTTCCTCCGAA
			Bzip1RXmaI	TCCCGGGTTAGACATTGAGGAGCTGTTCC
AT5G24430	CRK4	1785	Crk4FXmaI	ACCCGGG**ATG**GGTCATTGTTACAGCCGGA
			Crk4SacI	AACGAGCTCTCACCTAGGTCTCGAGCTT
AT4G09160	PATL5	2007	Patl5FNdeI	GACCAT**ATG**TCTCAAGATTCTGCAACT
			Patl5RXmaI	ACCCGGGTTACTCACAAGCTAAAGG
AT3G51670	PATL6	1230	Patl6FNdeI	GAGCAT**ATG**GATGCTTCATTGTCTCCA
			Patl6RXmaI	ACCCGGGTTAGACGGTTGTAGTAGATT
AT3G50630	KPR2	630	Krp2FNdeI	GAGCAT**ATG**GCGGCGGTTAGGAGAA
			Krp2RXmaI	ACCCGGGTCATGGATTCAATTTAACCCACTC
AT5G04470	SIM	384	SimFNdeI	GAGCAT**ATG**GATCTTGATTTAATACAAGATCTGC
			SimRXmal	ACCCGGGTCATCTTCGTGAACAAGAACGGA
AT3G10525	SMR1	387	Smr1FNdeI	GAGCAT**ATG**GATCTTGAATTACTACAAGATTTGT
			Smr1RXmaI	ACCCGGGTCATCTTCGAGAACAATAAGGGT

Table 2.3: Genes and sequences of primers used for amplifying full length gene coding regions for cloning into Y2H GAL4-AD vector pGADT7

2.4.7 Y2H Protein Pair Transformation Assays

Yeast strain AH109 (Clontech Laboratories, USA) containing BD-CPR5TM0, BD-CPR5TM1, and BD-53 plasmids respectively, were grown on SD/-Trp media plates for 4 days. Starter cultures for each construct were generated in 3x500mL Erlenmeyer flasks by inoculating a half plate of newly grown yeast (grown for 3-5 days) into 300mL sterile SD/-Trp liquid medium and aliquoted evenly between the 3 flasks. Cultures were incubated overnight at 30°C at 200 x rpm.

For each transformation, 60µl of fresh AH109 yeast cells containing BD-CPR5TM0, BD-CPR5TM1, and BD-53 respectively were transformed with GAL4-AD containing (AD-GOI-X) construct as per the protocols in section 2.4.2. Positive transformants were selected for on media lacking tryptophan and leucine (SD/-Trp/-Leu). Plates were sealed with Parafilm and incubated for 5 days at 30°C until colonies appeared.

Transformation positive clones were restreaked on medium stringency selection plates (SD/-His/-Trp/-Leu) and high stringency plates (SD/-Ade/-His/-Trp/-Leu/X-α-gal). Plates were sealed with Parafilm, wrapped in foil and incubated in darkness for 5 days at 30°C. Pictures of plates showing colony growth were taken with a Nikon D7000 with an AF Micro Nikkor 60mm lens and tripod.

2.5 Bimolecular Fluorescence Complementation (BiFC)

2.5.1 Generating Plasmids for BiFC and Transformation into *Agrobacterium tumefaciens*

BiFC was conducted using the pGreenII 0229 62-SK expression vector (Appendix 5) optimized for plant transformation via *Agrobacterium tumefaciens (Agrobacterium*) infiltration. Three pGreenII 0029 62 SK plasmid constructs containing the HA epitope tag and MCS from pGADT7 (HA-MCS) as well as cYFP or nYFP were constructed for subsequent gene cloning into the newly constructed plasmids (Figure 2.3).

cYFP and *nYFP* fragments were amplified with added restriction sites using *YFP* specific primers specific to each construct from previously cloned into expression vector pICH41155 (Appendix 4, 6A). HA tag sequence and MCS was amplified from pGADT7 using sequence specific primers (Appendix 6A). Gene coding regions for CPR5 and *EDS1* were amplified from cDNA (Appendix 6C) (section 2.2.1). All *GOI-Y* coding regions were excised from previously cloned into Y2H expression vector pGADT7 (Appendix 6D). Expression vector pGreenII 0029 62-SK was digested with the restriction enzymes specific to constructs p (HA::cYFP), p (cYFP::HA) and p (nYFP::HA) (Appendix 6B). All PCR products were purified and digested with the appropriate restriction enzymes (Appendix 6B), (section 2.2.2).

p (HA::cYFP), p (cYFP::HA) and p (nYFP::HA) were constructed from *nYFP*, *cYFP*, and HA-MCS ligation into previously digested pGreenII 0229 62 SK and cloned into *E. coli* DH5α. Transformants were analyzed via Colony PCR with all 35S promoter primer, HA specific primer and YFP specific primers (Appendix 6). Successful clones were sequenced by Macrogen, Inc. (Korea). (section 2.2.4, 2.2.5)

Positively identified and sequenced plasmids were used to construct completed expression plasmids p (cYFP::HA::GOI-X), p (GOI-X::HA::cYFP), and (p (nYFP::HA::GOI-Y)) (Figure 2.3). p (HA:;cYFP), p (cYFP::HA) and p (nYFP::HA) were digested with restriction enzymes specific to each gene and ligated with previously digested PCR amplified gene coding regions (Appendix 6D). Successful cloning of gene coding regions into p (HA::cYFP), p (cYFP::HA) and p (nYFP::HA) was determined via colony PCR using the cDNA amplification primers (Table 2.3) and subsequent sequencing by Macrogen, Inc. (Korea). (Appendix 6)

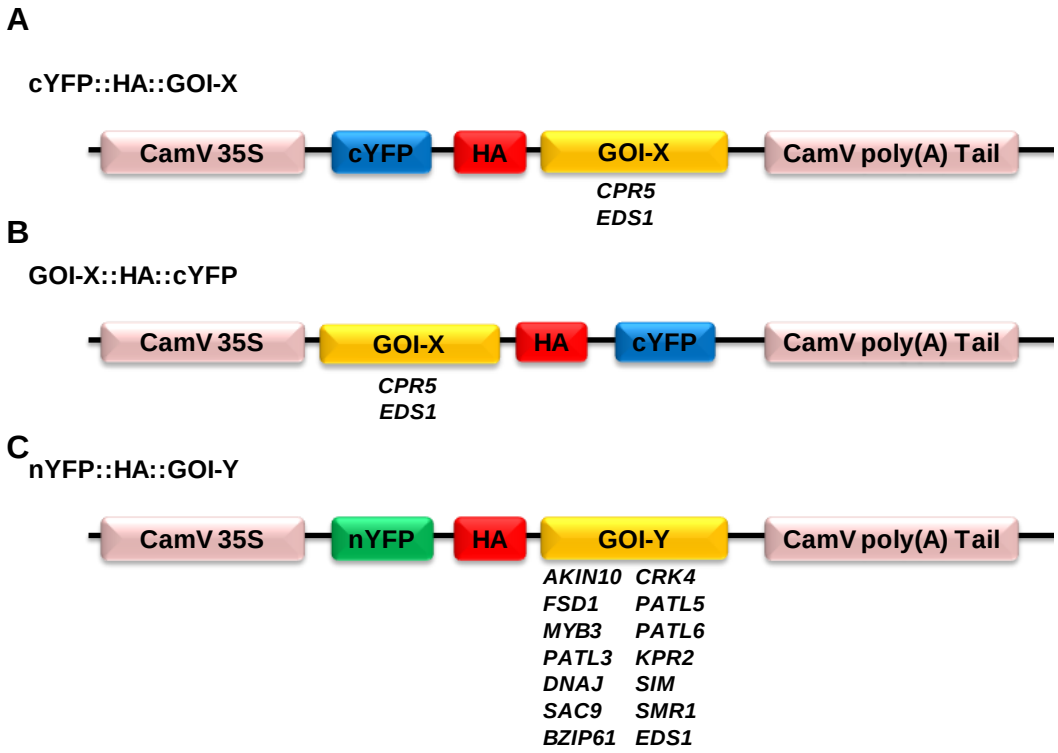

Figure 2.3: Plasmid Construction for BiFC Assay.
A total of 3 plasmid constructs carrying nYFP, and cYFP in specific orientations were constructed for insertion of gene coding regions. Two plasmid were constructed so that cYFP would be fused to the **A**) N-terminal (p (cYFP::HA::GOI-X)) and **B**) C-terminal (p (GOI-X::HA::cYFP)) of the Gene of Interest-X (GOI-X). **C)** One pGreenII 0229 62 SK plasmid was constructed so that nYFP would flank the N-terminal of GOI-Y (p (nYFP::HA::GOI-Y)). The genes subcloned into each final expression vector are listed.

2.5.2 *Agrobacterium tumefaciens* Transformation and Infiltration

Positively identified plasmids were amplified via alkaline lysis miniprep from previously cloned into DH5α cells, and transformed into *Agrobacterium* strain GV3101 already containing the helper plasmid pSOUP. Electro-competent cells of GV3101 (obtained from PhD colleague Muhammad Faisal) were transformed with pGreenII 0229 62 SK plasmid constructs by electroporation. Plasmid was added to thawed GV3101 competent cells and transferred to a pre-chilled Gene Pulser® 0.2cm electrode electroporation cuvette. Cells were electroporated using a Cell-Porator Electroporation System (Life Technologies Corporation, Auckland, New Zealand) following the instructions provided by the manufacturer. The electroporated cells were then transferred to 900µl of LB media and shaken at 30°C for 2 hours at 250 x rpm. After incubation, the transformed cells were selected by plating 100µl of the cell mixture on LB plates containing 20µg/mL gentamycin

(for selection of the helper plasmid pSOUP), 60µg/ml kanamycin (selection for pGreenII 0229 62SK) and 10µg/ml tetracycline (selection for GV3101) (LB/Tet/Kan/Gen) for 2 days at 30°C until colonies have formed (Table 2.1). A single colony was then restreaked onto a fresh plate. Bacteria grown from the newly streaked plate was tested for positive transformation of the correct plasmid using gene specific primers based colony PCR (section 2.2.4, Table 2.3)

Agrobacterium strains containing positively transformed expression vectors were grown in LB/ Tet/Kan/Gen media overnight at 30°C at 250 x rpm. Relevant cultures were pelleted at 5,000 x rpm for 4' and resuspended in 1ml of $MgCl_2$ (10mM). Cells were diluted and mixed with the appropriate accompanying cell culture so that the OD of the combined cell cultures had a final OD600 of 0.4 in 1ml of mixed cultures. Infiltration of 2-3 leaves of *Nicotiana benthamiana* were performed for each sample mixture. After 3 days, leaf discs were sampled.

2.5.3 Confocal Microscopy

Imaging was carried out using the Leica DM6000B SP5 confocal laser scanning microscope system running LAS AF software (version 2.7.3.9723; Leica Microsystems CMS GmbH). Images were acquired with a HCX PL Fluotar 40x (N.A. 0.75) dry. DAPI was imaged through excitation at 405nm (405 diode) and emission collection at 415-491nm; EYFP was imaged through excitation at 496nm (argon) and emission collection at 501-600nm; chloroplasts were imaged through excitation at 633nm (HeNe 633) and emission collection at 643-746nm. Brightfield was imaged simultaneously using 496nm.

2.6 Quantitative Real-Time PCR (qRT-PCR)

2.6.1 Isolation of total RNA and Quantification

2.6.1.1 RNA Extraction

A total of 14 lines of *Arabidopsis thaliana* were chosen for qRT-PCR (Table 2.4). Total RNA was extracted using the Zymogen Quick-RNA™ MiniPrep kit. 3 replicates of six plants each were harvested per line (a total of 18 plants harvested per line). One hundred milligrams of tissue per replicate was ground in liquid nitrogen and cells were lysed by adding 800 µl of RNA lysis buffer and vortexing for 15" Subsequently samples were centrifuged at

12,000 x rpm for 3' at room temperature. gDNA contamination was minimized by transferring the supernatant into Spin-Away™ filter in a collection tube and centrifuging at 10,000 x rpm for 1'. After adding an equal volume of 100% ethanol, the RNA was isolated by transferring the filtrate to Zymo-spin™ IIICG column in a collection tube and centrifuging at 10,000 x rpm for 1 min. The filtrate was discarded and 400 µl of RNA prep buffer was added to the column followed by centrifugation at 10,000 x rpm for 1'. The RNA was washed with an addition of 700 µl of RNA wash buffer followed by centrifugation at 10,000 x rpm for 1'. 9. Another 500 µl of RNA wash buffer was added to the column and centrifuged for 2' at 12,000 x rpm to remove traces of ethanol. Purified RNA was eluted by addition of 50µl of DNAse/RNAse free water into the column in a 1.7ml microcentrifuge tube followed by centrifugation at 12,000 x rpm for 1'. The RNA was quantified using the Qubit™ RNA Assay Kit and the Qubit® 2.0 Fluorometer (Life Technologies, Carlsbad, USA).

***Arabidopsis* Lines of Interest**	**Parent Line 1**	**Parent Line 2**
Col-*0*	Col-*0*	
cpr5-2	*cpr5-2*	
akin10	SALK_127939	
fsd1	SALK_036006C	
patl3	SALK_093994C	
patl5	SALK_124448	
crk4	SALK_009503C	
bzip61	SALK_138883	
cpr5-2 akin10	*cpr5-2*	SALK_127939
cpr5-2fsd1	*cpr5-2*	SALK_036006C
cpr5-2 patl3	*cpr5-2*	SALK_093994C
cpr5-2 patl5	*cpr5-2*	SALK_124448
cpr5-2 crk4	*cpr5-2*	SALK_009503C
cpr5-2 bzip61	*cpr5-2*	SALK_138883

Table 2.4: Summary of *Arabidopsis* Plant Lines and Parent Lines

2.6.1.2 DNAse Treatment

For qRT-PCR experiments, genomic-DNA free RNA was prepared using Roche RNase-free recombinant DNase treatment. The total RNA extracted (2-5 µg) as described in section 2.6.1.1, was mixed with 5µl of 10 x incubation buffer supplied with the enzyme and 1µl of DNase (10U), 1µl of Protector RNase inhibitor (10U) before water was added to give a final volume of 48.4µl. The mixture was incubated at 37°C for 20' after which the reaction

was stopped by the addition of 1.6μl of 0.25 M EDTA (pH 8.0) and heating at 75°C for 10'. The final volume was 50μl.

2.6.2 cDNA Synthesis

Synthesis of cDNA was performed using the Transcriptor First Strand cDNA Synthesis kit (Roche).

One μg of total RNA was combined with Oligo (DT)15 primer in a 0.2ml tube and the volume adjusted to 13μl with DEPC-treated water. The RNA solution was denatured at 65°C for 10' in Axygen® MaxyGene™ II thermal cycler (Axygen Inc.) and placed immediately on ice. After cool down, 7μl of the master reaction mixture containing x5 Transcriptor RT Reaction Buffer, protector RNase inhibitor (40U/μl), 10 mM dNTP-Mix and Transcriptor Reverse Transcriptase (20U/μl) were then added. The reaction mixtures were placed back into the thermal cycler and cDNA synthesis was carried out at 55°C for 30'. Subsequently heat inactivation of the reserve transcriptase was carried out at 85°C for 5'.

2.6.3 qRT-PCR Amplification

qRT-PCR was performed using the LightCycler 480 Real-Time PCR (Roche) system and LinReg PCR analysis software. For each cDNA prep (20 x dilution), 3 technical replicates for each reaction were performed. SYBR green I (Roche) was used as a florescent dye. qRT-PCR single reactions included 2.5μl of diluted cDNA, sense and antisense primers (final concentration of 0.5uM per primer), 5μl SYBR Green I Master Mix and sterile DNase and RNase free water up to 10μl (Table 2.5). Three (3) technical replicates of the 10μl reactions were plated on a 96 well plate and quantified using LightCycler 480 Real-Time PCR (Roche) with the following cycling conditions:

Pre-incubation		95°C	10'	
Amplification	Denaturation	95°C	10"	|
	Annealing	60°C	10"	| x40 cycles
	Extension	72°C	10"	|
Melting curve		95°C	5'	
Cooling		4°C		

Three potential housekeeping genes, *At2G31270, AtUBC9, and AtTUB5*, were chosen based on the literature (Table 2.5) (Czechowski, Stitt, Altmann, Udvardi, & Scheible, 2005). Analysis of the relative abundance of housekeeping gene transcripts yielded 2 usable housekeeping genes, *At2G31270 and AtTUB5*, due to their stable expression across all *Arabidopsis* lines tested. The relative abundance of targeted transcript (*AtPR1* and *AtPDF1.2*) was determined by comparative quantification to the geometric mean of the 2 reference genes *AtTUB5 and At2G32170*. Fluorescence measurements were performed at 72°C for each cycle and continuously during the final melting (melting curve).

Gene	Primer	Sequence
At2G32170	At2G32170-F	ATCGAGCTAAGTTTGGAGGATGTAA
	At2G32170-R	TCTCGATCACAAACCCAAAATG
AtUBC9	AtUBC9-F	TCACAATTTCCAAGGTGCTGC
	AtUBC9-R	TCATCTGGGTTTGGATCCGT
AtTUB5	AtTUB5-F	GCGATTGCCTTCAAGGGTTTC
	AtTUB5-R	CGAAGATCCGAGAGGAGTATC
AtPDF1.2	AtPDF1.2-F	CTTGTTCTCTTTGCTGCTTTCGAC
	AtPDF1.2-R	GTGCATTAACCTTGAAGGAGCCAA
AtPR1	AtPR1-F	ACACGTGCAATGGAGTTTGTGG
	AtPR1-R	CAGTGAGACTCGGATGTGCCA

Table 2.5: Primer Sequences used for q-RT-PCR (*A. thaliana*)

2.6.4 qRT-PCR Statistical Analysis

qRT-PCR data was extracted using LC480Conversion-software (http://www.hartfaalcentrum.nl/)

Primer efficiency for each set was determined by using the LinReg PCR software (Ruijter et al., 2009). Statistical analysis for qRT-PCR was performed using Microsoft Office Excel 2010 in accordance to the mathematical pfaffl equation.

$$R = \frac{(E_{target})^{\Delta CPtarget\ (control - sample)}}{(E_{ref})^{\Delta CPref\ (control - sample)}}$$

T-tests performed between data sets were done using a $p<0.05$ as the threshold to determine significance.

2.7 Plant Propagation and Harvesting Methods

Unless stated otherwise, *Arabidopsis thaliana* plants were grown in temperature controlled growth rooms with 16h light 8 hour at 22°C and 65% humidity.

2.7.1 Plant Genetic Crosses

Single mutant SALK lines were obtained from The *Arabidopsis* Information Resource (TAIR) (Appendix 7). *cpr5-2* double mutant plant lines were generated using the pollen from the homozygous SALK mutant plants to fertilize homozygous *cpr5-2* plants. Crosses were performed after cpr5-2 plants have developed 3-4 inflorescences to ensure that flower buds were developed and larger in size as cpr5 inflorescences were generally smaller than WT *Col-0* inflorescences. Successful crosses were determined via PCR based genetic screening of cDNA synthesized from chosen plants to check for heterozygosity of the TDNA insertion.

PCR Reactions containing Promega Master Mix (10µl), PCR-grade H2O (7.5µl), cDNA (1µl), Primer LBb1.3 (0.5µl) and each of gene/cDNA specific LP (0.5µl) and RP (0.5µl) primers were performed:

Pre-incubation		95°C	3’	
Amplification	Denaturation	95°C	30”	|
Annealing		53°C	30”	| x35 cycles
Extension		72°C	2’	|
Cooling		4°C		

All PCR reactions were visualized via agarose gel electrophoresis (section 2.1.3). By using all 3 primers, plants with wild-type genes (no TDNA insertion) yield a product of wild-type gene size only. Plants homozygous for the T-DNA insertion gene yield a PCR product that was the expected size of the T-DNA insert plus the homozygous mutant gene. Plants heterozygous for the T-DNA insertion yields products of both wild-type and homozygous mutant gene, and exhibits 2 bands when visualized via agarose gel (Table 2.6). Plants yielding heterozygous PCR products (F1 generation) were allowed to self-pollinate to produce homozygous double mutants.

Potential homozygous double mutants were detected in the F2 generation based on the smaller phenotype exhibited by *cpr5-2* and cDNA (section 2.6.2) was extracted from the chosen plants. PCR was conducted on cDNA extracted from F2 generation plants.

Plants exhibiting the dwarfed *cpr5-2* phenotype and yielding 1 PCR products specific to the homozygous SALK mutant were allowed to self-pollinate and seeds (F3) harvested were used to perform various assays.

Gene	Primer	Sequence	Wild-type expected size (bp)	Homozygous mutant expected size(bp)
	LBb1.3	ATTTTGCCGATTTCGGAAC		
AKIN10	AKIN10-RP	ACCACACGTTGGAAACTTTTG	1075	578
	AKIN10-LP	ACATGAAGTGCAGATGGGTTC		
FSD1	FSD1-RP	TTGGCATATGGTTTACCCATC	1295	986
	FSD1-LP	GAGGAGTTCATTTGTAACGCC		
PATL3	PATL3-RP	ATGGCTGAAGAACCTACTACT	1787	563
	PATL3-LP	TTAGAGAGGTTTGACATTGAA		
BZIP61	BZIP61-RP	ATGGGATGAGAAACAAACCAG	1093	898
	BZIP61-LP	GCATTGCATTGTCATAAATTCC		
CRK4	CRK4-RP	CTTCGAAGTTCTTCCCAAACC	1009	517
	CRK4-LP	CTTCGAAGTTCTTCCCAAACC		
PATL5	PATL5-RP	ATGTCTCAAGATTCTGCAACT	2398	1802
	PATL5-LP	TTACTCACAAGCTAAAGGCT		

Table 2.6: Primer Sequences for Genotyping of Arabidopsis T-DNA SALK Lines

2.7.2 Plant Dark and Sugar Treatment

Seeds were surface sterilized in 70% ethanol for 1' and washed 3 times with sterile water. Sterile seeds were plated on 100mmx100mmx15mm square plates containing MS media containing either 0/0.5/1/2% sucrose. Plates were sealed with Parafilm, wrapped in foil and imbibed in dark at 4°C for 3 days. Plates were then subjected to 1 hour light treatment to synchronize germination, rewrapped in foil and grown in a climate controlled room at 22°C, 65% humidity for 3 and 5 days. Plants were then transferred to fresh plates under Green safe-light conditions (all wavelengths filtered except for green) to simulate pseudo dark conditions as plants do not have receptors that absorb green wavelength light, which ensures minimal effects on the seedlings by exposure to visible light. Exposure to the visible light spectrum was kept at a minimum, but was used to photograph the plants. Shoot apical hook angles and root and hypocotyl lengths were also measured using ImageJ software (http://imagej.nih.gov/ij/)

2.7.3 Plant Propagation for Morphological Studies

Plant lines were grown under normal short day conditions (12h light/12h dark) at 22°C, 65% humidity for 21 days. Photographs were taken after 21 days.

2.7.4 Plant Drought Tolerance

Plant lines were grown under normal short day conditions (12h light/12h dark) at 22°C, 65% humidity for 30 days. Plants were then fully hydrated with water overnight and subsequently placed into a dry tray the next morning. Observations of drought tolerance were performed 1 week after removal from water.

Chapter 3: Results

3.1 Yeast-Two-Hybrid Identification of Protein-Protein Interactions

3.1.1 Introduction to Yeast Two Hybrid

CPR5 involvement in various plant pathways has remained unclear despite numerous studies involving CPR5 regulation of hormones and other regulatory pathways. A definitive way to determine CPR5 involvement in plant regulatory processes is to determine the proteins with a direct interaction with CPR5, as these proteins would provide much needed insight on the upstream regulation of CPR5 as well as downstream regulation by CPR5. Until recent, no proteins had been identified to directly interact with CPR5, making specific protein-protein interaction assays such as Co-immunoprecipitation difficult. However, a screening assay can be used that allows for the screen of numerous proteins to identify any potential protein partners of CPR5. Direct protein interactions can be identified and studied with the help of methods such as yeast two hybrid and bimolecular fluorescence complementation. These methods provide systems to visualize protein interactions using the interaction of fusion proteins in different host systems as to provide the basis for analysis. The methods, which make protein-protein interactions visible can not only reveal interacting partners, but can provide insight on the localization of such interactions. This is important in the study of proteins like CPR5 as establishing CPR5 localization and interacting would provide greater insight on the complex involvement of CPR5 *in planta*.

The Y2H system is a method for investigating protein-protein interactions using a yeast host system. This system does not depend on high amounts of purified protein or the use of antibodies. The Y2H system is very flexible and can be used to screen individual proteins for interaction or used to screen a large number of proteins to identify potential protein partners using a constructed or commercially available cDNA transcriptome library (Brueckner, Polge, Lentze, Auerbach, & Schlattner, 2009; Huang & Bader, 2009; Koegl & Uetz, 2007; Maier, Maier, & Onder, 2011).

Within the Y2H system there is a “bait” protein and a “prey” protein. The cloning of the “bait” protein coding region downstream of the GAL4-BD gene sequence and “prey”

protein coding gene downstream of the GAL4-AD sequence of the GAL4 transcription factor (TF) results in the translation of 2 fusion proteins (Appendix 2). Generally, the bait protein is the main protein of study and the prey protein is any potential interacting protein, or library of proteins. The Y2H system is based on the reconstitution and activation of a functional GAL4 TF, which allows for the binding of an upstream activating sequence (UAS) and recruitment of RNA polymerase II, leading to the transcription of downstream reporter genes. As the GAL4-BD is responsible for binding the UAS, and the Gal4-AD is responsible for the activation of transcription, both components are required for activation of any downstream gene targets. When an interaction occurs between a prey and bait protein, the proximal interaction that occurs between the Gal4-AD and Gal4-BD will provide enough of a connection between the two domains to activate the transcription of the downstream gene targets, as shown in figure 3.1A. In the current Y2H system, more than one reporter gene is used to increase the stringency of the protein screens, as the activation of more than reporter genes requires a more stable transcriptional activation as is the result of a stable bait and prey protein interaction. Yeast strain AH109, which contains 3 independent reporter genes, *HIS3, ADE2, and MEL1/lacZ.* Activation of transcription of *HIS3* and *ADE2* allows the yeast to grow on minimal media and allows for selection of yeast based on the capability of yeast to survive on highly stringent media. Activation of the *MEL1/lacZ* gene provides a colorimetric reaction when yeast is grown on media treated with X-α-galactosidase, resulting in blue yeast colonies (Figure 3.1A). Together, the Y2H library screening system was expected to provide potential protein partners of CPR5, and the more direct Y2H protein pair assays was expected to provide insight on reliability of the library screening in identifying true CPR5 protein partners (Clontech Laboratories, 2009, 2013, 2015).

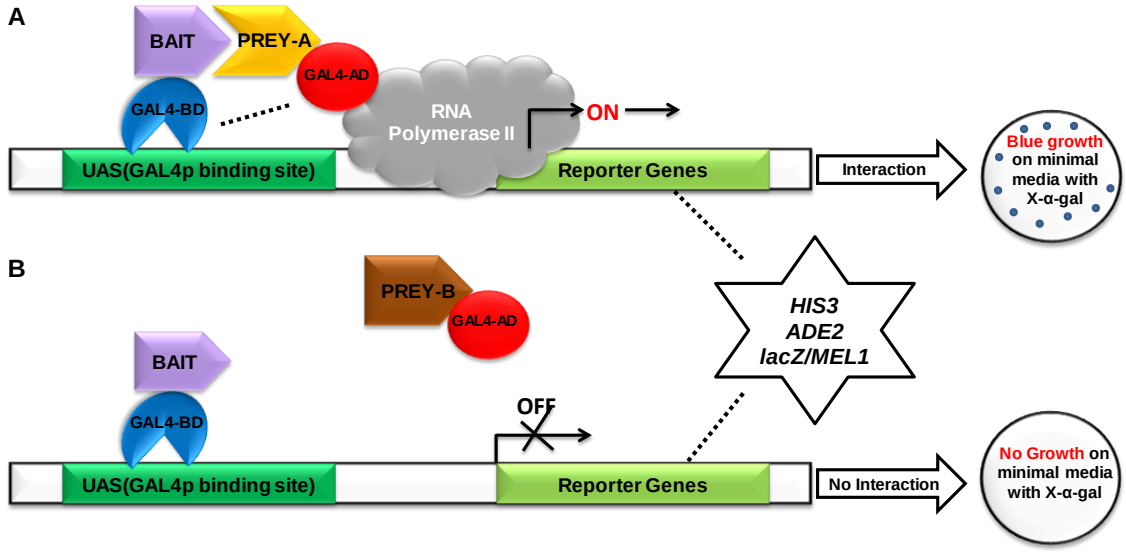

Figure 3.1: The Theory of Y2H assay.
The N-terminus of the protein of interest (bait) is fused to the C terminus of the GAL4-BD. The N-terminus of the proteins to be tested for interaction (Prey) is fused to the C-terminus of the GAL4-AD. **A)** The Bait and Prey-A proteins were interacting proteins so the GAL4-BD and GAL4-AD come into close enough proximity to activate the GAL4 transcription factor allowing for the recruitment of RNA Polymerase II to activate the expression of reporter genes *HIS3, ADE2, and lacZ/MEL1*. **B)** Prey-B is not an interacting partner of the bait protein and does not allow for the proximal activation of the GAL4 protein so no expression of reporter genes, *HIS3, ADE2* and *lacZ.MEL1* are expressed. (Figure modified from Clontech Laboratories, 2013)

3.1.2 Cloning of CPR5 into Y2H GAL4-BD Vector

Due to the putative transmembrane domain regions annotated in the CPR5 protein sequence, truncated forms of the CPR5 protein were used for the Y2H experiment. As the number of transmembrane domains within CPR5 has only been predicted using *in silico* analysis (Gao, et al., 2011; Daniel Perazza, et al., 2011; Yoshida, et al., 2002), two truncated forms of CPR5 were chosen for the Y2H experiment (Section 2.4.1). Some programs predict the presence of 4 transmembrane, while others predict the presence of 5 transmembrane regions. The 1st truncation chosen, CPR5TM0, excises the1st ambiguous transmembrane region as well as the 4 commonly predicted terminal transmembrane regions. The second truncation, CPR5TM1, excises only the 4 terminal transmembrane regions (Figure 2.2, Appendix 1).

Truncated forms of *CPR5* cDNA were cloned in frame into Y2H plasmid pGBKT7 that includes an upstream sequence encoding the GAL4-BD protein domain (Appendix 2A). Cloning was performed such that the GAL4 protein domain was fused to the N-terminus of the CPR5 proteins when expressed in yeast (Figure 2.2). The coding region of the truncated CPR5 genes were inserted into pGBKT7 plasmids through the use of 5' to 3'

restriction sites introduced by standard PCR and subsequent restriction digestion and ligation procedures (section 2.2). Successful subcloning was confirmed first by restriction digestion of the isolated plasmids and by diagnostic colony PCR amplification. Sequencing of the constructs confirmed that no altered sequence amplification during PCR amplification occurred and that the constructs were properly constructed at the correct *CPR5* truncation points.

3.1.3 Expression of GAL4-BD Fusion Proteins

Before testing of CPR5 in Y2H protein pair assays for protein-protein interactions, test assays were performed to determine whether the CPR5 truncation constructs were expressing the fusion proteins necessary for proper interaction.

In order to determine the expression of the fusion proteins, the empty pGBKT7 plasmid and pGBKT7-53 positive control plasmid, CPR5TM0, CPR5TM1 were independently transformed into yeast strain AH109. Yeast protein was crudely extracted and subjected to Western Blot Analysis probing with antibodies to the c-Myc epitope tag present in the pGBKT7 vector. Yeast lacking in any introduced GAL4-containing plasmids (AH109) were used as a negative control.

Fusion protein was expressed in yeast host AH109 and crudely extracted. The theoretical size of the fusion proteins was determined to be 57kD (BD-CPR5TM0) and 66kD (BD-CPR5TM1) (Figure 3.2A) (http://web.expasy.org/protparam/). Purified yeast protein fractionated on a 10% 1D-SDS-PAGE yielded a major band of ca. 57kDa and 66kDa respectively when probed with c-Myc monoclonal antibodies (Figure 3.2B, C). The empty pGBKT7 vector yielded a major band at of ca.21.7kDA consistent with the translation of a GAL4-BD::c-Myc fusion protein lacking any inserted protein (Figure 3.2A, B). This 21kDa protein represents GAL4-BD::c-Myc N-terminal region of the CPR5TM1, CPRTM0, p53 fusion proteins expressed.

The presences of observable stained bands at positions that correlate to the bands of the protein ladder indicate that proteins of similar size were found in the yeast protein extract (Figure 3.2). These bands confirm that BD-CPR5TM0 and BD-CPR5TM1 are being expressed and are nontoxic to the yeast host, as no difference in yeast growth was observed between BD-CPR5TM0, BD-CPR5TM1, and controls BD-p53, and pGBKT7 empty vector (data not shown).

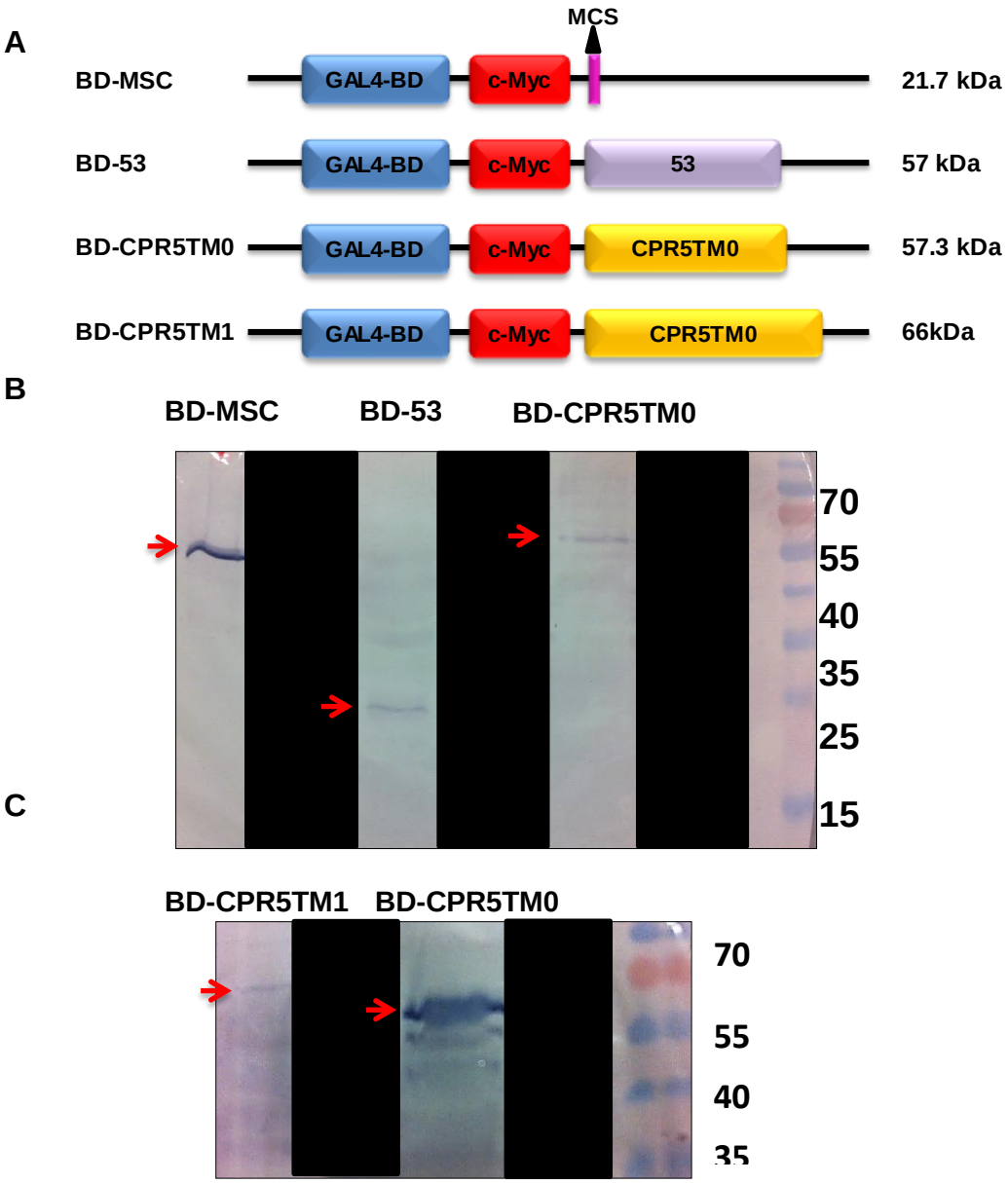

Figure 3.2: Western Blot Analysis of BD-CPR5TM0 and BD-CPR5TM1
Yeast containing 4 BD-plasmid constructs was probed with c-Myc antibodies to determine the expression and proper translation of the fusion proteins. **A)** The coding regions translated for each construct are shown and the total size of the fusion proteins translated is noted. BD-MCS contains no coding region insert but does translate the MCS with the GAL BD and the c-Myc tag. SDS PAGE gel and western blot analysis showing positive expression GAL4-BD::c-Myc fusion proteins **B, C)** BD-CPR5TM0 **C)** and BD-CPR5TM1 recognized by antibodies raised again c-Myc. **B)** Positive control BD-53 plasmid and BD-MCS empty vector were used as positive controls and yielded expression of fusion proteins at the indicated sizes. Protein ladder and sizes (kDa) are indicated on the right side of each Western blot.

3.1.4 Establishment of Protein Pair Y2H Mating Assays

Confirmation of the expression of the BD-CPR5TM0 and CPR5TM1 fusion proteins provides viable constructs to be used in Y2H assays. However, before utilizing the constructs in interaction assays, test assays were performed to determine whether the Y2H system was working, and if any auto-activation GAL4-mediated transcription was occurring using these constructs. Initially, the internal positive control plasmids pGBKT7-53 and pGADT7-T (BD-53 and AD-T) of the Matchmaker GAL4 Two-Hybrid System (Clontech Laboratories, USA) were transformed into yeast strain AH109 and Y187, mated, and tested for growth on yeast plates with different selection stringencies (section 2.4). Three different auxotrophy plates were used to test for the strength of the reporter gene activation. The first plate lacking in leucine (-Leu) and tryptophan (-Trp) (SD/-Trp/-Leu) selected for the presence of the GAL4-BD and GAL4-AD plasmids only. Selective agar plates lacking in leucine, tryptophan and histidine (SD/-Trp/-Leu/-His) were used to select for moderate reporter gene activation (medium stringency). Selective plates lacking in Trp, Leu, His and adenine (-Ade) were used to select for strong reporter activation (SD/-Trp/-Leu/-His/-Ade) (high stringency).

Mated yeast containing both control plasmids (pGBKT7-53 and pGADT7-T) exhibited robust growth when plated on all 3 plate stringencies indicating that positive interaction can be observed using the Y2H system. In contrast, the negative control assays including only one positive control vector (BD-53 or AD-T) and one negative control empty vector pGADT7/pGBKT7 (GAL4-AD or GAL4-BD) exhibited growth only on low stringency plates (SD/-Trp/-Leu) indicating that no interaction is occurring between the fusion proteins being expressed by each plasmid. The negative control assays including control vectors (GAL4-AD and GAL4-BD) yielded growth only on the SD/-Trp/-Leu plates indicative of the presence of the GAL4-BD and GAL4-AD plasmids, but no interaction between the recombinant proteins encoded by the two plasmid. The interaction of a protein containing GAL4 domain plasmid (pGBKT7-p53, pGBKT7-CPR5TM0, pGBKT7-CPR5TM1, pGADT7-T) with an empty vector (pGBKT7, pGADT7) containing the second GAL4 domain was unable to auto-activate the expression of GAL4-mediated gene expression indicating that the Y2H system is working properly. Additionally, no interaction was observed in yeast transformed with 2 empty vectors (pGBKT7, pGADT7). All positive and negative controls yielded yeast growth on the appropriate auxotrophic media indicating that the Y2H system is working correctly, and that the CPR5 constructs are viable for Y2H assays.

3.1.5 Identification of Novel CPR5 Proteins Interactions

Two Y2H library screenings were performed using BD-CPR5TM0/BD-CPR5TM1 and a normalized universal *Arabidopsis* transcriptomic library (Clontech Laboratories, USA) respectively. BD-CPR5TM0 yeast was grown and mated with an aliquot containing a normalized *Arabidopsis thaliana* transcriptome plated on SD/-His/-Trp/-Leu media and yielded thousands of colonies. Colonies that grew up to 2mm were deemed to be potential interactants and were streaked onto new SD/-His/-Trp/-Leu plates in order to confirm their growth and were incubated for 5 days at 30°C. Once grown, the positively growing colonies were streaked onto SD/-His/-Trp/-Leu/-Ade plates in order to test for interaction. A total of 1623 clones were isolated and screened over 3 successive generations to segregate individual colonies and to confirm stable yeast lines. Further screening of these clones yielded 390 yeast lines (Figure 3.3) able to grow on high stringency media (SD/-His/-Trp/-Leu/-Ade). A total of 697 colonies were isolated from the Y2H library screening with BD-CPR5TM1 and 48 were identified to grow on high stringency media, SD/-His/-Trp/-Leu/-Ade and SD/-His/-Trp/-Leu/-Ade/X-α-gal.

Despite using a normalized library in the Y2H screening, positive yeast clones can contain plasmids with identical copies of the same gene coding region. Yeast colony PCR followed by digestion with a high frequency cutter restriction enzyme and visualization via agarose gel electrophoresis yielded several duplicate band patterns indicative of multiple identification of the same interaction. A total of 82 clones were identified to have unique gel digestion patterns, 47 associated with BD-CPR5TM0 and 35 associated with BD-CPR5TM1. Despite choosing unique digestion patterns from the hundreds of clones, several genes were identified from multiple cloned sequenced from each screening. Of the 82 clones sequenced, sequences aligning to genes *MYB3, PATL3, DNAJ* and *CRK4* were identified from the sequenced coding regions of several different clones (table 3.1). Sequencing, BLAST analysis and sequence analysis of the 82 clones yielded ten genes of interest that were in frame with the GAL4-AD. Five genes, *AKIN10, FSD1, MYB3, PATL3*, and *BZIP61* were identified from the coding region of the AD-plasmid constructs found to interact with CPR5TM0. 4 genes, *DNAJ, SAC9, PATL5,* and *PATL6* were identified from the coding region of the AD-plasmid constructs to interact with CPR5TM1. *CRK4* was identified from the coding region of constructs found in both Y2H library screenings.

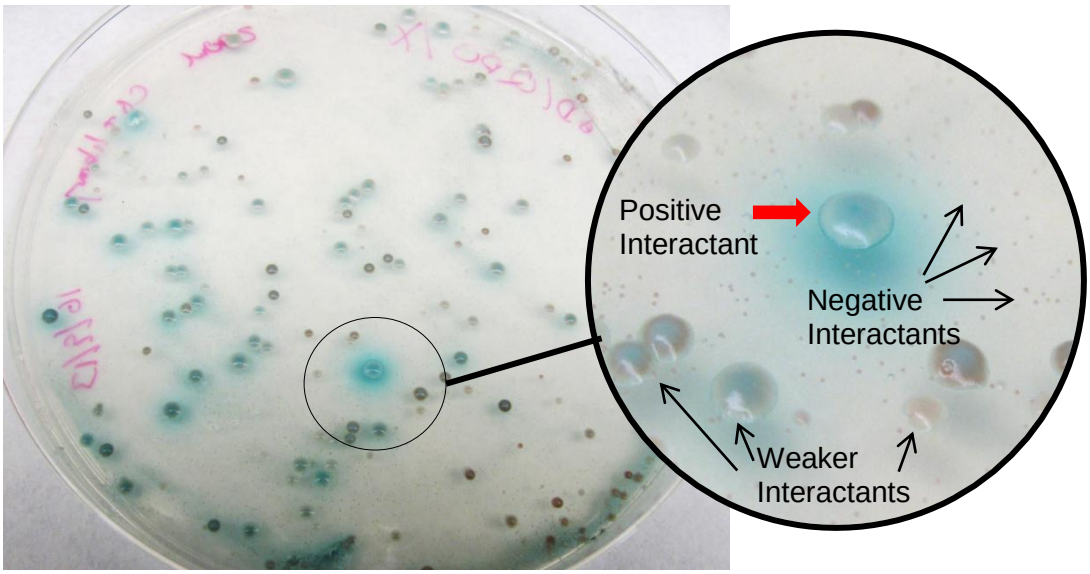

Figure 3.3: Representative Plate of Yeast Grown on SD/-His/-Trp/-Leu/-Ade/X-A-Gal and Subsequent Screening Plate.
Yeast exhibiting robust growth (~3mm) and a clear blue color and lacking any red hue a representative of a "strong" positive interactants. Yeast exhibiting smaller yet noticeable growth (1-2mm) or a red hue are representative of weaker interactants to be tested further. Small red colonies (<1mm) are representative of negative interactants. Yeast colonies identified as strong and weaker interactants were screened over 4 successive generations.

			CDS Consensus Alignment			
Gene	**Screen**	**CDS Size (nt)**	**Start(nt)**	**End (nt)**	**Total Size**	**Protein Region**
AKIN10	TM0	1608	1249	1608	359	N-terminal
FSD1	TM0	639	0	639	639	Whole Protein
MYB3	TM0 (x2)	774	127	774	647	N-terminal
PATL3	TM0	1473	838	1473	635	N-terminal
			844	1473	629	N-terminal
BZIP61	TM0	990	73	990	917	N-terminal
CRK4	TM0 (x2) TM1	1785	1078	1785	707	N-terminal
DNAJ	TM1	1329	769	1329	560	N-terminal
			703	1329	626	N-terminal
			772	1329	557	N-terminal
SAC9	TM1	4944	4255	4944	689	N-terminal
PATL5	TM1	2007	1417	2007	590	N-terminal
PATL6	TM1	1230	781	1230	449	N-terminal
Average Size of Library AD-Plasmid Coding Region					615.6	

Table 3.1: Genes Identified in CPR5TM0/CPR5TM1 Y2H Library Screenings.
The Y2H screen that yielded the plasmid containing specific gene coding region is listed and the number of duplicate identifications of the same constructs is also noted in parenthesis. Sequence alignment of the coding regions obtained from the Y2H commercial library plasmids identified the consensus alignment of gene coding regions. The total CDS sizes of each gene identified as well as the total size of the gene coding region obtained from each AD-plasmid is listed. The start nt and end nt of the consensus coding region obtained from each sequenced construct is listed and the total size of the coding regions is listed. The average size of the coding regions obtained from the library plasmids is noted at the bottom. As constructs containing different sized coding regions for *PATL3*, and *DNAJ* were identified, the different coding regions identified are listed.

As two Y2H library screenings were performed, and different potential interacting proteins were found in each screening, it was necessary to determine if the proteins identified were able to interact with only one of the two CPR5 constructs. To determine whether the interaction was isolated to one truncation, the plasmids containing the identified gene coding regions were purified and subjected to protein pair Y2H assays with both truncated CPR5 constructs. Interaction was determined by growth selection on high stringency SD/-His/-Trp/-Leu/-Ade and SD/-His/-Trp/-Leu/-Ade/X-α-gal plates. CPR5TM0 exhibited growth indicative of interaction when transformed with 9 out of 10 of the constructs, and showed poor interaction with the CRK4 containing construct (Figure 3.4A). CPR5TM1 interacted with 9 out of 10 identified genes containing protein constructs and did not yield any growth when transformed with BZIP61 (Figure 3.4B). All interactions yielded blue growth on SD/-His/-Trp/-Leu/-Ade/X-α-gal plates indicating that activation of the *lacZ/MEL1* gene was occurring, a marker for strong interactions (Figure 3.4A, B).

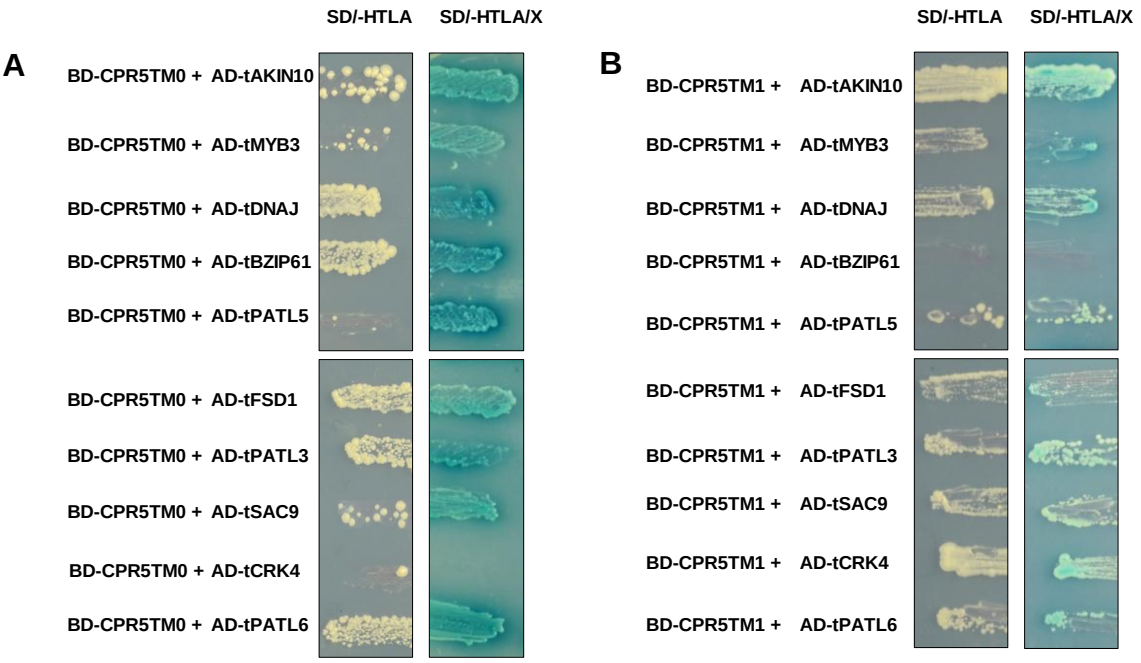

Figure 3.4: Protein Pair Y2H Transformation Assays of Constructs Rescued from Y2H Screening

Plasmids isolated from yeast of positive interactants identified in the 2 Y2H screens with **A)** CPR5TM0 **B)** CPR5TM1 with AD-tAKIN10, AD-tFSD1, AD-tMYB3, AD-tPATL3, AD-tDNAJ, AD-tBZIP61, AD-tCRK4, AD-tPATL5, AD-tPATL6, AD-tKPR2, AD-tSIM, AD-tSMR1), were transformed into AH109 yeast strain containing CPR5TM0 and CPR5TM1 respectively and tested from interaction on SD/-HTLA and SD/-HTLA/X-α-gal media.

3.1.6 Examination of Physical Interactions Of CPR5TM0/CPR5TM1

The commercial Y2H normalized transcriptome does not include all full length cDNA genes; rather the transcriptome contains cDNA that was size (1.0-2.4kb) selected prior to cloning into the GAL4-AD plasmid. Sequence analysis of the constructs identified in the Y2H library screenings confirms this size selection as only one of the identified coding regions (*FSD1*) translated a full length protein. The coding regions of all other sequenced constructs included partial cDNA coding regions.

To further investigate whether the genes of interest code for interacting protein partners of CPR5, full length coding sequences were cloned into the multiple cloning site of GAL4-AD containing vector pGADT7, and subsequently transformed into AH109 yeast containing one of 3 Gal4-BD constructs (BD-CPR5TM0, BD-CPR5TM1, or negative control BD-53) (Appendix 3). Additionally, as CPR5 has been shown to interact with SIM, SMR1 and KRP2 (S. Wang, et al., 2014), the full length coding regions of these 3 proteins was also cloned into pGADT7 and transformed with each of the 3 GAL4-BD plasmid containing yeast. No construct was created for the full length *SAC9* coding region due to the inability of amplifying the full coding region of *SAC9* without mutations. Twelve protein pair Y2H assays was performed with each GAL4-BD construct, giving a total of 36 interactions tested for growth. All transformations yielded growth on low stringency media SD/-Trp/-Leu indicating that successful transformation of yeast occurred, and that all yeast contained both a GAL4-BD and GAL4-AD plasmid. Three independent colonies from each transformation were streaked onto medium stringency media SD/-His/-Trp/-Leu. Yeast containing either CPR5TM0 or CPR5TM1 and AKIN10, MYB3 or BZIP61 constructs yielded robust growth on SD/-His/-Trp/-Leu (Figure 3.5). All other transformed yeast yielded little growth on SD/-His/-Trp/-Leu indicative of a weaker interaction or no interaction occurring between two fusion proteins. Yeast from SD/-His/-Trp/-Leu plates were restreaked onto high stringency media SD/-His/-Trp/-Leu/-Ade and SD/-His/-Trp/-Leu/-Ade/X-α-gal to test for strong interaction between the two fusion proteins in the yeast transformants. Under high stringency conditions, Full length MYB3 was able to interact with both CPR5TM0 and CPR5TM1 (Figure 3.6A, B), full length BZIP61 was found to interact with only CPR5TM0 (Figure 3.6A) and full length CRK4 was found only to interact with CPR5TM1 (Figure 3.6B) under high stringency conditions.

In addition, CPR5TM0 was found to interact with the control full length SIM fusion protein under high stringency conditions, but did not yield a strong blue color indicative of activation of the highly stringent *lacZ* gene.

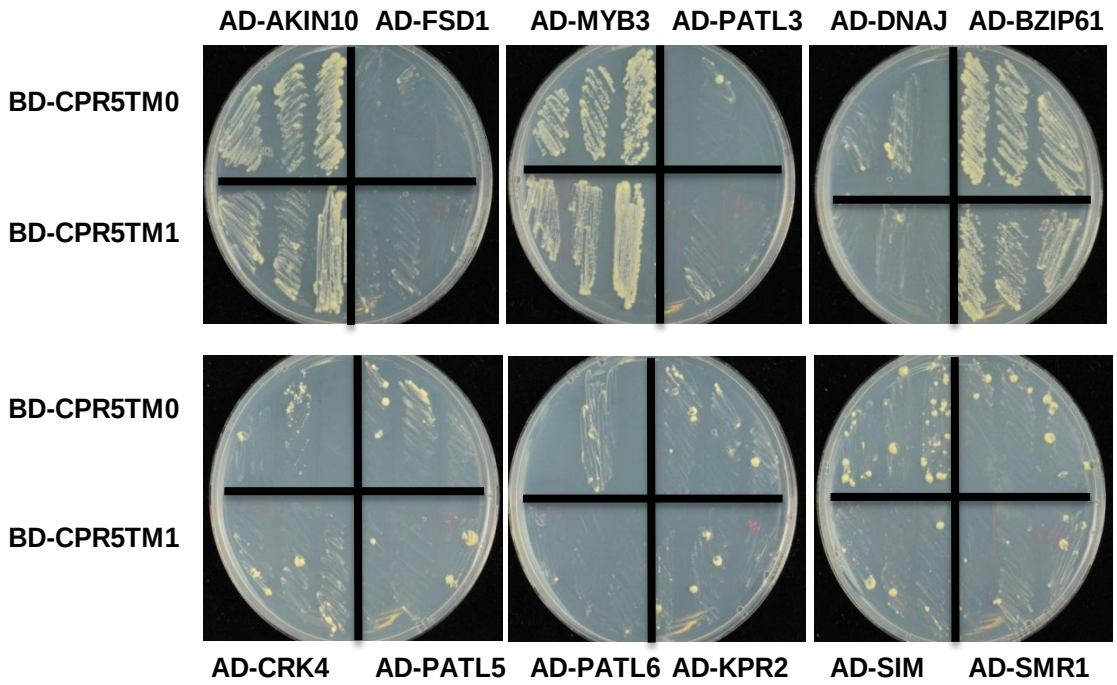

Figure 3.5: Protein Pair Y2H Transformation Assay on Medium Stringency Media
Protein pair Y2H transformation assays between BD-CPR5TM0/BDCPR5TM1 and GAL4-AD full length gene constructs (AD-AKIN10, AD-FSD1, AD-MYB3, AD-PATL3, AD-DNAJ, AD-BZIP61, AD-CRK4, AD-PATL5, AD-PATL6, AD-KPR2, AD-SIM, AD-SMR1), 3 individual colonies per mating assay were plated on medium stringency (SD/-His/-Trp/-Leu) media. Both CPR5TM0 and CPR5TM1 interact with AKIN10, MYB3, and BZIP61. All other interactions appear to be weak indicated by minimal growth of yeast.

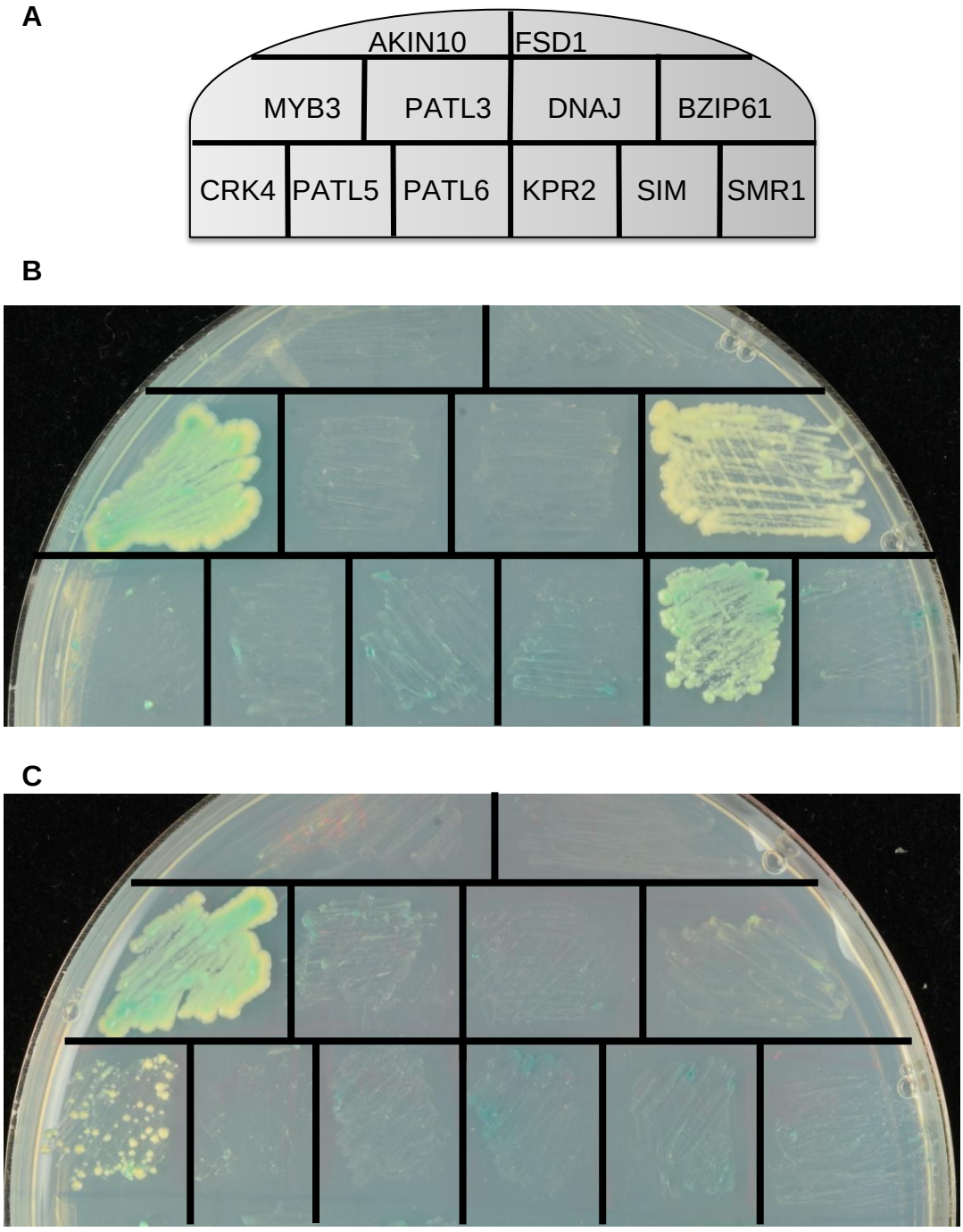

Figure 3.6: Protein Pair Y2H Transformation Assay on High Stringency Media.
A) Representative plate listing the names of protein tested with CPR5TM0 and CPR5TM1 Protein pair Y2H transformation assays between **B)** BD-CPR5TM0 and **C)** BDCPR5TM1 with GAL4-AD full length gene constructs AD-AKIN10, AD-FSD1, AD-MYB3, AD-PATL3, AD-DNAJ, AD-BZIP61, AD-CRK4, AD-PATL5, AD-PATL6, AD-KPR2, AD-SIM, and AD-SMR1 plated on high stringency media (SD/-His/-Trp/-Leu/-Ade/X-α-gal. Yeast growth was observed when **B)** Yeast growth was observed when CPR5TM0 containing yeast (AH109) was transformed with plasmids containing full length MYB3, BZIP61 and SIM. **C)** Yeast growth was observed when CPR5TM1 containing yeast was transformed with plasmids containing full length MYB3 and CRK4.

3.1.7 Summary of Y2H Results

The two independent Y2H screens identified a total the proteins of interest from 82 sequenced clones. Of those ten clones, nine of the protein region containing plasmid was found to interact with both construct, and only tBZIP61 was not found to interact with CPR5TM0. However, CRK4 interaction with CPR5TM0 was not observed when the plasmid was rescued despite finding CRK4 in the CPR5TM0 screen. Protein pair Y2H assays using full length proteins of interest identified under medium stringency media, interaction with AKIN10, MYB3, and BZIP61 with both CPR5TM0 and CPR5TM1. Under high stringency conditions (SD/-HTLA), MYB3 observed to be able to interact with both CPR5TM0 and CPR5TM1. CPR5TM0 was also found to interact with BZIP61 and SIM, the previously published CPR5 interactants (S. Wang, et al., 2014) (Figure 3.7). CPR5TM1 was only found to interact with one protein besides CRK4. It is evident from the results that the full length proteins interact differently than the truncated proteins obtained from the initial Y2H library screenings.

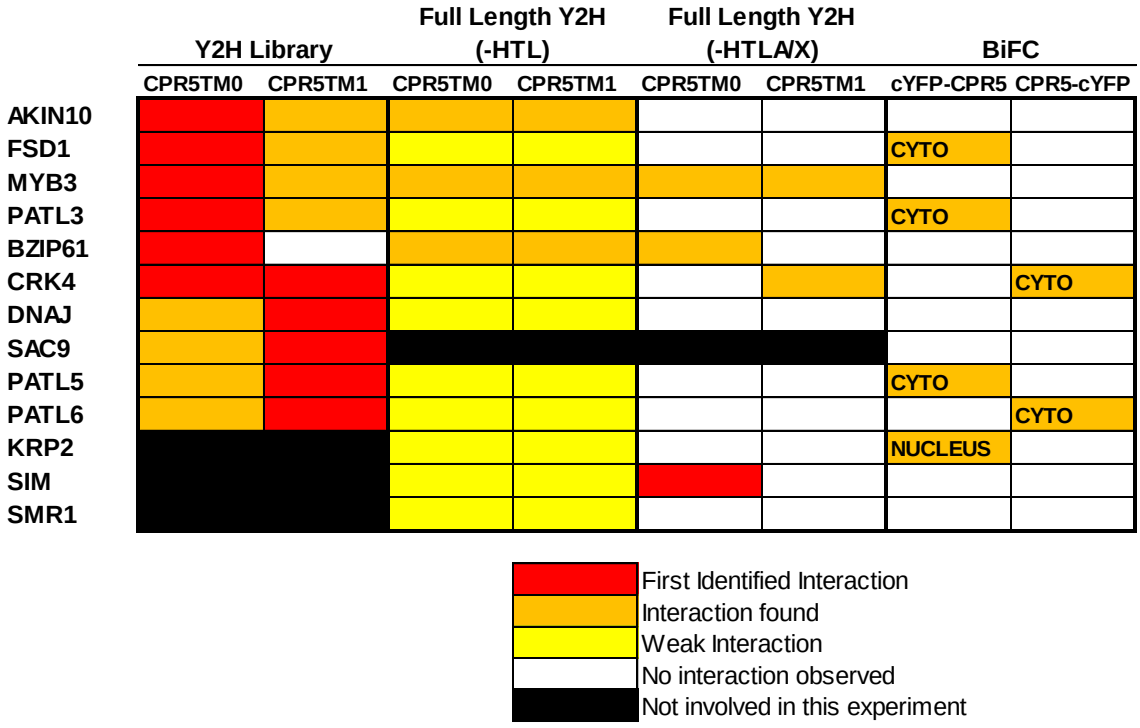

Figure 3.7: Heat Map Summary of Interactions Identified via Y2H and BiFC.
Red indicates the CPR5 construct the protein interaction was first identified. Orange denotes that an interaction was found. Yellow indicates either weak interaction as measured by little to no yeast grown observed on medium stringency media SD/-His/-Trp/-Leu (SD/-HTL). White and black denote no interaction observed or protein not involved in the experiment. The localization of interaction via BiFC is indicated where appropriate (NUCLEUS=nuclear localization, CYTO=cytoplasmic).

3.2 BiFC Assay

3.2.1 Introduction to Bimolecular Fluorescence Complementation

Bimolecular Fluorescence Complementation (BiFC) is a fairly recent method for the direct visualization of protein-protein interactions in a variety of living host (Walter et al., 2004). BiFC is based on the reconstitution of a fluorescent protein function when two non-fluorescent non complementary fragments of a fluorescent protein are brought together by a pair of interacting proteins (Figure 3.8A). Studies have shown that when the YFP fluorescent protein can be split at specific sites within a β-strand or be split at a loop; that the resulting two fragments of protein are (C. D. Hu, Chinenov, & Kerppola, 2002) capable of functioning as one functional fluorescing protein when brought into close enough proximity, similar to the two halves of the GAL4 domain in the Y2H system. The BiFC utilizes a two fusion protein system where in a protein of interest is fused to either the N-terminal or the C-terminal half of a fluorescent protein, and the second protein of interest is fused to the other half of the fluorescent protein(C.-D. Hu, Grinberg, & Kerppola, 2006). The reconstitution of the fluorescent protein function allows for the imaging of the fluorescence emitted. Fluorescent proteins cannot be seen under visible light, and require excitation by specific wavelengths of light to be visualized using confocal microscopy (Figure 3.8).

Functional fluorescing proteins are able to absorb a photon of higher energy and emit a photon with a lower energy longer wavelength that can be measured using a confocal microscope(Kerppola, 2006). A variety of fluorescence protein are compatible with BiFC, including the enhanced yellow fluorescence protein (YFP) is used, but other fluorescence proteins have also been used in studies, including the green fluorescent protein (GFP), and blue fluorescent protein (BFP)(Weinthal & Tzfira, 2009).

For the purposes of this study, Enhanced YFP (YFP) was used. The two nonfluorescent protein fragments, the C-terminal half of YFP (cYFP) and the N-terminal half of YFP (nYFP), are fused to two putative interacting partners. If interaction occurs between the two putative protein partners, the positive interaction can result in the proximal reconstitution of the YFP fluorescent protein and will emit an observable yellowish-green fluorescence (Figure 3.8A). If no interaction occurs between 2 proteins, no fluorescence should be observed as no reconstitution of the fluorescent signal can occur without a proximal interaction to bring the YFP halves together (Figure 3.8C).

There are several locations where a fluorescent protein can be split. For YFP, there are two places that the YFP can be split according to previously published data. The first location is at amino acid 155. The second location is between amino acid 173 and 174(C.-D. Hu, et al., 2006; Kerppola, 2006). For this study, YFP was split between amino acids 155 and 156(Appendix 4).

BiFC is a relatively simple method of investigating protein-protein interactions and provides a platform that can be used to study protein-protein interactions in a more native host model. The system has been reported to be very sensitive in the detection of low expressing protein-protein interactions (C.-D. Hu, et al., 2006; Kerppola, 2006; Walter, et al., 2004). BiFC allows for the use of a plant host to test for protein-protein interactions, thereby providing a host system that is similar to the native Arabidopsis host. The use of a similar host organism greatly improves the chances of proper protein translation, folding, and subsequent interactions.

In order to provide a more accurate model for CPR5 interaction assays, a *Nicotiana benthamiana* plant model was chosen for transient infiltration of *Agrobacterium* and subsequent bimolecular fluorescence complementation.

If CPR5 interaction with the identified proteins orients the two YFP fragments at opposite ends of the protein complex, the YFP halves will not be in close enough proximity to reconstitute YFP function (Figure 3.8B). In order to ensure that the fusion proteins allow for the fragments of YFP to associate with each other when a protein of interest interacts with CPR5, several different constructs of CPR5 were produced to account for the orientation of potential protein interactions. The N-terminal YFP segment was tagged to the N-terminal of all genes of interest and the C-terminal YFP segment was tagged to both N-terminal and the C-terminal of CPR5 (cYFP-CPR5/ CPR5-cYFP). By fusing the cYFP segment of the YFP protein to both the C-terminal and the N-terminal of CPR5 respectively, we account for the possibility that the N-terminal region of the proteins of interest interaction will be in close proximity to either the C-terminal or N-terminal region of CPR5.

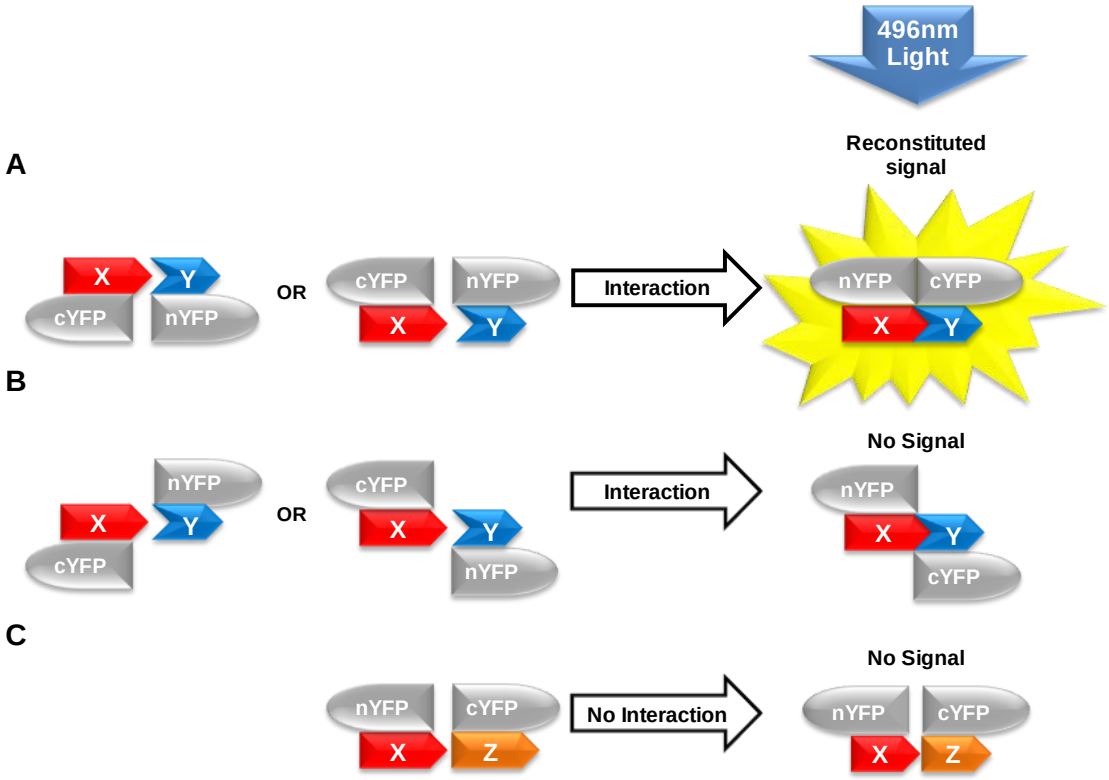

Figure 3.8: The Theory of BiFC assay.
Functional YFP fluorescent proteins are able to emit fluorescence when excited with 496nm wavelength light (argon). A) Proteins that are able to interact (X and Y) with the cYFP and nYFP tags fused to the proper protein terminals provide the close enough proximity for the YFP fragments to reconstitute function and emit a fluorescent signal. B) Interacting proteins with cYFP and nYFP fused to nonproximal terminals do not provide the proximity required for reconstitution of signal despite interaction between X and Y. C) Proteins that do not interaction (X and Z) are unable to provide the proximity required to reconstitute signal. The precise structures and flexibilities specific to each protein must be taken into account in order to determine the most viable terminal region for YFP fusion. (Figure was modified from Weinthal & Tzfira, 2009)

3.2.2 Examination of Physical Protein Interactions via BiFC

Confocal microscopy of *Nicotiana benthamiana* leaves infiltrated with both an N-terminal YFP fusion protein-encoding plasmid, and C-terminal YFP fusion protein-encoding plasmid was used to determine the interaction between CPR5 and the proteins identified in the Y2H screening. Full length coding regions of each protein were used for cloning.

To confirm that the BiFC assay works efficiently and properly, EDS1 from *Arabidopsis thaliana* was used as a control gene to optimize the BiFC assay. The interaction of the positive control (EDS1+EDS1) in this experiment has been confirmed by many studies

(Feys, Moisan, Newman, & Parker, 2001). EDS1 interaction with itself is known to occur within the nucleus as well as the cytoplasm. Prior to the use of the YFP nonfluorescent halves in BiFC analysis, visible YFP fluorescence was confirmed as well as EDS1 localization. EDS1 fused to full length YFP was transiently transformed to Nicotiana and fluorescence was observed confirming YFP fluorescence can be observed in the cytoplasm and the nucleus (Figure 3.9). Additionally, as a positive control for BiFC interaction, nYFP-EDS1 and cYFP-EDS1 (Figure 3.10B) or EDS1-cYFP (Figure 3.11B) were transiently transformed into Nicotiana and fluorescence was observed, however little interaction was observed within the nucleus as compared to full length YFP-EDS1 which exhibits bright fluorescence in the nucleus (Figure 3.9, 10B). The nuclear fluorescence caused by the interaction of EDS1 within the nucleus may not have been within an observable threshold (Figure 3.9) (Feys, et al., 2001).

To further confirm the system, the following negative controls were tested. Agrobacterium containing plasmids coding for nYFP-EDS1+cYFP-CPR5 (Figure 3.10A), nYFP-EDS1+CPR5-cYFP (Figure 3.11A), cYFP-CPR5+nYFP, cYFP+nYFP-EDS1, cYFP-EDS1+nYFP, and EDS1-cYFP+nYFP (data not shown) was transiently transformed into *Nicotiana benthamiana* and no detectable YFP fluorescence was detected indicating that the YFP protein was not reconstructed because no interactions were occurring between any of the proteins and protein fragments.

To study protein-protein interactions of CPR5, *Agrobacterium* containing plasmids coding for CPR5 and one of the 10 genes of interest, or one of the published control genes (SIM, SMR1 and KRP2) were infiltrated into tobacco *N. benthamiana*. Nine of ten of the proteins of interest, SIM, SMR1 and KRP2 were tested with both cYFP-CPR5 and CPR5-cYFP. SAC9 was not assayed due to the inability to obtain the SAC9 coding sequence without mutation. As no confirmed positive control has been extensively tested and proven for CPR5, no known CPR5 true positive control could be used, however any interaction with SIM, SMR1 and KRP2 will be considered confirmation of their published interaction with CPR5.

YFP signal was observed between N-terminal tagged, C-terminal YFP-CPR5 (cYFP-CPR5) and PATL3, PATL5, and FSD1 in the cytoplasm (Figure 3.10C, D, and E). The fluorescence suggests that CPR5 interacts with PATL3, PATL5, and FSD1 outside of the nuclear envelope. YFP signal was also observed between cYFP-CPR5 and KRP2 in the nucleus (Figure 3.10F), suggesting that interaction of the two proteins occurs in the nucleus as observed by Wang et al, (2014).

YFP signal was also observed between C-terminal tagged, C-terminal YFP-CPR5 (CPR5-cYFP) and N-terminally tagged, N-terminal YFP-CRK4 (nYFP-CRK4) (Figure 3.11B) and PATL6 (nYFP-PATL6) (Figure 3.11C) respectively, in the cell periphery or cytoplasm.

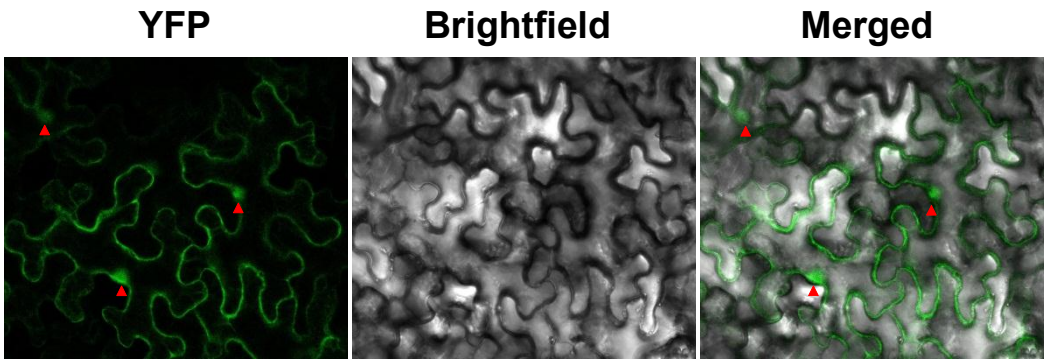

Figure 3.9: EDS1-YFP Fluorescence in the cytoplasm and nucleus.
EDS1-YFP was transiently transformed into Nicotiana leaves, and was visualized using a confocal microscope 3 days after transformation. YFP is positively visualized at 501-600nm. EDS1-YFP fluorescence is positively observed in the nucleus and cytoplasm. EYFP was visualized at 501-600nm. Bright field was visualized was taken simultaneously using 496nm. Nuclei are noted in red.

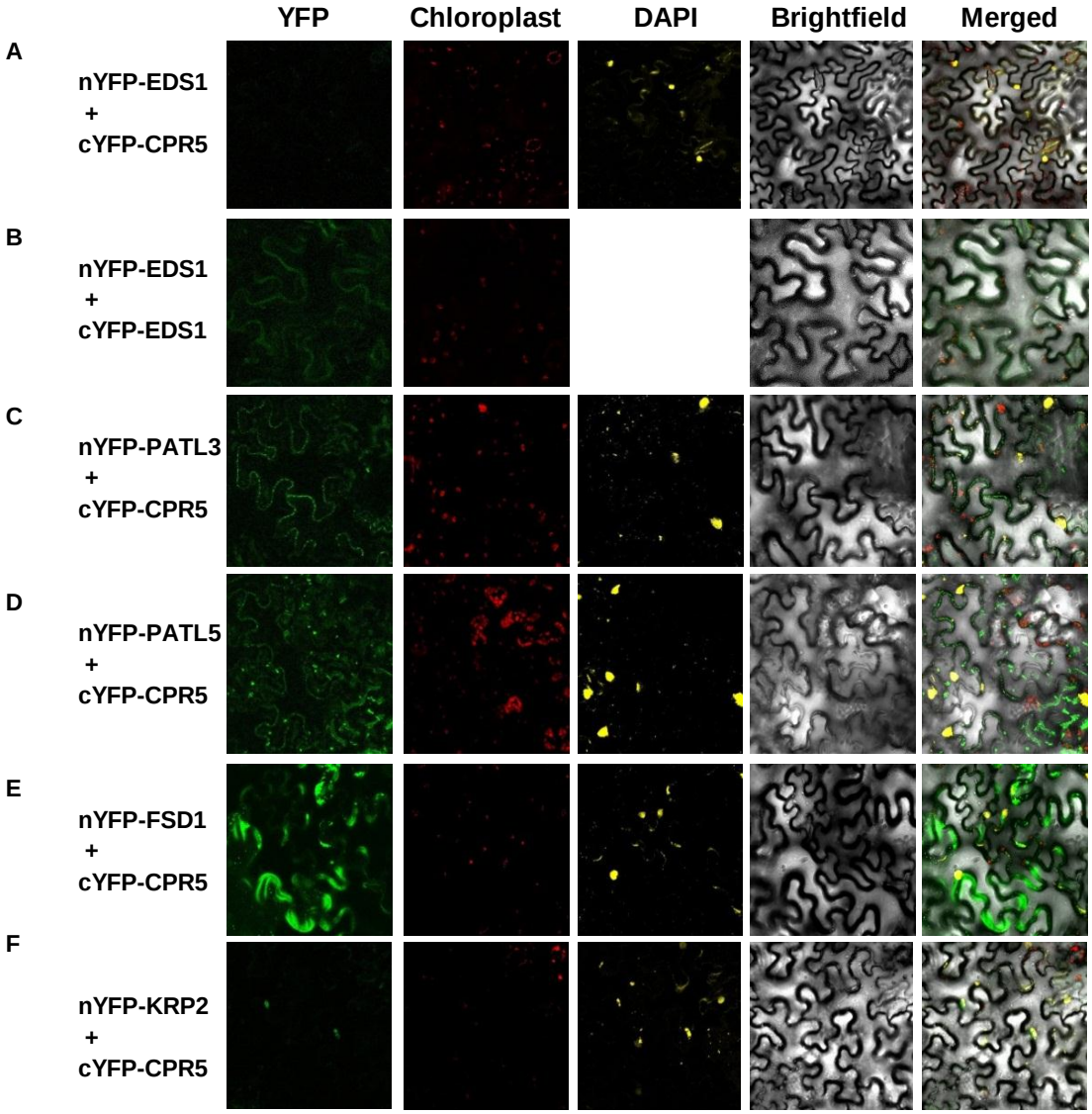

Figure 3.10: BiFC Signal form N. benthamiana Expressing N-terminal tagged, C-terminal-YFP-CPR5 and N-terminal tagged, N-terminal-YFP-GOI.
BiFC assay was carried out in *Nicotiana benthamiana* leaves. N terminal tagged C-terminal YFP-Full Length CPR5 (cYFP-CPR5) was used for all assays. The N and C terminus of YFP were fused to **A)** EDS1(nYFP-EDS1) and full length CPR5(cYFP-CPR5) as a negative control, **B)** EDS1(nYFP-EDS1) and EDS1(cYFP-EDS1), **C)** PATL3(nYFP-PATL3) and CPR5(cYFP-CPR5), **D)** PATL5(nYFP-PATL5) and CPR5(cYFP-CPR5), **E)** FSD1(nYFP-FSD1) and CPR5(cYFP-CPR5), **F)** KRP2(nYFP-KRP2) and CPR5(cYFP-CPR5). EYFP was visualized at 501-600nm. DAPI served as a nuclear marker and was visualized at 415-491nm. Chloroplast were visualized at 643-746nm. Brightfield was visualized was taken simultaneously using 496nm.

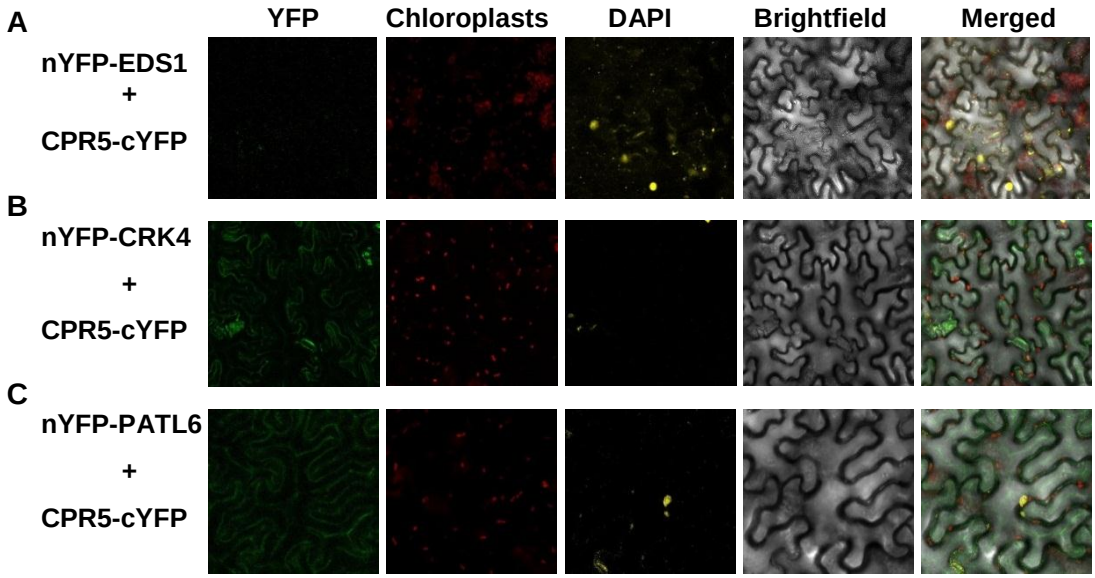

Figure 3.11: BiFC Assay was carried out in *N. benthamiana* Expressing C-terminal tagged, C-terminal-YFP-CPR5 and N-terminal tagged, N-terminal-YFP-GOI
C terminal tagged C-terminal YFP-Full Length CPR5 (CPR5-cYFP) was used for all assays. The N and C terminus of YFP were fused to **A**) EDS1 (nYFP-EDS1) and full length CPR5 (CPR5-cYFP) as a negative control, **B**) PATL6 (nYFP-PATL6) and CPR5 (CPR5-cYFP), **C**) CRK4 (nYFP-CRK4) and CPR5 (CPR5-cYFP). EYFP was visualized at 501-600nm. DAPI served as a nuclear marker and was visualized at 415-491nm. Chloroplast were visualized at 643-746nm. Brightfield was visualized was taken simultaneously using 496nm.

3.2.3 Summary of BiFC Results

Although CPR5 has been predicted to be a nuclear membrane bound protein, the orientation of CPR5 membrane binding and localization of the C-terminal nonmembrane bound portion of the protein has not been established. Assays such as BiFC can provide insight on the localization of the different regions of CPR5 based on the interactions that are identified and the location of the fused split YFP tag. BiFC analysis yielded several potential protein interactions occurring with CPR5 localized to both the nucleus and outside of the nucleus (Figure 3.7) As shown, FSD1, PATL3 and PAL5 interacts with cYFP-CPR5 indicating that the N-terminal region of these proteins are in close enough proximity to the C-terminal region of CPR5 to allow the split YFP fragments to reconstitute YFP function. CRK4 and PATL6 was found to interact with CPR5-cYFP suggesting that the N-terminal region of these proteins is in close enough proximity to the N-terminal region of CPR5 to reconstitute YFP fluorescent function and is also present in the nucleus. Additionally, KRP2, the published control protein was found to interact with cYFP-CPR5

within the nucleus. As KRP2 is a nuclear protein, KRP2 interaction with cYFP-CPR5 indicates that the C-terminal region of CPR5 is localized in the nucleus as well. The specific localization of the protein interactions observed outside of the nucleus cannot be exactly pinpointed based on the fluorescent signals as has been generally listed as cytoplasmic (Figure 3.7).

3.3 Changes in *cpr5-2* Morphological Phenotypes

cpr5-2 has very evident phenotypic differences to Col-*0*, which include smaller plant size, minimal trichome development, as well as aberrant responses to hormonal stress and to sugar (Aki, et al., 2007; Boch, et al., 1998; Bowling, et al., 1997; Gao, et al., 2011; H.-C. Jing, et al., 2007; H.-C. Jing & Dijkwel, 2008; H. C. Jing, et al., 2008; Kirik, et al., 2001; Yoshida, et al., 2002). Genetic crosses were performed to establish double mutants of *cpr5* and *akin10*, *fsd1*, *crk4*, *patl3*, *patl5*, and *bzip61*. Crosses with *dnaj*, *sac9*, and *patl6* mutant lines were unsuccessful and no double mutant line was produced. No *myb3* SALK T-DNA KO line was available from TAIR. Because *cpr5* is recessive, analysis of the effects of these double mutants was performed with plants from after the F2 generation. PCR screen of F2 plants and subsequent growth and harvest of seeds from selected double mutants was used to obtain homozygous double mutant populations. To determine the phenotypic differences between the double mutant plant lines and *cpr5-2*, several different assays were performed to determine any differences in phenotypes respectively.

3.3.1 Trichomes and Lesions

Trichome observations were conducted on plants grown in 12h light/12h dark for 22 days as the short day conditions have been observed to amplify phenotypic differences (section 2.7). Col-*0*, *cpr5-2*, the SALK TDNA KO lines, and the six double mutant lines were grown. In all six of the double mutant lines, trichome abundance appears to have no visible difference compared to the *cpr5-2* plants (Figure 3.12). There were also no visible differences in trichome development and abundance in the six single mutant lines as compared to Col-*0* wild-type plants (Figure 3.12). In addition to trichome development, HR-like lesions are known to form on the *cpr5-2* mutant (Boch, et al., 1998; Bowling, et al., 1997). HR lesion formation in Col-*0*, *cpr5-2*, SALK KO lines, and the double mutant lines was observed in the same plants used to observe trichome growth. These HR-like lesions were also observed on all double mutant lines similar to *cpr5-2*, but not on any of the single mutant lines or Col-*0* (Figure 3.12).

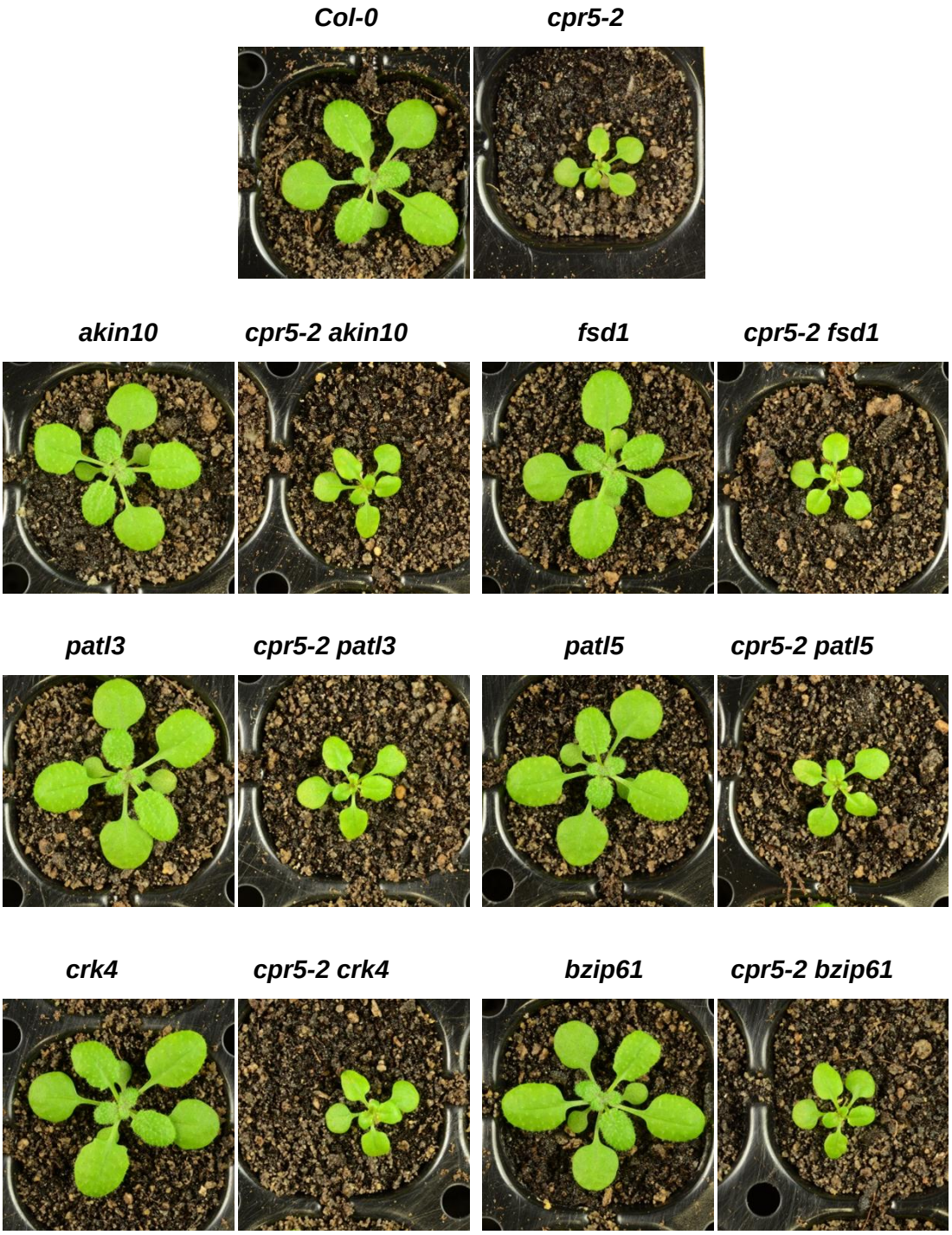

Figure 3.12: Representative Arabidopsis Plants Grown for 21 Days under Normal Short Day Conditions.
Representative physiological phenotypes of 21 day old Arabidopsis mutant and double mutant seedlings. F3 generation double mutant seedlings were grown at 22°C 12h/12h light/dark cycle.

3.3.2 Drought Tolerance

cpr5 mutant plants exhibit increased tolerance to abiotic stresses such as drought, salt and heat, thus it was important to observe the effect of abolishing the genes of interest on abiotic stress tolerance as compared to *cpr5-2* mutants. Plants were grown in 12h light/12h dark for 30 days before withholding water. After withholding water for 1 week, *cpr5-2* exhibited markedly higher tolerance to drought measured by the observable lack of wilting as compared to WT Col-*0* plants.

The SALK single mutant parent lines (akin10, fsd1, patl3, patl5, crk4 and bzip61) exhibited similar wilting to Col-0 indicative of a normal drought tolerance phenotype. Similar to *crp5-2* mutants, the double mutant lines, *cpr5-2 akin10*, *cpr5-2 fsd1*, *cpr5-2 patl3*, *cpr5-2 patl5, cpr5-2 crk4, cpr5-2 bzip61* all exhibited high drought tolerance as measured by the lack of observable wilting as compared to WT Col-*0* and the SALK single mutant lines. (Figure 3.13)

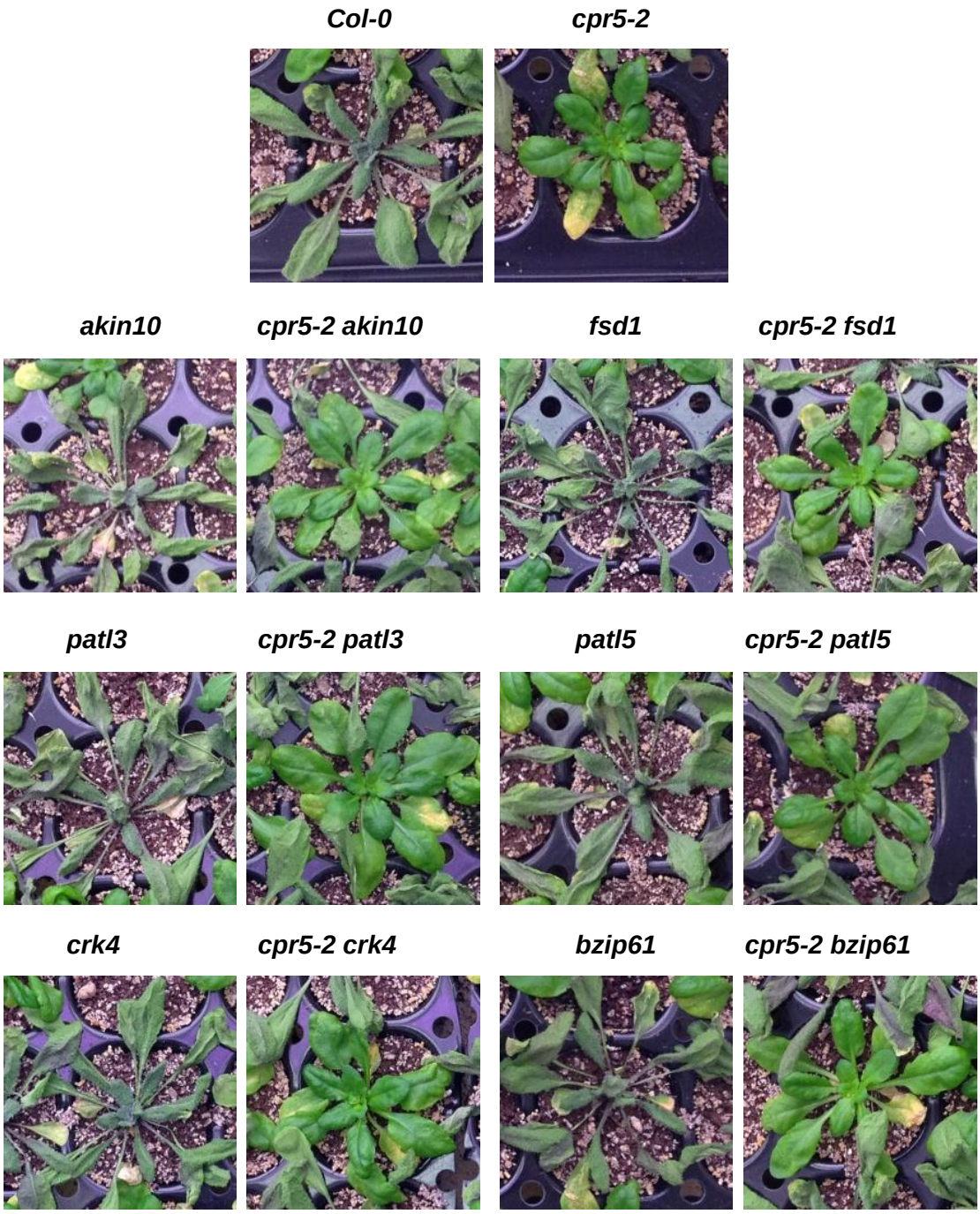

Figure 3.13: Representative Drought Tolerance Phenotypes of 5-Week Old Arabidopsis Mutant and Wild Type Seedlings.
F2 generation double mutant seedlings were grown at 22°C 12h/12h light/dark cycle for 4 weeks. Plants were well water overnight and placed into a dry tray. Photos were taken after 1 week of withholding water.

3.3.3 Dark and Sugar Treatment

Exogenous application of sugar has an observable negative effect on Arabidopsis seed germination and development; however, *cpr5* mutants exhibit similar repression of germination and development under significantly lower concentrations of applied sugar (Yoshida, et al., 2002). In order to assess the effect of exogenous application of sugar on the germination and development of *Arabidopsis* seedlings, they were grown in darkness to remove the variable light factor that contributes to germination. Additionally, the effects of dark treatment and sugar treatment were uncoupled by assessing the phenotypes of all Arabidopsis mutant lines on media containing 0% sucrose in dark.

3.3.3.1 *cpr5-2* morphological phenotypes under dark and sugar treatment

Arabidopsis seedlings were germinated in darkness and various sucrose concentrations. When germinated in darkness, *cpr5-2* seedlings exhibit inhibited hypocotyl elongation as compared to *Col-0*. This elongation is suppressed in *cpr5-2* seedlings, yielding hypocotyl lengths roughly half the length of Col-*0* hypocotyls when grown on sucrose for 3 and 5 days respectively ($p<0.05$) (Figure 3.15).

Sugar sensitivity was determined by growth of seedlings for 3 and 5 days in darkness on 1/2MS media containing 0.5%, 1% and 2% sucrose. Col-*0* and *cpr5-2* seedlings both exhibited similar trends of down-regulation of hypocotyl elongation when grown on 0.5%, 1% and 2% sucrose for 3 days, and similar inhibition when grown on 1% and 2% sucrose for 5 days as compared to 0% sucrose dark treatment (Figure 3.14A). The inhibition of hypocotyl elongation was more pronounced with treatment of higher concentrations of sucrose.

Sucrose treatment of *cpr5-2* mutants for 3 days yielded no observable difference in root elongation as compared to dark treated seedlings. However, Col-*0* seedlings treated with sucrose for 3 days and Col-*0* and *cpr5-2* seedlings treated with sucrose for 5 days, exhibited similar trends of upregulated root elongation phenotypes. However, high concentration of sucrose treatment did not yield more pronounced up-regulation of root elongation (Figure 3.14B). Treatment of *cpr5-2* seedlings with 0.5% sucrose and 2% sucrose for 5 days yielded roots roughly 4mm longer than roots measured under dark treatment for 5 days.

Similarly, the apical hook curvature of *cpr5-2* seedlings was markedly more pronounced as sucrose concentrations increased. Col-*0* apical hook curvature was observably more

pronounced under 0.5% sucrose but maintained similar apical hook angles under 1% and 2% sucrose treatment as 0% sucrose dark treatment. (Figure 3.14C)

In order to determine whether the phenotypes exhibited by the *cpr5-2* double mutants is due to the knockout of the two genes, or due to an epistatic or additive effect, the SALK parent line of the double mutant was compared to Col-*0* to determine any phenotypes that may be exhibited by the single mutant lines, that could affect the double mutant.

Although *cpr5-2* hypocotyls are markedly shorter than Col-*0* when grown under dark treatment, both *cpr5-2* and Col-*0* exhibited similar downward trend of hypocotyl lengths with increasing sucrose concentrations. There is no noticeable difference in root lengths of Col-*0* and *cpr5-2* seedlings grown under dark treatment, but exposure to sucrose resulted in an overall upward trend of elongation with increasing sucrose concentrations.

In order to assess the effect of abolishing CPR5 potential partners, *cpr5-2* double mutants were treated in identical conditions to *cpr5-2* and Col-*0* seedlings to determine any phenotypic differences between *cpr5-2*, Col-*0*, the SALK mutant lines, and the *cpr5-2* SALK double mutant lines (Table 2.4). A total of 14 lines were grown in darkness and treated with 3 different sucrose concentrations over a period of 3 days and 5 days respectively.

As the SALK mutant lines all exhibited WT Col-*0* like morphology when grown under normal growth conditions. The SALK mutant lines were compared to Col-*0* in order to assess any effects of dark or sugar treatment which could yield a similar phenotype in *cpr5-2* SALK double mutant lines.

The overall phenotypic trend of treatment with a sucrose gradient was observed as well as measure of any differences in hypocotyl lengths, root lengths, and apical hook curvatures.

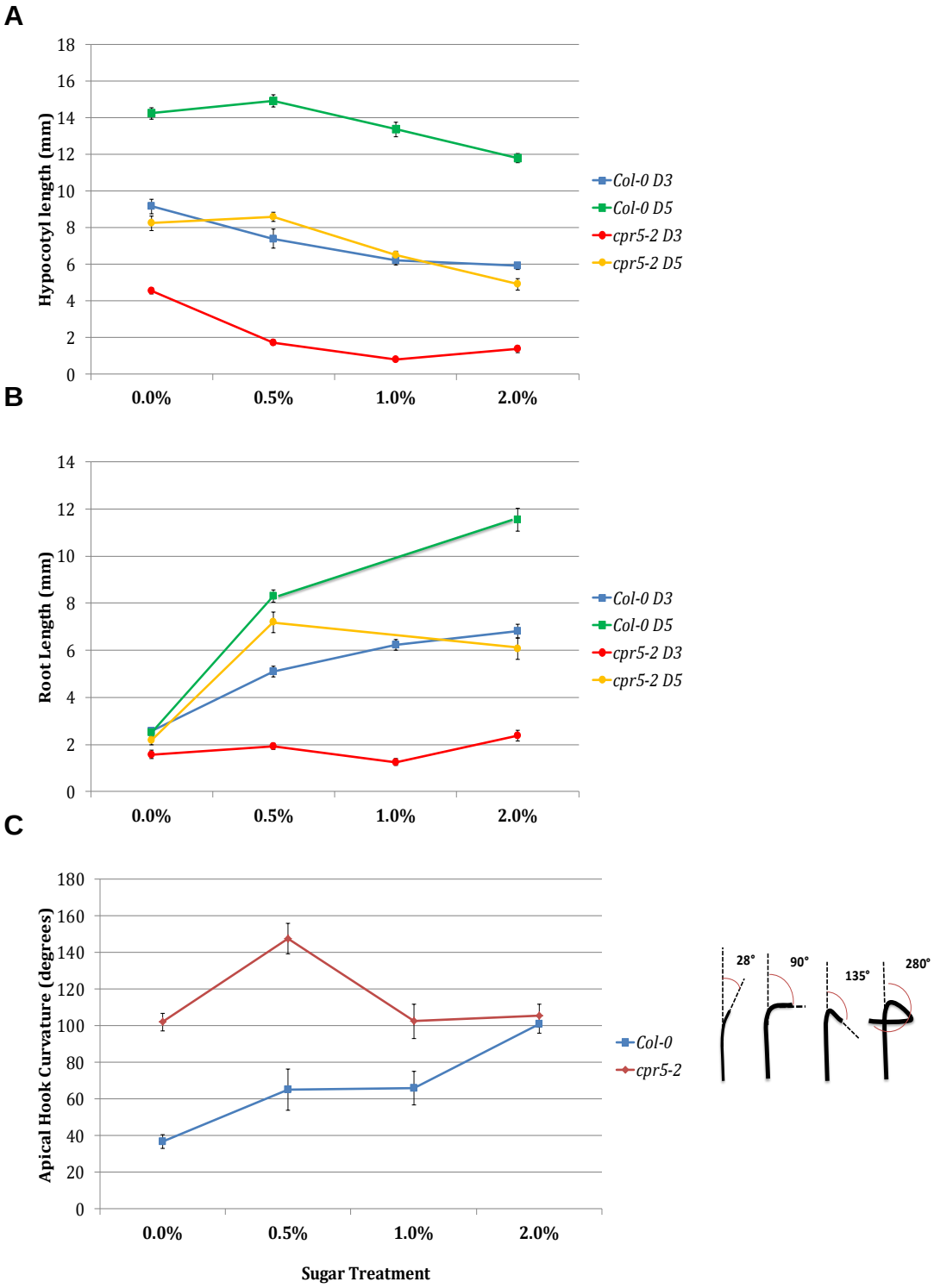

Figure 3.14: *Arabidopsis crp5-2* and Col-*0* Seedlings under Dark and Sugar Treatment. *cpr5-2* and Col-*0* plants were grown under darkness (0%) and darkness+sucrose treatment (0.5%, 1%, and 2%) for 3 and 5 days. **A**) Hypocotyls, **B**) Roots, and **C**) Apical Hook curvature were measured at 3 and 5 days after germination in darkness. Angles were measured based on diagram shown. Each bar represents average measured length of 10 seedlings (n=10)

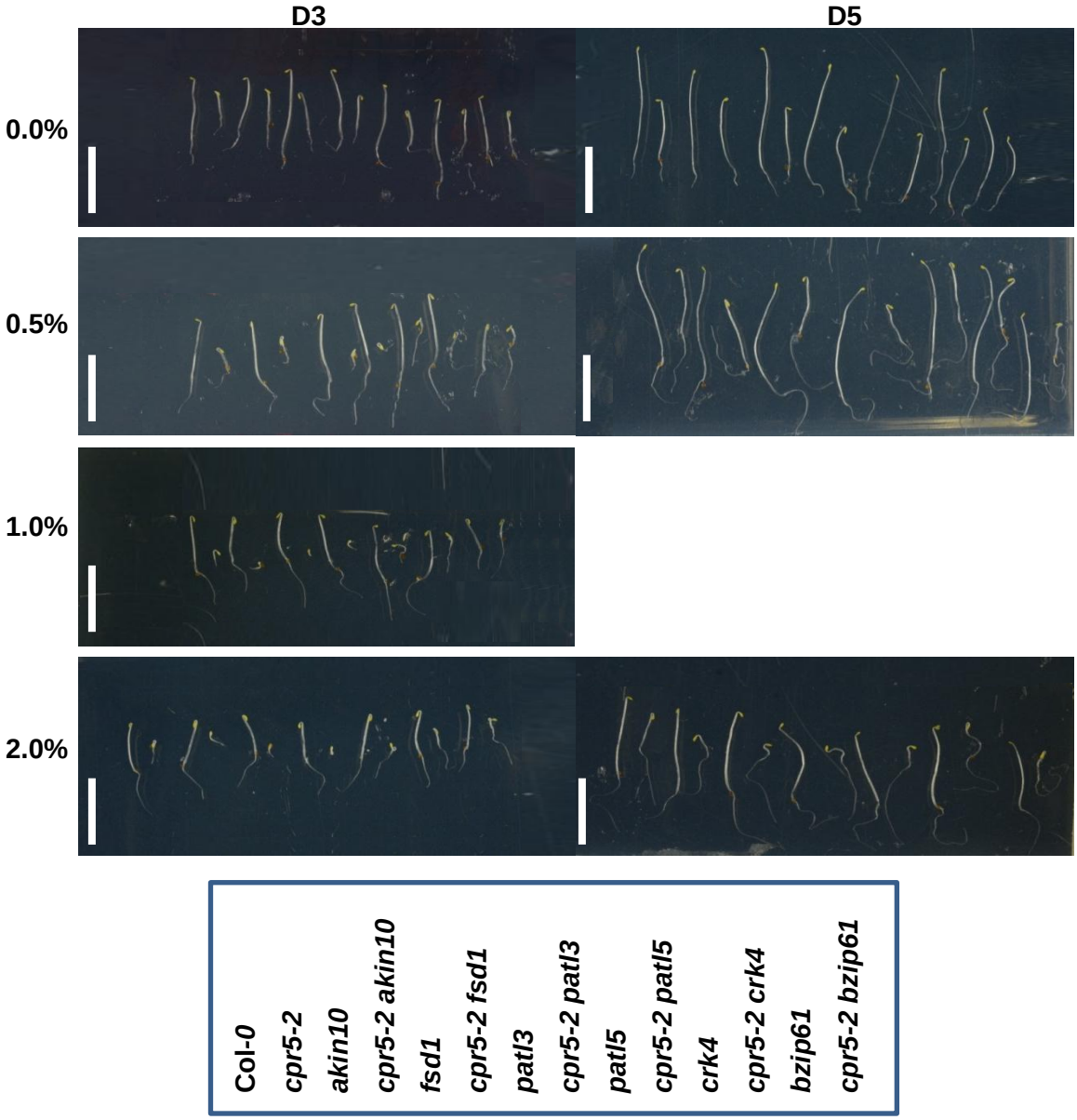

Figure 3.15: Representative Arabidopsis Seedlings from Dark and Sugar Treatment for 3 and 5 Days

Arabidopsis seedlings grown in sucrose media (0%, 0.5%/1%/2%) for 3 and 5 days at 22°C 65%. Plates were wrapped foil wrapped and seedlings grown in darkness. Seedlings Left to Right: (Col-*0*, *cpr5-2*, *akin10*, *cpr5-2 akin10*, *fsd1*, *cpr5-2 fsd1*, *patl3*, *cpr5-2 patl3*, *patl5*, *cpr5-2 patl5*, *crk4*, *cpr5-2 crk4*, *bzip61*, *cpr5-2 bzip61*) Bar represents 1cm.

3.3.3.2 *akin10* and *cpr5-2 akin10*

Plant lines were treated with 3 different sucrose sugar concentrations (0.5%, 1.0%, and 2%) in darkness and were also treated with only darkness and 0% sucrose as a control and as a dark treatment assay (Figure 3.15).

akin10 single mutant seedlings exhibited no difference in hypocotyl length, root length and apical hook angle when compared to *Col-0* under darkness, or sucrose treatment. This indicates that the single mutant does not exhibit any sugar sensitivity or altered skotomorphogenic development similar to cp5-2 seedlings (3.16A, B, 3.17A, B, 3.18A, B). Under 0% dark treatment, *cpr5-2 akin10* seedlings yielded hypocotyls 21.8% and 27% longer than *cpr5-2* seedlings ($p<0.05$) at both 3 and 5 days after treatment, respectively (Figure 3.16A, B) . 1% and 2% sucrose treatment for 3 days of *cpr5-2 akin10* seedlings grown in darkness inhibited hypocotyl elongation yielding hypocotyls that were 60% and 77% the length of *cpr5-2* hypocotyls ($p<0.05$) (Figure 3.16A, B).

cpr5-2 akin10 seedlings also exhibited root lengths 116% and 79% longer than *cpr5-2* seedlings when grown in darkness(Figure 3.17A, B). *cpr5-2 akin10* seedlings grown under sucrose treatment (1% and 2%) for 3 days showed significantly shorter roots ($p<0.05$) than those of *cpr5-2* seedlings (Figure 3.17A). *cpr5-2 akin10* seedlings exhibited inhibited root elongation in the presence of any sucrose for 5 days (Figure 3.17B), but the overall average length of the roots was still longer than *cpr5-2* seedling roots ($p<0.05$).

cpr5-2 akin10 also exhibited a more pronounced mean apical hook curvature angle of 102° than the *cpr5-2* mean angle of 76.7° when measured at day 5 ($p<0.05$) (Figure 3.18A) under darkness. At day 5, the apical hook curvature of *cpr5-2 akin10* seedlings was also more pronounced than *cpr5-2* under 0.5% sucrose treatment ($p<0.05$), similar to the angles of seedlings measured under 0% sucrose dark treatment, and less pronounced than *cpr5-2* under 2% sucrose ($p<0.05$) (Figure 3.18A). No apical hook angles were measured at day 3 due to the immaturity of the seedlings. It was difficult to obtain accurate angles as the hypocotyl and roots growth had not initiated.

Hypocotyls, roots and apical hook curvatures were generally upregulated and more pronounced in *cpr5-2 akin10* seedlings grown in darkness (Figure 3.19). *cpr5-2 akin10* seedlings generally exhibited down regulation of hypocotyl length after 5 days of sucrose treatment, as well as down regulation of root elongation after 3 days of sucrose treatment as compared to *cpr5-2* seedlings. However, at day 5 *cpr5-2 akin10* seedling roots were generally longer than *cpr5-2* seedlings, and there was no trend for apical hook curvature in *cpr5-2 akin10* seedlings in the presence of sugar.

3.3.3.3 *fsd1* and *cpr5-2 fsd1*

fsd1 single mutants exhibited hypocotyls 34% longer than *Col-0* seedlings ($p<0.05$) under 0.5% sucrose treatment and showed a similar trend under 0% sucrose dark treatment ($p=0.059$) (Figure 3.16C, D). *cp5-2 fsd1* exhibited hypocotyl lengths similar to *cpr5-2* under dark treatment, but exhibited inhibited hypocotyl elongation as compared to *cpr5-2* seedling hypocotyl lengths under 0.5% ($p=0.069$), 1% ($p<0.05$) and 2% ($p<0.05$) when measured at day 3 (Figure 3.16C), ranging from 79% to 57% of *cpr5-2* hypocotyl lengths, and showed similar inhibition of growth at day 5 under all 3 sucrose conditions ranging from 78% to 56% of *cpr5-2* mean hypocotyl lengths (Figure 3.16D).

Although no differences in hypocotyl elongation was observed, *fsd1* seedlings did however exhibited 25% and 33% longer root lengths under dark treatment at day 3 (Figure 3.17C) and 5 (Figure 3.17D) ($p<0.05$), as well as under 0.5% sucrose treatment measured at day 3 ($p<0.05$), but showed inhibited root elongation under 2% sucrose treatment with roots only 80% the length of *Col-0* mean root lengths ($p<0.05$) (Figure 3.17C, D). Similar to *fsd1* seedlings, *cpr5-2 fsd1* seedlings were observed to have increased root elongation under dark treatment at day 3 (Figure 3.17C), with roots 81% longer than *cpr5-2* seedlings, and showed a similar trend of increased hypocotyl elongation at day 5 ($p<0.106$) (Figure 3.16D) but was not statistically significant. Conversely, at day 3, *cpr5-2 fsd1* seedlings exhibited decreased root elongation under 1% and 2 % sucrose treatment (Figure 3.17C) but, by day 5, seedling mean root length was 59% and 33% longer than *cpr5-2* seedling root lengths(Figure 3.17D).

No major differences were exhibited in apical hook curvature between *fsd1* and *Col-0* seedlings in any of the treatments (Figure 3.18B). *cpr5-2 fsd1* Apical hook curvature was measured at a more pronounced angle of 144° as compared to *cpr5-2* average angle of 79° under the same 0.5% sucrose treatment ($p<0.05$) (Figure 3.18B).

cpr5-2 fsd1 seedlings exhibited *cpr5*-2 like phenotypes when grown under darkness, however fsd1 seedlings exhibited longer root phenotype. c*pr5-2 fsd1* seedlings also exhibited a trend of down-regulated hypocotyl elongation in treatment for 3 and 5 days. Sucrose treatment of *cpr5-2 fsd1* seedlings however yielded seedlings with a general trend of down-regulated hypocotyl elongation at day 3, but an up-regulated hypocotyl elongation at day 5 yielding shorter and longer root lengths respectively. Additionally, apical hook curvature was generally more pronounced in *cpr5-2 fsd1* seedlings subjected to sucrose treatment (Figure 3.19).

3.3.3.4 *patl3* and *cpr5-2 patl3*

patl3 seedlings exhibited increased hypocotyl elongation as compared to *Col-0* under dark and 0.5% and 1% sucrose treatments ($p<0.05$), but had similar lengths to *Col-0* under 2% sucrose treatment when measured at day 3 (Figure 3.16E) however, it did not yield any statistically significant differences in hypocotyl length by day 5 under any treatment (Figure 3.16F). *cp5-2 patl3* seedlings under dark treatment yielded seedlings with longer hypocotyls on average after 3 days of treatment ($p=0.057$), but was statistically significant as compared to *cpr5-2* hypocotyl lengths (Figure 3.16E). Conversely, under all sucrose treatments, hypocotyls measured at both 3 and 5 days were 71% to 59% the length of *cpr5-2* hypocotyls ($p<0.05$) (Figure 3.16E, F).

Dark treatment yielded *patl3* seedlings with an 18% higher average root length than *Col-0* seedlings at day 3 ($p<0.05$) and showed similar trends at day 5 ($p=0.076$), but yielded shorter root lengths under 2% treatment at day 5 ($p<0.05$) with a similar trend at day 3 ($p=0.10$) (Figure 3.17E, F). *cpr5-2 patl3* seedlings grown in darkness exhibited increased root growth with root lengths 108% and 51% longer than *cpr5-2* at day 3 and 5 respectively ($p<0.05$) (Figure 3.17E, F). 1% and 2% sucrose treatment of *cpr5-2 patl3* seedlings for 3 days yielded seedlings with roots significantly shorter than *cpr5-2* seedlings, at 42% and 25% of *cpr5-2* roots respectively (Figure 3.17E). Conversely, by day 5, 0.5% and 2 % sucrose treatment yielded roots that were 47% and 69% longer than *cpr5-2* seedling roots (Figure 3.16F).

There was no significant difference in apical hook curvature of *patl3* seedlings and *Col-0* seedlings (Figure 3.18C). The apical hook curvature of *cpr5-2 patl3* seedlings was more pronounced under dark treatment and 0.5% sucrose treatment ($p<0.05$) (Figure 3.18C). 2% sucrose treatment of *cpr5-2 patl3* seedlings however, did not yield any significant difference in apical hook curvature as compared to *cpr5-2*, and was very similar to the angles observed under 0.5% sucrose treatment (Figure 3.18C).

cpr5-2 patl3 and *patl3* both exhibited up-regulation of root elongation under dark treatment and patl3 exhibited general trends of up-regulated hypocotyl elongation under sucrose treatment for 3 days but was not observed on day 5. c*pr5-2 parl3* exhibited more pronounced apical hook under all treatments and a general up-regulated root phenotype at 5 days of sucrose treatment. Contrary to this was *cpr5-2 patl3* down-regulation of hypocotyl length under sucrose treatments for 3 and 5 days and root elongation at 3 days (Figure 3.19).

3.3.3.5 *patl5* and *cpr5-2 patl5*

patl5 seedlings grown in darkness exhibited no difference in hypocotyl lengths, root lengths, or apical hook curvature as compared to *Col-0* seedlings (Figure 3.16G,H, 3.17G, H, 3.18D).

Sucrose treatment (0.5%, 1%, and 2%) of *patl5* seedlings for 3 days yielded 27%, 23%, and 18% longer hypocotyls than Col-*0* seedlings ($p<0.05$) (Figure 3.16G), but no significant differences were observed from seedlings treated for 5 days. *cp5-2 patl5* seedlings grown in darkness for 3 and 5 days yielded seedling with longer hypocotyls than *cpr5-2* at day 3 ($p<0.05$) and day 5 ($p=0.056$), as well the hypocotyls of seedlings measured under sucrose treatment for 3 days ($p<0.05$) (Figure 3.16G, H). Conversely, *cpr5-2 patl5* hypocotyls were significantly shorter than *cpr5-2* when subjected to any sucrose treatments for 5 days ($p<0.05$) (Figure 3.16F).

No differences in root length growth were observed under sucrose treatments between *patl5* and Col-*0*. Root length of *cpr5-2 patl5* seedlings show a trend of increased root elongation to those grown under darkness (Figure 3.17G, H). Seedlings treated with sucrose for 3 days yielded roots longer than *cpr5-2,* but the difference in root length decreased as concentrations of sucrose increased with root lengths from 265% of *cpr5-2* seedlings at 0.5% sucrose, to 221% and 142% of *cpr5-2* root lengths when grown on 1% and 2% sucrose media ($p<0.05$) (Figure 3.17G, H). Seedlings treated with 0.5% and 2% sucrose for 5 days yielded 64% and 103% longer root lengths than *cpr5-2* ($p<0.05$) (Figure 3.17H).

Although no differences in apical hook curvature was observed between *patl5* and Col-*0* under any treatment, c*pr5-2 patl5* seedlings exhibited more pronounced apical hook angles when exposed to sucrose. This was only significantly more pronounced than *cpr5-2* when grown on 0.5% sucrose media ($p<0.05$) (Figure 3.18D).

cpr5-2 patl5 exhibited down-regulation of hypocotyl elongation under sucrose treatment and down-regulation of root length at 3 days of sucrose treatment, whereas at day 5, sucrose treatment generally caused an up-regulation of root elongation yielding overall longer roots than *cpr5-2* seedlings. c*pr5-2 patl5* seedlings also exhibited more pronounced apical hook under all treatments. Contrary to *cpr5-2 patl5, patl5* exhibited longer hypocotyls after 3 days of sucrose treatment (Figure 3.19).

3.3.3.6 *crk4* and *cpr5-2 crk4*

crk4 seedlings yielded seedlings with increased hypocotyl elongation when grown in darkness for 3 and 5 days, (Figure 3.16I, J). In *crk4* seedlings, after 3 days in 0.5% sucrose (Figure 3.16I) and after 5 days at 2% sucrose treatment (Figure 3.16J), the seedlings exhibited 31% and 10% more elongated hypocotyls as compared to *Col-0* seedlings ($p<0.05$). Similar to *crk4* seedlings, *cpr5-2 crk4* seedlings grown in darkness for 3 and 5 days yielded seedlings with increased hypocotyl lengths as compared to *cpr5-2*, but no significant difference in root lengths (Figure 3.16I, J, 3.17I, J). *cpr5-2 crk4* grown for 3 days in 0.5%, 1% and 2% sucrose treatments yielded increased hypocotyl lengths 101%, 137% and 45% greater than *cpr5-2* seedlings ($p<0.05$) (Figure 3.16I), but no observable difference in lengths was observed after 5 days of similar treatment (Figure 3.16J).

crk4 seedlings yielded seedlings with as increased root elongation when grown in darkness for 5 days ($p<0.05$) (Figure 3.17I, J). No significant difference was observed in root lengths of seedlings grown for 3 days under darkness (Figure 3.17I). *crk4* seedlings after 3 days in 0.5% and 1% sucrose showed increases of 30% and 14% root elongation ($p<0.05$). Although no difference was observed in the root lengths of dark treated seedlings, in 0.5% ($p<0.05$), 1% ($p<0.05$) and 2% ($p<0.05$) sucrose treatment of *cpr5-2 crk4* seedlings for day 3, measured roots were 159%, 240%, and 144% significantly longer than *cpr5-2* seedlings under the same treatments (Figure 3.17I). Similarly, *cpr5-2 crk4* seedlings grown in 0.5% ($p=0.053$) and 2% ($p<0.05$) sucrose treatment for 5 days yielded roots 22% and 150% longer than control *cpr5-2* seedlings (Figure 3.17J).

Sucrose treatments did not have any visible effect on the apical hook curvature of *crk4* as compared to Col-*0* (Figure 3.16E).

No significant difference was observed in the apical hook curvature of *crk4* and *Col-0* under any sucrose treatments (Figure 3.18E). Apical hook curvature of *cpr5-2 crk4* seedlings was more pronounced at an average angle of 115° as compared to *cpr5-2* average angle of 77° (Figure 3.18E). Sucrose treatment did not have any observable effect on apical hook curvature of *cpr5-2 crk4* as compared to *cpr5-2* seedlings (Figure 3.18E).

cpr5-2 crk4 exhibited generally longer hypocotyls at day 3 of sucrose treatment, but exhibited *cpr5-2* like hypocotyls after 5 days of treatment. Root elongation was generally upregulated in *cpr5-2 crk4* and no affect was observed in apical hook curvature in the double mutant (Figure 3.19).

3.3.3.7 *bzip61* and *cpr5-2 bzip61*

bzip61 seedlings grown in darkness and sugar treatment show an overall trend of shorter hypocotyls than *Col-0* seedlings (Figure 3.16K). Converse to *bzip61* seedlings, *cpr5-2 bzip61* seedlings grown in darkness for 3 days yielded hypocotyls 28% longer than *cpr5-2* seedlings (Figure 3.16K). After 3 days of sucrose treatment (0.5%, 1%, and 2%), hypocotyls were visibly longer than *cpr5-2* hypocotyls by 98% ($p<0.05$), 127% ($p<0.05$) and 36% ($p<0.05$) for each treatment respectively (Figure 3.16L). Conversely, after 5 days of 0.5% and 2% treatment, *cpr5-2 bzip61* seedlings yielded hypocotyls shorter than *cpr5-2* seedlings(Figure 3.16L).

In *bzip61*, shorter root lengths were measured under dark and sucrose treatments for 3 days compared to Col-*0* (Figure 3.17K), and at 2% sucrose treatment for 5 days ($p<0.05$) (Figure 3.17L). Contrast to *bzip61* seedlings, *cpr5-2 bzip61* seedlings exhibited significantly longer root growth when compared to control *cpr5-2* plants ($p<0.05$) under all dark (36% and 58% longer), and sugar treatments (104%-207% longer) except 5 days in 0.5% sucrose treatment ($p=0.105$) (Figure 3.17G, H).

In dark treatment, *bzip61* seedlings exhibited more pronounced apical hook angles than *Col-0*, but were not visible different under sucrose treatment (Figure 3.18F). In *cpr5-2 bzip61* plants after 5 days on 2% sucrose media, apical hook curvature was significantly more pronounced than *cpr5-2* seedlings ($p<0.05$) (Figure 3.18F).

cpr5-2 bzip61 mutants exhibited a general up-regulation of hypocotyl lengths at two days of sucrose treatment, up-regulation of root length in all treatment as well as more pronounced apical hook curvature under sucrose treatments. Contrary to this, *bzip61* seedlings exhibited down-regulation of hypocotyl and root elongation under darkness and sucrose treatment as well as more pronounced apical hook curvature under dark treatment (Figure 3.19)

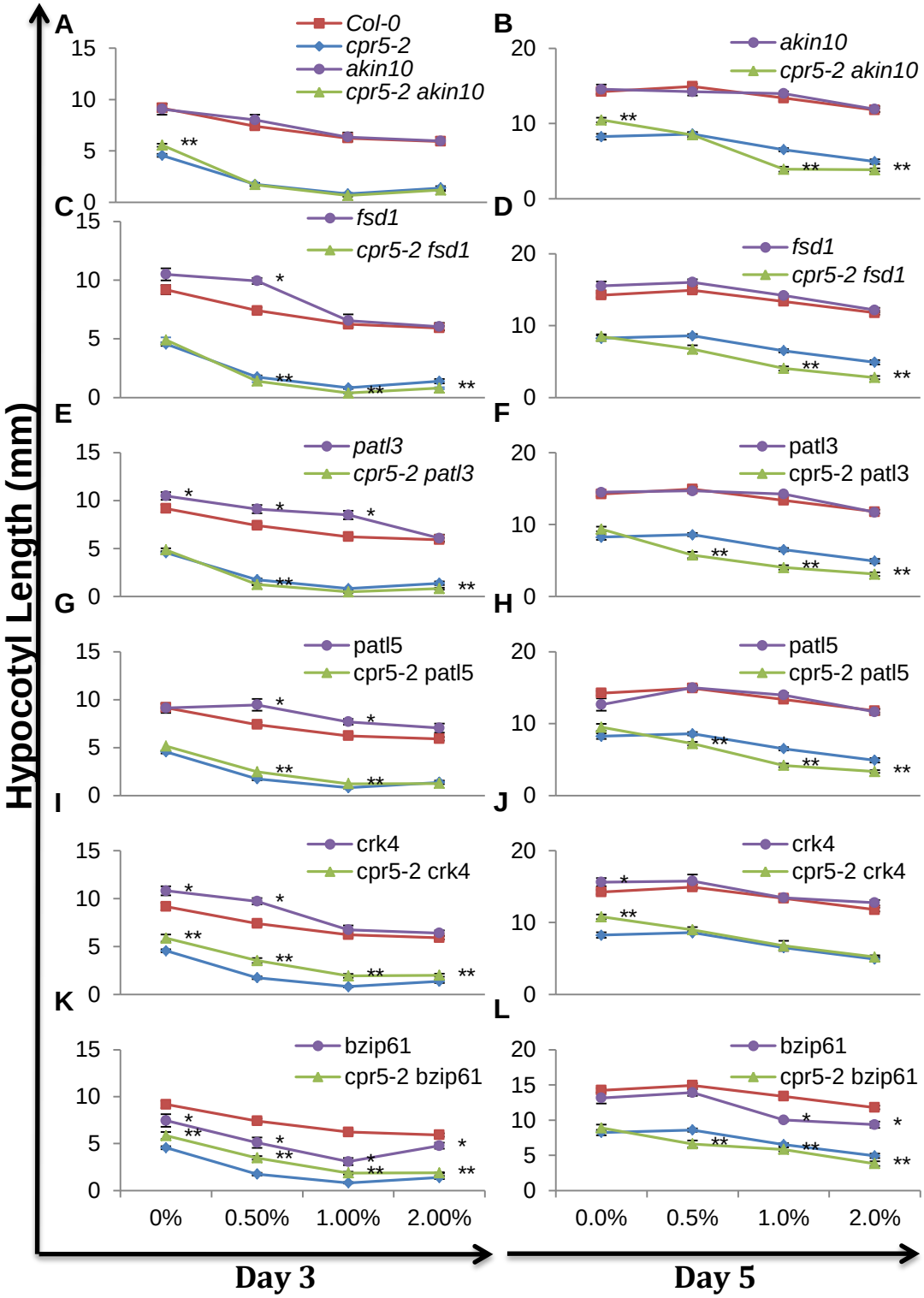

Figure 3.16: Hypocotyl Length of 3 and 5 Day Old Dark and Sugar Treated Seedlings 3 and 5-day old seedlings were grown in darkness on 0%, 0.5% 1%and 2% sucrose media at 22°C. Hypocotyl length of seedlings **A, B**) *cpr5-2 akin10*, akin10 **C, D**) *cpr5-2 fsd1*, *fsd1* **E, F**) *cpr5-2 patl3 patl3*, **G, H**) *cpr5-2 patl5*,*patl5* **I, J**) *cpr5-2 crk4 crk4*, **K, L**) *cpr5-2 bzip61*, *bzip61* grown in treatments for 3 days **A, C, E, G, I, K**)5 days and (**B, D, F, H, J, L**)5 days. Each bar marker represents average measured length of 10 seedlings (n=10). ** indicates statistical significance ($p<0.05$) when compared to *cpr5-2* and * indicates statistical significance from Col-*0* as calculated using *students t-test*.

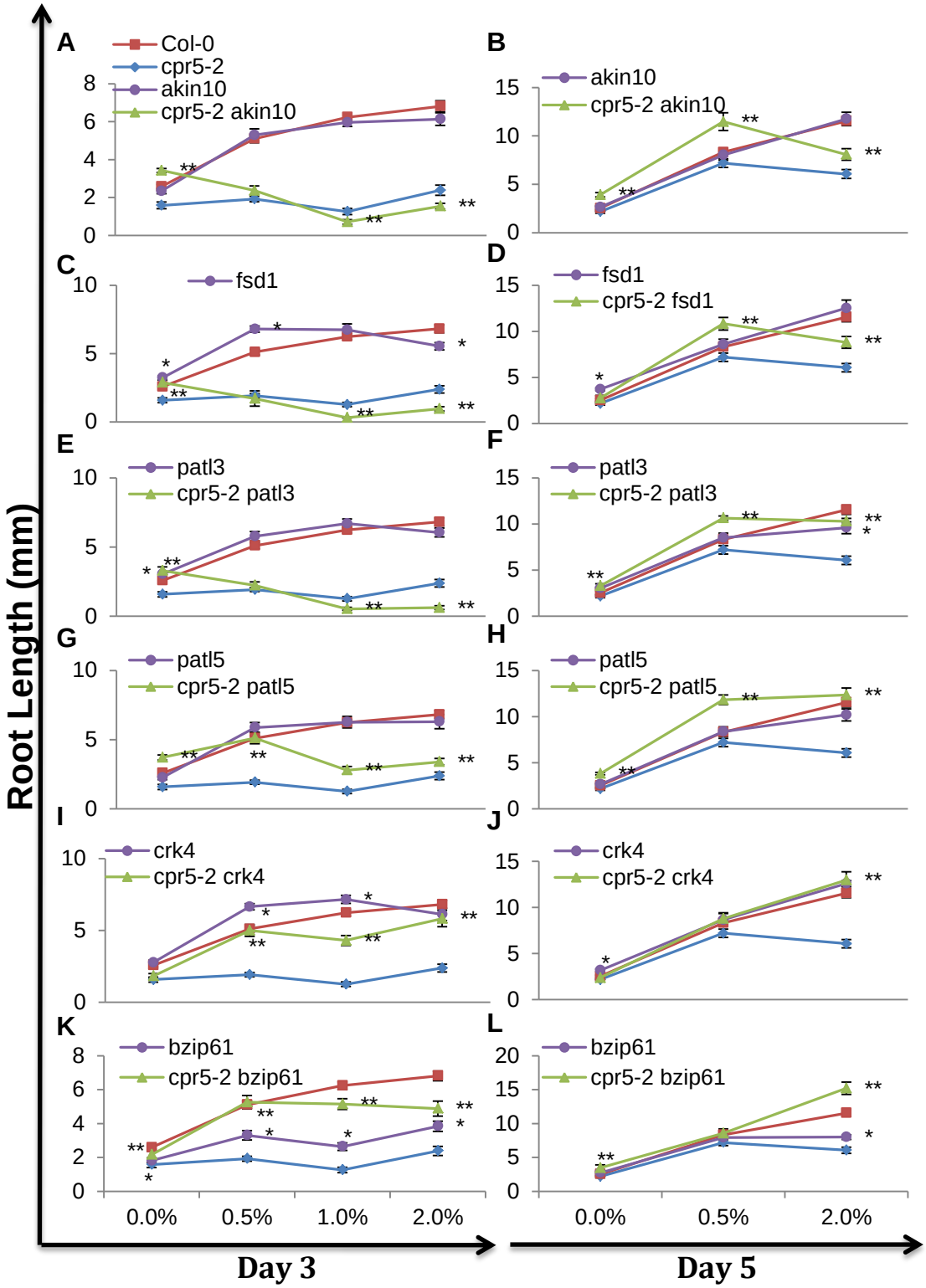

Figure 3.17: Root Length of 3 and 5 Day Old Dark and Sugar Treated Seedlings
3 and 5-day old seedlings were grown in darkness on 0%, 0.5% 1%and 2% sucrose media at 22°C. Root length of seedlings **A, B**) *cpr5-2 akin10*, akin10, **C, D**) *cpr5-2 fsd1*, *fsd1,* **E, F**) *cpr5-2 patl3, patl3*, **G, H**) *cpr5-2 patl5,patl,5* **I, J**) *cpr5-2 crk,4 crk4*, **K, L**) *cpr5-2 bzip61*, and *bzip61* grown in treatments for **A, C, E, G, I, K**)3 days and **B, D, F, H, J, L**) 5 days. Each bar marker represents average measured length of 10 seedlings (n=10). ** indicates statistical significance ($p<0.05$) when compared to *cpr5-2* and * indicates statistical significance from Col-*0* as calculated using *students t-test*.

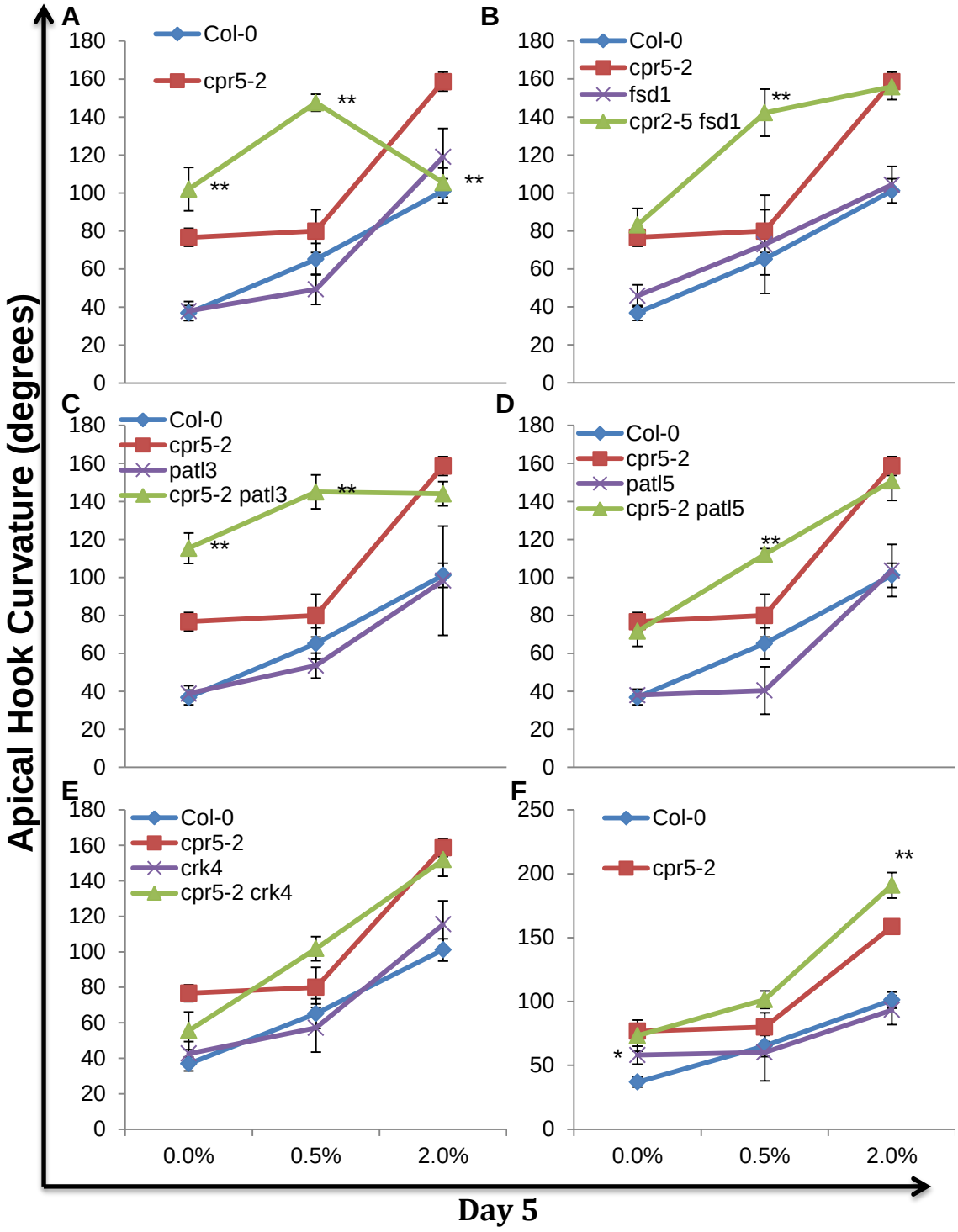

Figure 3.18: Apical Hook Curvature of 3 and 5 Day Old Dark and Sugar Treated Seedlings
Five-day old seedlings were grown in darkness on 0%, 0.5% and 2% sucrose media at 22°C. Apical hook curvature angles of **A**) *cpr5-2 akin10*, *akin10* **B)** *cpr5-2 fsd1, fsd1*, **C)** *cpr5-2 patl3*, *patl3* **D)** *cpr5-2 patl5*, *patl5* **E**) *cpr5-2 crk4*, *crk4* **F)** *cpr5-2 bzip61*, *bzip61* are compared to *cpr5-2*and Col-*0* apical hook curvatures respectively. Each bar represents average measured length of 10 seedlings (n=10). * indicates statistical significance ($p<0.05$) as calculated using students t-test. ** indicates statistical significant as compared to *cpr5-2* and * indicates statistical significance from Col-*0*

A

	Dark treatment cpr5-2					Sugar treatment cpr5-2				
	Hypocotyl (mm)		Root (mm)		Apical Hook (°)	Hypocotyl (mm)		Root (mm)		Apical Hook (°)
	D3	D5	D3	D5	cpr5-2	D3	D5	D3	D5	D5 (0.5%)
	4.56	8.25	1.58	2.18	76.68					
cpr5-2 akin10	5.55	10.47	3.43	3.91	102.05					
cpr5-2 fsd1										
cpr5-2 patl3			3.30	3.30	115.35					
cpr5-2 patl5			3.71	3.81						
cpr5-2 crpk4	5.88	10.80								
cpr5-2 bzip61	5.85		2.16	3.46						

B

	Dark treatment Col-0					Sugar Treatment Col-0				
	Hypocotyl (mm)		Root (mm)		Apical Hook (°)	Hypocotyl (mm)		Root (mm)		Apical Hook (°)
	D3	D5	D3	D5	Col-0	D3	D5	D3	D5	D5
Col-0	9.17	14.24	2.58	2.52	36.82					
akin10										
fsd1			3.24	3.71						
patl3	10.49		3.05	3.03						
patl5		12.65								
crpk4	10.82	15.62		3.18						
bzip61	7.45		1.81		57.99					

Figure 3.19: Heat Map Summary of Arabidopsis Seedlings Grown under Dark and Sugar Treatment for 3 and 5 Days.
A) Results were determined by comparing elongation and apical hook curvature of double mutant lines indicated to *cpr5-2.* **B)** Single mutant lines were compared to Col-*0* to determine their elongation and apical hook phenotypes. Red denotes up-regulation of elongation or more pronounced apical hook curvature as compared to *cpr5-2* or Col-*0* as indicated above each column. Green denotes down-regulation of elongation or less pronounced apical hook as compared to *cpr5-2* or Col-*0* as indicated about each column. Dark treatment results were calculated based off plants grown on 0% sugar media. Sugar treatment results were determined based off the trending phenotype observed across all sugar treatments (0.5%, 1%, and 2%). White denotes no significant change was observed as compared to *cpr5-2* /Col-*0*. Yellow denotes that conflicting phenotypes were observed across sugar treatments. Orange denotes trending up or down regulation of elongation (see value in square to determine regulation changes)

3.4 qRT-PCR

3.4.1 Identification of Stable Housekeeping Genes

qRT-PCR is a quantitative representation of transcription expression, and is used to determine any differences in transcriptional expression across different plant lines or exposed to different treatments. qRT-PCR requires the use of housekeeping genes, genes whose expression is stable across all plant lines of interest or across any treatments. 3 genes, *AT2g31270*, *AtTUB5*, and *AtUBC9* (Czechowski, et al., 2005) were chosen, and tested for housekeeping expression in all lines. Analysis of the 3 housekeeping genes indicated that AtUBC9 expression was not stable across all lines, and was removed as a housekeeping gene (Figure 3.20). However, *At2G31270* and *AtTUB5* were found to show stable expression across all lines as measured by the near parallel Cq values when graphed (Figure 3.20). The transcript abundance of genes of interest are then normalized against housekeeping genes using the Pfaffl method (section 2.6.4) and referred to as relative transcript abundance (data not shown). As AtUBC9 did not yield stable expression as measured by the nonlinear Cq values shown in figure 3.20, only At2G31270 and AtTUB5 were used to determine the relative expression of *PR1* and *PDF1.2* in all plant lines measured (section 2.6.4).

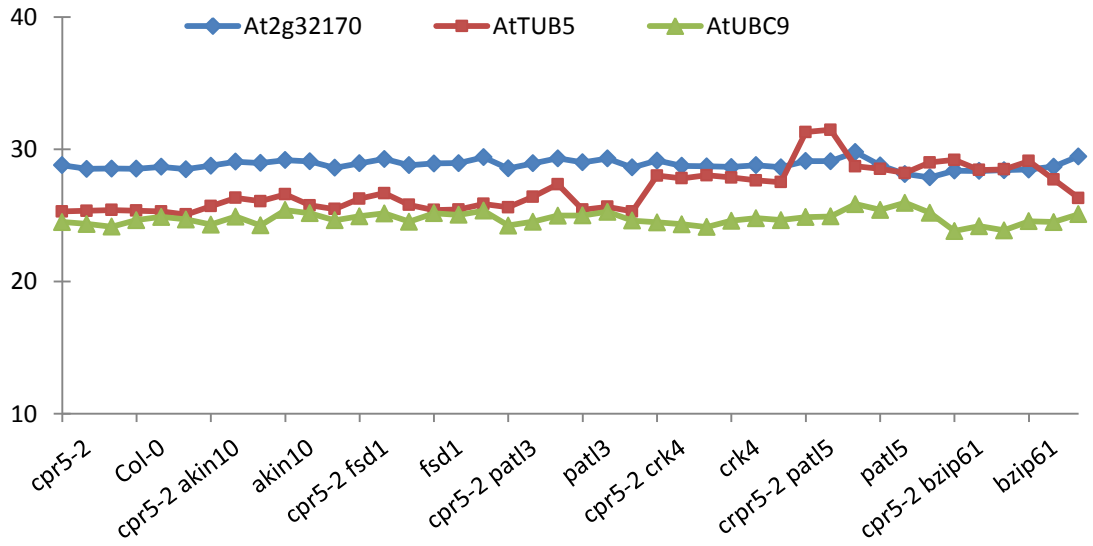

Figure 3.20: Expression of Housekeeping Genes, *At2G31270*, *AtTUB5* and *AtUBC9* Across All Lines Investigated.
3 housekeeping genes, *At2G31270*, *AtTUB5* and *AtUBC9* were tested for stable expression in *cpr5-2*, Col-*0*, *cpr5-2 akin10*, *akin10*, *cpr5-2 fsd1*, *fsd1*, *cpr5-2 patl3*, *patl3*, *cpr5-2 patl5*, *patl5*, *cpr5-2 crk4*, *crk4*, *cpr5-2 bzip61*, and *bzip61. The average Cq value of each biological replicate (x3 per line) is shown.*

3.4.2 qRT-PCR of *PDF1.2* and *PR1* in *Arabidopsis* Lines

Gene expression of *PR1* and *PDF1.2* is markedly upregulated in *cpr5-2* plants as compared to Col-*0* (Bowling, et al., 1997). As no double plant mutant produced significantly different observable phenotypes from the *cpr5-2* single mutant when grown under normal growth conditions or drought conditions (Figure 3.12, 3.13), qRT-PCR was used to quantify any changes to *cpr5-2* up-regulation of *PR1* and *PDF1.2* expression when *AKIN10*, *FSD1*, *PATL3*, *PATL5*, *CRK4*, or *BZIP61* is abolished in a *cpr5-2* background.

The relative transcript abundance of plant resistance and stress genes *PR1* and *PDF1.2* of the double mutants was compared to the *cpr5-2* mutant line. Additionally, Col-*0* plants were compared to the single mutant lines obtained originally, all of which exhibited morphological phenotypes similar to Col-*0*. All SALK single mutant lines exhibited significant down-regulation of *PR1* and *PDF1.2* as compared to *cpr5-2*, thus no comparison of the single mutant lines with *cpr5-2* (data not shown) ($p<0.01$). Col-*0* was also used to compare to the relative expression in the single mutant lines to determine if any underlying effect on *PR1* or *PDF1.2* was exhibited by the single mutant lines that would explain the alterations to *cpr5-2* expression of *PR1* or *PDF1.2*.

In whole plant tissue excluding the root system of plants harvested at 25 days, there were no statistically significantly differences in *PDF1.2* transcript levels of single mutant lines as compared to Col-*0* (Figure 3.21B). The relative transcript abundance of *PDF1.2* was significantly ($p<0.05$) down-regulated in the *cpr5-2 fsd1* line (Figure 3.21A). Additionally, *cpr5-2* patl3 exhibited trending down-regulation of *PDF1.2* ($p=0.055$) but was not statistically significant.

Conversely, *akin10* and *crk4* appear to have a down-regulation of *PR1* expression as compared to Col-*0* (Figure 3.21D). This down-regulation did not translate to the double mutant *cpr5-2 akin10* or *cpr5-2 crk4* mutant lines which showed similar expression levels as *cpr5-2*. *PR1* was significantly upregulated in *cpr5-2 patl3* ($p<0.05$) and down-regulation in *cpr5-2 bzIp61* ($p<0.05$) double mutant lines (Figure 3.21C).

Although no visible phenotypes are observed in the double mutant lines grown under normal or drought conditions, qRT-PCR indicates that *PDF1.2* expression is down-regulated in 2 double mutant lines, *cpr5-2 fsd1* and *cpr5-2 patl3,* but was not down-regulated in the single mutant parent lines which exhibited Col-*0*-like expression of *PDF1.2* (Figure 3.21E). Conversely, *PR1* expression was affected in two single mutant lines that were not observed in the related double mutant lines, and two double mutant lines

exhibited differential regulation of *PR1* expression that was not observed in the parent single mutant lines (Figure 3.21E)

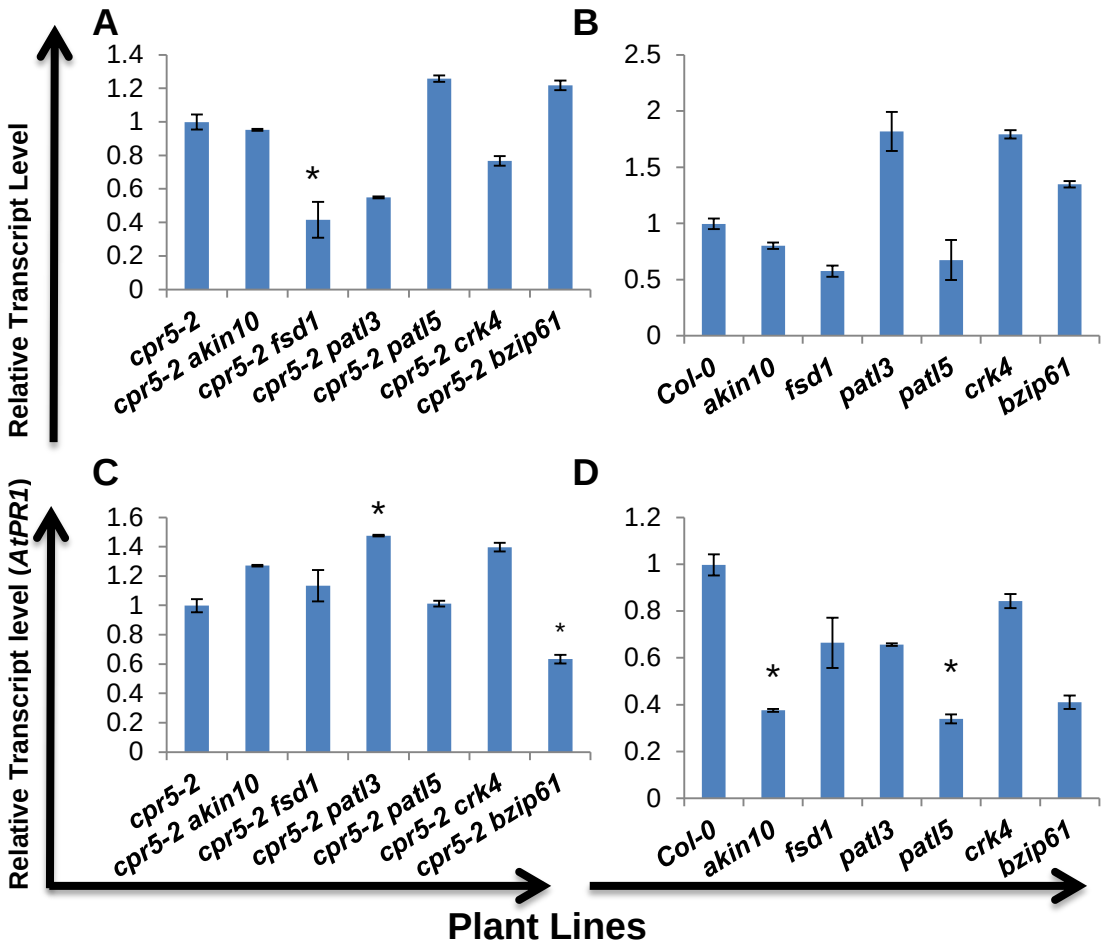

E ***AtPDF1.2***

	cpr5-2		*Col-0*
cpr5-2	1	***Col-0***	1
cpr5-2 akin10	0.952	***akin10***	0.801
cpr5-2fsd1	0.415	***fsd1***	0.576
cpr5-2 patl3	0.550 (T)	***patl3***	1.817
cpr5-2 patl5	1.257	***patl5***	1.793
cpr5-2 crk4	0.767	***crk4***	0.675
cpr5-2 bzip61	1.217	***bzip61***	1.348

F ***AtPR1***

	cpr5-2		*Col-0*
cpr5-2	1	***Col-0***	1
cpr5-2 akin10	1.271	***akin10***	0.376
cpr5-2 fsd1	1.134	***fsd1***	0.665
cpr5-2 patl3	1.475	***patl3***	0.657
cpr5-2 patl5	1.397	***patl5***	0.843
cpr5-2 crk4	1.012	***crk4***	0.340
cpr5-2 bzip61	0.633	***bzip61***	0.410

No significant difference in expression
Up-regulation of expression
Down-regulation of expression
(T) trending (not statistically significant)

.

Figure 3.21: Transcriptional Changes of Defense-Related Genes PR1 and PDF1.2 in Arabidopsis Mutant Plant Lines
Transcriptional changes in A, B) PR1 and C, D) PDF1.2 in wild-type, single and double mutant Arabidopsis thaliana. Relative transcript abundance (fold change) was determined by qRT-PCR and was normalized to cpr5-2 single mutant plants using two internal reference genes AT2G31270 and TUB5. E, F) Heat map visual summary of results with relative transcript levels. Error Bars represent mean SEM of 3 biological replicates. * indicates statistically significant ($p<0.05$) differential expression when compared with control cpr5-2 (A,C) and Col-0 (B,D) plants.

Discussion

CPR5 was first identified in a screening for mutants with altered resistance, and was named constitutive repressor of pathogenesis related genes 5 (Bowling, Clarke, Liu, Klessig, & Dong, 1997). However, since its discovery, *cpr5* has been extensively studied and evidence suggests that *CPR5* plays a role in various plant processes; and mutation of this gene confers a variety of altered phenotypes. These altered phenotypes include not only morphological changes, but also confer hypersensitivities to various hormones and sugars, resistance to various pathogens, as well as other stresses such as drought, heat, etc. *cpr5* mutant plant lines exhibit constitutively high levels of ROS as well as high expression of defense related genes such as PR1 and PDF1.2 (Aki et al., 2007; Boch, Verbsky, Robertson, Larkin, & Kunkel, 1998; Bowling, et al., 1997; Gao et al., 2011; H.-C. Jing, Anderson, Sturre, Hille, & Dijkwel, 2007; H.-C. Jing & Dijkwel, 2008; H. C. Jing et al., 2008; Kirik et al., 2001; Perazza et al., 2011; Yoshida, Ito, Nishida, & Watanabe, 2002).

The first published interaction assays involving CPR5 indicated that CPR5 interacts with several cell cycle related genes (CKI's), namely *SMR1, SIM* and less strongly to *KRP2* (S. Wang, et al., 2014). This suggests that CPR5 might be a multifunctional protein with numerous protein partners. The confirmed physical interaction with these 3 proteins using proteomic assays, corroborates that CPR5 interacts with proteins within the nucleus. SIM and CPR5 interaction was confirmed via Y2H pairwise assay where the transformation of AD-SIM and BD-truncated-CPR5 (S. Wang, et al., 2014) expression vectors into yeast, resulted in interaction between the expressed SIM and CPR5 fusion proteins. This interaction was observed as yeast capable of growing on highly stringent media (S. Wang, et al., 2014). KRP2 and CPR5 interaction was observed using BiFC and fluorescent signals were observed in the nuclei from reconstructed florescent proteins (S. Wang, et al., 2014). This study takes into account these published interactions and conducts similar assays to determine the validity of these reported interactions.

With limited data available and in-depth analysis yet to be performed for all the newly identified proteins, the data described here constitutes an important first step towards identifying protein that's physically interact with CPR5; and how CPR5 fits into the regulatory pathways of plant processes it has previously been associated.

4.1 Interaction Studies Identified and Confirmed Protein Interactions

4.1.1 Y2H Identification of CPR5 Potential Protein Partners and Interacting Domains

The initial Y2H assay consisted of a commercial screen (Clontech Laboratories, 2013) that allows interaction studies using a normalized transcriptome library of *Arabidopsis thaliana*, but the coding regions cloned in the AD-vector are not full length gene coding regions (Clontech Laboratories, 2015). Rather, a technique called SMART cDNA library construction was used to create the cDNA library (Clontech Laboratories, 2015; Maier, et al., 2011) which consists of cDNA synthesized from the mRNA of 11 different *Arabidopsis* tissues and was normalized to reduce the copy number of highly represented mRNA and to increase the copy; of lowly expressed transcripts (Clontech Laboratories, 2015; DeGrado-Warren et al., 2008). In addition, the library of cDNA was sized selected (1.0-2.4kb). This selection of cDNA, averaging 1.2kb in length, was not intended to yield full length cDNAs; rather it was designed to express protein domains for protein-protein interaction. Analysis of the 82 constructs sequenced confirmed that a majority of the coding regions cloned into the GAL4-AD plasmid were not full length coding regions, and a majority of coding regions observed were 1.0-1.5kb confirming that the library contained selected cDNA of specific sizes (data not known).

Some types of protein-protein interactions are inherently missed in Y2H due to the limitations of the system (Brueckner, et al., 2009; Huang & Bader, 2009; Koegl & Uetz, 2007). The yeast cell does not provide a suitable environment for interactions involving membrane proteins, or proteins requiring post-translational activation, transcriptional activation, or specific localization or complex formation (Brueckner, et al., 2009). However researchers have had great success with the Y2H library system as it allows for high throughput analysis of proteins(Brueckner, et al., 2009).

The unique Y2H library construction model provides a mode of detecting protein-protein interactions by only providing protein domains for interaction with the protein of choice, in this case CPR5 (Brueckner, et al., 2009). As such, the library screening provides a method of bypassing the requirements of any protein modification or environment to stabilize a protein for interaction by only translating important protein domains, and essentially truncating the protein similar to what was done to CPR5 in this study. The translation of these protein domains yields an opportunity to detect protein interactions

that would normally not be detectable in a yeast host due to any number of parameters required to translate a fully functioning plant protein in a yeast host, and to provide the correct environmental conditions and localization to positively allow for interaction.

The Y2H screening identified CRK4, a protein that is annotated to be a cytosolic membrane bound protein (Du, Wang, Liang, & Lu, 2005; Harmon, 2003; Hofmann & Stoffel, 1993). Due to the differences in cell morphology, this plant membrane protein may not adopt the proper conformation in yeast without being membrane bound. Consequently, this interaction may have been missed if the CRK4 protein was fully translated. Consistent with this suggestion, was the lack of medium and strong interaction between CPR5TM0 and CRK4 despite the truncated CRK4 (tCRK4) interacting with both CPR5TM0 and CPR5TM1 (Figure 3.7). Sequence analysis of the 3 library tCRK4 constructs revealed that the 3 individual constructs included the coding region for the N-terminal end of the CRK4 protein starting at aa359, which is truncated directly after the predicted transmembrane regions (aa 251-267, and aa 328-348) (Table 3.1) (Hofmann & Stoffel, 1993), consistent with the suggestion that the truncation of transmembrane regions may be the reason this interaction was identified. Given that CPR5 was truncated to overcome the issue of the protein binding to the yeast membrane, it is likely that many of the interactions observed with CPR5 in the Y2H screening was a result of translating only specific protein domains.

Also notable was AKIN10 interaction with both CPR5TM0 and CPR5TM1 constructs under medium stringency media but not high stringency media indicative of a weaker interaction occurring between CPR5 and AKIN10. As a strong interaction is observed between CPR5 and truncated AKIN10 (tAKIN10), this difference in observable interaction may be due to restrictions of the AKIN10 CPR5-interacting protein domain by the full AKIN10 protein structure, or potential misfolding of AKIN10 in yeast.

Protein binding sites and interaction sites often require some protein activation or modification making it difficult to know if proteins are being correctly folded in yeast. As protein domains and interaction sites are conserved across numerous proteins and within protein families, the observed interaction of CPR5 with what is believed to be a protein domain of one protein could be the mirroring the interaction CPR5 would have with another protein with the same or similar protein domain. Although identification of CPR5 interaction with a specific domain does not necessarily identify the protein CPR5 interacts with, it could provide insight on how CPR5 functions within the cell.

For instance, truncated CPR5 was found to interact with PATL3, PATL5, and PATL6 protein domains in the Y2H screen. As these 3 proteins have been annotated to have a conserved Sec14 lipid binding domain and Golgi dynamics domains (Peterman, 2004), it is possible that CPR5 observed interaction with the 3 protein domains constructs was due to CPR5 interaction with the conserved Sec14 or Golgi dynamics protein domain, rather than with the specific consensus sequence of the protein identified. CPR5 interaction with specific protein domains could provide insight on which proteins to explore in future research.

Alternatively, the protein domain may be missing crucial coding regions that are required to interact with CPR5 either directly or concurrently with CPR5. Sequence analysis of constructs found to include fragments of the same gene, but with different segments of gene coding regions inserted into the GAL4-AD plasmid indicate that interacting proteins may have been missed due to the partial coding regions being translated. As mentioned earlier, CPR5 interaction with these protein domains may be a false positive as CPR5 may interact with these domains in other proteins not identified. Without the necessary protein elements to regulate interaction with important protein domains, nonspecific binding to these protein elements is likely to occur. The Y2H library screening provides the initial basis for determining CPR5 interacting proteins and interacting protein domains, but does not provide a definitive answer as to whether or not the proteins identified are protein partners of CPR5.

As mentioned, the library includes multiple constructs with partial or full coding regions to the same gene/protein. If the coding region is not cloned into the MCS in the proper reading frame, translation of the coding region will not result in the protein of interest being translated, and therefore an interaction should not have been identified. Analysis of the sequenced constructs identified a majority of the coding regions were not in frame with the GAL4-AD domain. These frame-shifted coding regions indicate that many of the coding regions may not translate accurate protein domains.

In order to supplement the results of the Y2H library screening, and to account for the limitations of the library screens, Y2H protein pair assays were used to provide further evidence that the genes identified in the Y2H commercial library screen are protein partners of CPR5. Using this method to analyze interactions of CPR5 with full length proteins of interest, CPR5TM0 interaction was observed with MYB3, BZIP61 and SIM, whereas CPR5TM1 was observed to interact with MYB3 and CRK4 as identified by yeast growth exhibiting a blue hue on highly stringent media (Figure 3.7). Interestingly, BZIP61 was only able to interact with CPR5TM0 similar to truncated BZIP61 indicating that the

interaction may require the truncation of the putative transmembrane domain not truncated from CPR5TM1. CPR5 interaction with these full length proteins, coupled with CPR5 interaction with their respective protein domains give credence to the possibility of these being true CPR5 interacting partners.

However, this method, although widely used, does not detect the direct interaction of two proteins, but rather detects the ability of two proteins to activate the expression of the reporter genes via interaction of the GAL4BD and GAL4AD. As such, this method to determine the interaction of two proteins does not provide the most accurate means of detecting the direct interaction of two proteins. However, this limitation has largely been addressed by the use of numerous reporter genes (Clontech Laboratories, 2013). The difference in outcome from the Y2H commercial screening and the Y2H protein pair assay may be due to the length of the coding region. As the full length coding region was cloned into the GAL4-AD vector rather than selected protein domains, the use of an artificial host system disregards the possibility that any of the proteins of interest may require post translational modification, specific localization, or complex formation not possible in yeast, to interact with CPR5. Alternatively, the difference in results between the two Y2H assays may be due to the use of different GAL4-AD plasmids. The commercial library was cloned into plasmid pGADT7-RecAB, whereas the full length coding regions were cloned into pGADT7 (Clontech Laboratories, 2013, 2015). Although there are no major differences between the two plasmids, the difference in the multiple cloning sites may have affected the conformation of the GAL4-AD fusion protein.

Despite the inherent flaws, the interactions observed using the Y2H system provided evidence that CPR5 may be able to interact with multiple protein partners of varying functions, but these interactions may not mirror those that would occur in an *in vivo* assay. As the yeast host system is far less complex than the plant host, it is difficult to ascertain the validity of these interactions without further experimentation using full length CPR5 proteins in a less foreign host. However, the ability of the interacting fusion proteins to activate all the reporter genes provides promising evidence for the interaction of truncated CPR5 with these proteins, and the ability to interact with CPR5 as protein domains and as full length proteins.

4.1.2 BiFC Identified 6 different Protein-Protein Interactions *in planta*

In order to address some of the limitations of the Y2H system, BiFC was used to provide further insight on the interactions of CPR5 as well as the localization. BiFC is an experimental tool typically used to validate protein-protein interactions (C.-D. Hu, et al., 2006; Kerppola, 2006). This protocol, however, has its limitations. It has been reported that the orientation of the fluorescent tag halves and proteins must be correctly aligned to provide proper protein-protein interaction and subsequent fluorescent tag reconstitution (Horstman, Tonaco, Boutilier, & Immink, 2014; C.-D. Hu, et al., 2006; Kerppola, 2006). Alternatively, the location of the tag on the protein N or C terminus may affect the protein folding and function. However this limitation can be overcome with the proper controls and use of all combinations of fusion constructs. It is also important to note that BiFC utilizes a transient *Nicotiana benthamiana* system, which, although is a plant system can vary from Arabidopsis and may yield improperly folded or localized proteins that are native to *Arabidopsis thaliana*. However, *Nicotiana benthamiana* has been shown to be an excellent model for transient expression assays and an excellent model for *in planta* studies (Kerppola, 2006; Ohad, Shichrur, & Yalovsky, 2007; Waadt et al., 2008). Several researchers have predicted CPR5 to be a nuclear membrane bound protein with a nuclear localization signal, which may interact with proteins on both sides of the membrane (Daniel Perazza, et al., 2011; S. Wang, et al., 2014). If the predicted model is true, then depending on the location of the fluorescent tag, different proteins may yield positive fluorescence. It has also been noted that CPR5 may be truncated after translation (Daniel Perazza, et al., 2011) and depending on the location, of the fluorescent tag segments, the tag may be excised along with CPR5, causing nonspecific localization or dual localization depending on the functionality of this putative protein fragment.

It is also important to note that, due to the use of the 35S promoter, the fluorescence exhibited by positively identified protein-protein interactions may be due to false positives due to the saturation of cells with the two fusion proteins (Gookin & Assmann, 2014; Horstman, et al., 2014), which can cause high background signal (Horstman, et al., 2014). However, advancements in fluorescent protein processing, and development of new fluorescent tags has largely accounted for possibility of false positives due to high background signal (Gookin & Assmann, 2014; Horstman, et al., 2014; C. Wang et al., 2012). Consistent with this was the use of the enhanced YFP tag in this study and the lack of visible background observed in the negative control BiFC assays.

Fluorescence from the interaction of the two BiFC complexes in living cells has been reported to be less than 10% of that produced by an intact fluorescent proteins (Kerppola, 2006). The lack of observable fluorescence within the nucleus of the EDS1/EDS1 positive control confirms this observation as EDS1 is known to dimerize within the nucleus (Figure 3.7A, 3.8A) (Feys, et al., 2001). Despite the use of a 35S promoter to provide constitutive expression of the fusion proteins, fluorescence was not observable in a majority of the living cells analyzed. As such, several interactions may have been missed due to low fluorescence levels or the infrequency of fluorescent cells due to low cell transformation levels.

Many of the initial limitations of BiFC have been overcome as the technique has advanced. The remaining limitations can be overcome with the use of good positive and negative controls, as well as constructing fusion proteins with the YFP fragments attached in both ends of each protein of interest as one done in this study (Fang & Spector, 2010; C.-D. Hu, et al., 2006; Kerppola, 2006; C. Wang, et al., 2012). However, in this study, not every conformation of constructs was produced, suggesting that interactions may have been missed. Additionally, although only one interaction was identified to occur in the nucleus, and no fluorescence was observed with transcription factor proteins MYB3, BZIP61, or AKIN10 in the nucleus, this does not discount that an interaction does exist. As the positive control EDS1+EDS1 was able to emit fluorescence from the cytoplasm (Figure 3.10B), this interaction was unable to emit visible fluorescence in the nucleus as observed when EDS1-YFP was transiently transformed into *Nicotiana benthamiana*. Despite the limitations mentioned, observable fluorescence was detected with six different proteins of interest with the two CPR5-YFP constructs indicative of positive interaction between CPR5 and the aforementioned proteins (Figure 3.7). CPR5 interaction with these six proteins provides further evidence of the already observed interactions found in the Y2H screening and protein pair assays.

4.2 Effect of mutation of potential interacting proteins on *cpr5-2* hypersensivity to sucrose

4.2.1 Effects of Dark Treatment on *cpr5-2* Double Mutant Seedlings

cpr5-2 mutants grown under skotomorphogenic conditions (dark conditions) exhibit shorter hypocotyls than WT Col-*0* seedlings (Yoshida, et al., 2002), making the study of *cpr5-2* double mutant lines under similar conditions, making it a viable approach to observing any rescue or alteration of cpr5 skotomorphogenic response. Skotomorphogenic development consists of several survival mechanisms adopted by plants (Josse & Halliday, 2008). These mechanisms include, repressing root elongation in favor of hypocotyl elongation in order to locate a light source necessary for normal plant development. As well as, the formation of an apical hook occurs, which is traditionally due to the need to break through soil or other barriers in order to seek light (Josse & Halliday, 2008). Apical hook formation protects the apical meristem as well as the unfolded cotyledons and becomes less pronounced as the seedling develops (Josse & Halliday, 2008).

Skotomorphogenic development appears to be affected in several of the double mutants and is not observed in the single mutant parent lines. Most notably, *cpr5-2 akin10, cpr5-2 fsd1, cpr5-2 patl3, cpr5-2 patl5* all exhibit elongated roots when grown under darkness for 3 days, and *cpr5-2 akin10 and cpr5-2 patl3, and cpr5-2 patl5* exhibited similarly longer roots after day 5. As root elongation is suppressed during skotomorphogenesis, the elongated roots exhibited by these double mutants are suggestive of an alleviation of skotomorphogenic repression of root elongation, perhaps due to a misregulation of these developmental pathways.

4.2.2 *CPR5* and *BZIP61* Regulation of Root Elongation in Response to Exogenous Application of Sugar.

Analysis of the root elongation of *cpr5-2,* Col-*0,* SALK single mutants and *cpr5-2* SALK double mutants resulted in similar root phenotypes between a majority of the SALK lines and Col-*0*, and similarly between *cpr5-2* and *cpr5-2* SALK double mutants. However, *cpr5-2 bzip61 and bzip61* mutants exhibited markedly different root phenotypes than *cpr5-2*

seedlings and Col-*0* seedlings when germinated on sucrose supplemented media. *cpr5-2 bzip61* double mutant exhibited root lengths and elongation patterns similar to Col-*0* seedlings. Conversely, *bzip61* exhibited *cpr5-2* like root elongation when subjected to sucrose treatments, suggesting that *BZIP61* plays a regulatory role in sugar-dependent root elongation. Although the overall root lengths of *bzip61* were longer than *cpr5-2* root lengths, they were markedly shorter than *cpr5-2 bzip61* and Col-*0* root lengths. *cpr5-2 bzip61* double mutant root lengths measured at day 5 under 2.0% sucrose treatment were longer than cpr5-2 roots and exhibited greater than WT root lengths, suggesting an interaction occurring between CPR5 and BZIP61 as abolishing BZIP61 in a *cpr5-2* background is able to rescue *cpr5-2* altered root phenotype in the presence of high sucrose treatment.

Although, hypocotyl lengths are negatively impacted by increased concentrations of sucrose treatment, the overall lengths of *bzip61* seedling hypocotyls was significantly shorter than Col-*0,* whereas the hypocotyl lengths of cpr5-2 bzip61 were significantly longer than cpr5-2 seedlings. Abolishment of BZIP61 in a *cpr5-2* background partially rescues the stunted hypocotyl elongation phenotype exhibited by cpr5-2 mutant seedlings. However, the *bzip61* single mutant exhibited shorter hypocotyls than Col-*0*. These observations suggests that CPR5 acts upstream of BZIP61 and positively regulates BZIP61 regulation of normal root growth under dark and sucrose treatment. However, as abolishing both CPR5 and BZIP61 is only partially able to rescue the down-regulated hypocotyl elongation exhibited in *cpr5-2* seedlings, there is likely an alternative mechanism influencing *cpr5-2* stunted hypocotyl elongation. Consistent with this theory is the difference in phenotype exhibited by *cpr5-2* and *cpr5-2 bzip61* mutant seedlings as compared to *bzip61* single mutant seedlings. Nevertheless the single and double mutant phenotypes are consistent with a physical interaction between CPR5 and BZIP61 as suggested by the Y2H results.

4.2.3 *CPR5* Regulation of *AKIN10* Sugar Starvation-dependent Activation.

AKIN10, is an isoform of sucrose nonfermenting-1-related protein kinase 1 (*SnRK1*), which acts as a cellular energy metabolism sensor that is activated by sugar deprivation (Jeong, Seo, Woo, & Park, 2015). *AKIN10* has been reported to be functionally redundant to AKIN11. Consistent with this concept is the lack of observable phenotype changes in *akin10* single mutants (Coello, Hey, & Halford, 2011; Fragoso et al., 2009). Also the

characteristics of redundant proteins, abolishment of both *AKIN10* and *AKIN11* were consistent in a double mutant resulted in impairment of starch degradation (Fragoso, et al., 2009). As *AKIN10* has been reported to be activated by sugar starvation conditions (Fragoso, et al., 2009; Tsai & Gazzarrini, 2012), abolishment of *AKIN10* could potentially lead to the misregulation of sugar starvation sensing and subsequent misregulation of cellular energy metabolism signaling as akin10 is involved in resource allocation during sugar starvation (Baena-González, Rolland, Thevelein, & Sheen, 2007; Fragoso, et al., 2009; Jeong, et al., 2015; Tsai & Gazzarrini, 2012).

Under dark treatment, abolishment of *AKIN10* in the *cpr5-2* background resulted in markedly longer hypocotyls and roots as compared to *cpr5-2* suggesting a partial rescue of *cpr5-2* inhibition of hypocotyl elongation and an exaggerated root elongation phenotype. Interestingly, sucrose treatment abolished the alleviation of *cpr5-2* inhibition of hypocotyl elongation, yielding hypocotyls similar in length to *cpr5-2* after 3 days of sucrose treatment. After 5 days of treatment, hypocotyl elongation was markedly decreased in *cpr5-2 akin10* with hypocotyls significantly shorter than *cpr5-2*.

cpr5-2 akin10 mutants exhibited longer hypocotyls under dark treatment, but near *cpr5-2* length hypocotyls after sucrose treatment indicating a more exaggerated inhibition of hypocotyl elongation in response to exogenous application of sugar. Sucrose treatment resulted in a 40% decline in *cpr5-2* hypocotyl length, whereas a 60% decline in hypocotyl length was observed in *cpr5-2 akin10* double mutant seedlings. As dark treatment appears to alleviate *cpr5-2* hypocotyl inhibition and sucrose treatment exaggerates it in *cpr5-2 akin10* mutants, there appears to be a genetic link between *CPR5* and *AKIN10*. However, the mechanism by which the two interact and regulate growth in response to skotomorphogenic conditions or sugar treatment is still to be determined.

As mentioned, *cpr5-2 akin10* roots exhibited longer average root lengths than *cpr5-2* when grown under dark treatment suggesting AKIN10 involvement in the negative regulation of root growth under skotomorphogenic conditions. However, this exaggerated root elongation phenotype was alleviated under sucrose treatment at 3 days suggesting that sucrose treatment has an antagonistic effect on AKIN10. As AKIN10 is believe to act as a negative regulator of plant development under sugar starvation conditions, abolishment of AKIN10 should lead to an inactivation of this mechanism, allowing *akin10* single mutants to grow uninhibited under sugar starvation conditions (dark 0% sucrose). This is not observed in *akin10* single mutants, but is observed in the *cpr5-2 akin10* double mutant, suggesting that interaction between AKIN10 and CPR5 is required for the regulation of AKIN10 sugar starvation-dependent activation.

A theoretical model that could explain this observed *cpr5-2 akin10* phenotype is CPR5 upstream negative regulation of AKIN10 sugar starvation-dependent response. As CPR5 acts as a negative regulator of AKIN10, abolishment of AKIN10 would lead to the misregulation of CPR5 suppression, leading to uninhibited growth similar to WT seedlings, as is observed. However, under sugar starvation, CPR5 is suppressed by some unknown mechanism thereby suppressing CPR5 negative regulation of AKIN10, allowing growth.

Alternatively, the difference in root elongation phenotype exhibited by *cpr5-2 akin10* after 3 days of sucrose treatment versus 5 days could be due to an independent mechanism of plant sugar response that indirectly influences AKIN10 and CPR5 regulation of root elongation. In the presence of sucrose or glucose, in planta levels of sugars was higher after two days but was markedly decreased by 5 days independent of the high sugar content still present in the media (Dijkwel, Kock, Bezemer, Weisbeek, & Smeekens, 1996). Taking this into account, the endogenous levels of sucrose are lower in the seedlings by day 5, thus sugar response may be reduced accordingly. The lower sugar content could be enough to activate an *akin10* redundant sugar response mechanism leading to a repression of growth despite consistently high sugar levels in the media.

This is consistent with AKIN10 activation under sugar starvation conditions, as sugar starvation leads to repression of plant growth and the reallocation of resources (Yu, 1999). As high sugar levels in theory act antagonistically on AKIN10 activation, abolishing *AKIN10* should lead to similar effects of exogenous application of high sugar levels, leading to a misregulation of controlled root growth. As sugar starvation conditions activate AKIN10, high sucrose levels should inactivate AKIN10 response to starvation conditions. In the presence of sucrose, AKIN10 negative regulation of growth and the positive reallocation of resources cannot occur. It has been reported that seedlings have an efficient mechanism for the removal or processing of extra sugars (Dijkwel, et al., 1996). In conclusion, the results suggest a genetic interaction between *CPR5* and *AKIN10*, consistent with a physical interaction between the encoded proteins as predicted by the Y2H data.

4.2.4 Uncoupling CPR5 Hypersensitivity to Sugar –Future Outlooks

The proposed mechanisms of CPR5 interaction based on the double mutant phenotypes observed is only speculation however and has no definitive evidence. The dark treatment

and sugar treatment assays performed constitutes a basic first step towards uncoupling the altered phenotypes observed in *cpr5-2* mutants and provides evidence of interaction with CPR5 via the partial rescue of *cpr5-2* hypersensitivity to sugar.

More research must be conducted in order to unlink the various partial phenotypes observed across all the double mutant lines. Analysis of a *cpr5-2 akin10 akin11* triple mutant would provide a basic first step in understand the mechanism behind *AKIN10* and *CPR5* interaction and regulation of sugar starvation and sugar signaling. Further studies must also be conducted to determine the effect of phytohormones on the *cpr5-2* SALK double mutant lines as *cpr5-2* exhibits markedly hypersensitive responses to a majority of phytohormones. Looking at the effects of antagonists such as ethylene and cytokinin will provide information on the possible influences phytohormones have on the altered sugar sensitivity phenotypes observed in the *cpr5-2* double mutants (Aki, et al., 2007).

4.3 Identification of Plant Processes Relating to CPR5 Interaction with the Identified Proteins of Interest

4.3.1 CPR5 may Confer Drought Tolerance through Interaction with Heatshock Protein DNAJ.

In order to address *CPR5* regulation of abiotic stresses, *cpr5-2* double mutants were observed for rescue of *cpr5-2* drought tolerance phenotype. Interestingly, none of the double mutant lines observed exhibited a rescue of the *cpr5-2* drought tolerance phenotype, rather they all exhibited *cpr5*-like increases in drought tolerance (Figure 3.13). Due to the absence of rescue of *cpr5*-2 enhanced drought tolerance, it can be postulated that the genes of interest code for proteins that work upstream of CPR5 to regulate drought tolerance, or that redundancy in interacting proteins exists. Alternatively, proteins not yet identified may be responsible for the regulation of CPR5 dependent drought tolerance.

This suggests that if CPR5 regulation of drought involves interaction with AKIN10, FSD1, BZIP61, CRK4, PATL3 OR PATL5, and that this interaction occurs upstream of CPR5 due to the lack of rescue exhibited by the *cpr5-2* double mutants of *cpr5-2* drought tolerance. Alternatively, as only six double mutant lines were generated, 4 proteins of interest were not further studied via analysis of double knockout mutants; and could be involved in the interaction necessary to regulate drought tolerance and other abiotic stresses that are enhanced in *cpr5-2* mutants.

As no drought or abiotic stress studies have been conducted on published CPR5 interacting partners SIM, SMR1 and KRP2, it is possible that DNAJ, a heatshock chaperone protein (Qiu, Shao, Miao, & Wang, 2006) annotated to play a regulatory role in NaCl stress tolerance (Zhao, et al., 2010) and identified in the Y2H screen, is responsible. DNAJ overexpression leads to tolerance of salt stress (Zhao, et al., 2010). Salt stress elicits a complex response from plants as salt toxicity also causes osmotic stress (Hasegawa, Bressan, Zhu, & Bohnert, 2000; Niu, Bressan, Hasegawa, & Pardo, 1995). Interestingly, DNAJ is a chaperone protein and known to hold proteins in an unfolded state (Qiu, et al., 2006), which provides an alternative model of DNAJ interaction with CPR5.

As heatshock proteins are well documented to help cells regulate the harmful effects of abiotic stresses such as NaCl, heat, and drought through proper protein folding and activation of regulatory pathways, DNAJ may regulate drought tolerance by binding and

inactivating CPR5 during times of stress. This theory is consistent with *cpr5* enhanced tolerance to drought due to the lack of a functional CPR5 protein. Additionally, *dnaj* single mutant plants exhibited wild-type like growth (data not shown), but no drought tolerance assays were performed to determine the effects abolishing *DNAJ* on drought tolerance.

DNAJ was also not extensively studied, as no *cpr5-2 dnaj* double mutant plant line was produced for further analysis. However production of a *cpr5-2 dnaj* to study the effects *dnaj* has on *cpr5-2* enhanced drought tolerance would provide insight on the mechanism by which *cpr5-2* confers enhanced drought tolerance.

ABA is involved in drought tolerance, however, studies suggest that *cpr5* increased tolerance to drought may be independent of ABA (Gao, et al., 2011; Swamy & Smith, 1999; Yan, Tsuichihara, Etoh, & Iwai, 2007). As DNAJ is a protein known to help in the regulation of stresses, it can be inferred that proper function of DNAJ would confer mediation of ROS levels. Observations of ROS levels in *dnaj* and *cpr5 dnaj* mutants could provide the interaction responsible for the up-regulation of ROS levels observed in *cpr5*. Given that DNAJ interaction with CPR5 may confer mediation of ROS levels, DNAJ interaction with CPR5 may be the regulatory mechanism that controls tolerance to abiotic stresses independent of the ABA-dependent drought tolerance regulation, whose misregulation confers *cpr5* enhanced tolerance to abiotic stresses caused by drought, heat, and NaCl.

4.3.2 CPR5 as a Putative Mediator of ROS via Interaction with a Superdismutase

ROS plays conflicting roles in plants. ROS can be detrimental to cellular functions and yet they are also important signalling molecules that are natively produced (Apel & Hirt, 2004). Plants have developed crucial mechanisms to deal with ROS, including modification of gene expression upon exposure, and maintenance of ROS scavenging mechanisms. ROS are capable of inducing superoxide, singlet and triplet oxygen, nitric oxide, and hydroxyl radicals that can cause damage to nucleic acids, proteins lipids through oxidation. To maintain the correct levels of ROS, plants have evolutionarily developed antioxidant systems (Apel & Hirt, 2004; Pallavi, et al., 2012; Tripathy & Oelmüller, 2014).

Environmental stresses are known increasers of superoxide production within plants, and plants are believed to rely on superoxide dismutase (SOD) enzymes to detoxify these reactive oxygen species (Kliebenstein, Monde, & Last, 1998; Pallavi, et al., 2012). Superoxide dismutases are enzymes that act as antioxidants. CPR5 has been suggested as

a mediator of ROS levels (Hebeler et al., 2008; H.-C. Jing & Dijkwel, 2008). Transcriptomic and proteomic analysis of pre-symptomatic *cpr5* mutants indicated that 3 of 5 universal ROS marker genes, 16 out of 27 genes induced by six ROS treatments, and one third of ROS-dependent putative transcription factors were upregulated in cpr5 mutants (Hebeler, et al., 2008; H.-C. Jing, et al., 2007; H. C. Jing, et al., 2008). These observations indicate that cpr5 is under intense oxidative stress, which is confirmed by the presence of high ROS levels in *cpr5* mutants. These also suggest that CPR5 may act as a mediator of ROS and that the changes in regulation in *cpr5* mutants are a result of the misregulation of ROS expression.

FSD1, an iron superoxide dismutase, is one protein identified via Y2H screening and whose interaction was also observed via BiFC. As FSD1 is one of several in a family of super dismutases, it is plausible that the CPR5 interacts with FSD1 to mediate ROS levels. FSD1 has been reported to be localized in the chloroplasts, plastids and cytoplasm (Kliebenstein, et al., 1998; Myouga et al., 2008); however BiFC analysis of FSD1 and CPR5 interaction yielded observable fluorescence that is not consistent one localization to the cytosol compared to the positive control or any one specific organelle or the nucleus. As the proteins are expressed through a 35S promoter, the overexpression of the nYFP-FSD1 and cYFP-CPR5 may have allowed a finite number of YFP halves to reconstitute function resulting in a false positive at nondescript localizations (Gookin & Assmann, 2014; Horstman, et al., 2014). Positive interaction between CPR5 and FSD1 via YFP fluorescence also supports that this interaction is occurring outside of the nucleus.

Although CPR5 has been proposed as a regulator of the ROS gene network, it is unclear whether the effects of cpr5 on ROS levels observed in *cpr5* mutants is due to misregulation of the ROS gene network, or due to misregulation of other regulatory pathways that indirectly affect the ROS gene network. The ROS signalling pathway is extensively complex and includes input from numerous signalling partners and pathways (Baxter, Mittler, & Suzuki, 2014; Mittler et al., 2011; Torres, Jones, & Dangl, 2006; Vellosillo, Vicente, Kulasekaran, Hamberg, & Castresana, 2010). As no one interaction is in charge of ROS regulation and signalling, it is not remarkable that the *cpr5 fsd1* double mutant exhibits similar phenotypes to *cpr5-2* under normal or drought conditions, as FSD1 would be only one of many mediators of ROS. However, *cpr5-2 fsd1* did exhibit a 2 fold down-regulation of *PDF1.2*, quantified by qRT-PCR. *PDF1.2* is a pathogen defense gene whose expression is increased as a result of pathogen attacks as well as abiotic stresses such as UV-B light exposure. The up-regulation of *PDF1.2* gene expression requires the presence of ROS. As ROS levels were not measured in the *Arabidopsis* mutants, it is difficult to determine the

role of *FSD1* in ROS maintenance. In addition, as it is unclear whether ROS levels were rescued in the *cpr5-2 fsd1* double mutant, it is difficult to conclude whether the down regulation *PDF1.2* was a result of a rescue of *cpr5-2* upregulated *PDF1.2* expression phenotype via ROS maintenance, or a direct regulation of pathogen resistance or abiotic stress tolerance. Studies of *fsd1* single mutants confirm that knockout of *FSD1* allows the plant to grow normally contrary to *fsd2* and *fsd3* single mutants which exhibited pale green leaves and retardation of growth (Myouga, et al., 2008). *FSD1* has a functional homolog, *CSD2*, in the cytosol suggesting that *FSD1* may play a redundant role in plant development under normal growth conditions (Kliebenstein, et al., 1998). *FSD1* transcripts were not detected under normal growth conditions but was observed under severe oxidative stress due to low copper levels in soil (Abdel-Ghany, Muller-Moule, Niyogi, Pilon, & Shikanai, 2005). Although no visible phenotypes were exhibited my *cpr5-2 fsd1* mutant plants, there is overwhelming evidence that suggests an interaction is occurring between FSD1 and CPR5. FSD1 is the only protein of interest identified through the Y2H screen to be a complete protein. Alternatively, interaction with CPR5 was identified via BiFC, and abolishing *FSD1* is a *crp5-2* background yielded a rescue of *cpr5-2* up-regulation of PDF1.2 suggesting that the abolishment of both CPR5 and FSD1 leads to an alleviation of the constitutive resistance observed in *cpr5-2* mutants. Taken together, *fsd1* single mutants and *cpr5-2 fsd1* mutants may exhibit responses to endogenous exposure to severe oxidative stress and further study of FSD1 involvement in CPR5 regulation of ROS and defense via pathological studies is required.

4.3.3 CPR5 may Modify PI Signalling through Interaction with SAC9 and Patellins

The Phosphoinositides (PIs) signalling pathway and PI involvement in plant processes is as complex as the hormone signalling pathways, and involved in the regulation of the same processes (Balla, 2013; McSteen & Zhao, 2008). PIs are cellular phospholipids that control numerous aspects of a cell through near universal signalling in eukaryotic cells. PI signalling involves the phosphorylation and dephophorylation of PIs as well as cleavage of PIs by specific PI kinases and relocalization of the modified signalling molecules (Balla, 2013; Williams, 2005). PIs regulate vesicular trafficking, and modulate lipid distribution through interaction with lipid transfer proteins (Peterman, 2004). PIs also regulate ion channels, pumps and transporters and control both endocytic and exocytic processes. PI's exist both in the cytoplasm as well as in the nucleus (Balla, 2013).

One of the most characterized PIs is PtdIns (4,5)P (2). Alteration of PtdIns (4,5)P (2) concentrations resulted in defects in the actin cytoskeleton and exocytosis (Desrivieres, Cooke, Morales-Johansson, Parker, & Hall, 2002; Tall, Spector, Pentyala, Bitter, & Rebecchi, 2000; Yin & Janmey, 2003). Additionally, PtdIns (4,5)P (2) and it's derivative accumulate during abiotically stressed plants (X. M. Wang, 2002). PtdIns (4,5)P (2) signalling is terminated through the action of inositol polyphosphate phosphatases and PI phosphatases including suppressor of actin mutation (SAC) domain phosphatases (Meijer & Munnik, 2003). SAC9 was identified in the initial Y2H screen for potential protein interactants of CPR5, but was not extensively studied due to the length of the *SAC9* coding region (5kb) making it difficult to clone, as well as the difficulty of creating a successful *cpr5-2 sac9* double mutant. The *sac9* mutant exhibits several phenotypes that mirror *cpr5-2* including constitutive stress response and overexpression of stress-induced genes, over-accumulation of ROS, dwarfism, and closed stomata (Williams, 2005). SAC9 phosphatase has been suggested to be involved in regulating PI signals during stress response, and if confirmed, CPR5 interaction with SAC9 suggests that *cpr5-2* high stress response may be due to the misregulation of the stress-dependent PI signalling response (Vollmer, Youssef, & DeWald, 2011; Williams, 2005).

Aside from SAC9, CPR5 has also been identified to putatively interact with 3 Sec14-like patellin proteins (PATL), PATL3, PATL5, and PATL6 suggested to play a role in PI binding and membrane trafficking, providing further evidence that CPR5 may be involved in PI signalling (Peterman, 2004). These 3 patellins have not been extensively studied; however analysis of the patellin family confirms the presence of a sec14-like domain conserved across all 6 patellin family members (Peterman, 2004). As the sec14 domain found in yeast and mammals are involved in the binding of PIs as well as in vesicle formation, cytokinesis, and cell plate formation, the 3 patellins identified may be involved in similar processes (Bankaitis, Malehorn, Emr, & Greene, 1989; Stocker & Baumann, 2003). Abolishment of a single patellin did not affect *cpr5-2* phenotypes which may be explained by the suggestion that there is redundancy within the patellin family. Additionally, CPR5 interaction with the patellin family may be redundant similar to CPR5 interaction with SIM and SMR1 (S. Wang, et al., 2014). Triple or quadruple knockout mutants may provide some insight on the true function of this protein family and to the validity of the interactions observed between CPR5 and the 3 members of the patellin family identified. Interestingly, *cpr5-2 patl3* exhibited a significant up-regulation of *PR1* ($p<0.05$) and a trending down-regulation of *PDF1.2* ($p=0.062$), indicating an uncoupling of the regulation of the two defense related gene. As *PR1* and *PDF1.2* are defense-related genes from two

independent plant resistance pathways, PATL3 may antagonistically regulate the expression of these two genes. It is unclear how the patellins, most likely involved in vesicle formation and cell cycle-related pathways (Peterman, 2004) are involved in the regulation of defense-related genes, however it is not out of the realm of possibility as all plant pathways are all interconnected (Balla, 2013; Gururani, et al., 2015; Khan, et al., 2014; Larrieu & Vernoux, 2015; Meijer & Munnik, 2003; Robert-Seilaniantz, et al., 2011).

4.3.4 CPR5 Involvement in Transcriptional Regulation.

Transcription factors are proteins involved in gene regulation (Singh, 1998; Spitz & Furlong, 2012). Generally TFs have several gene partners and work through binding specific DNA binding sites (enhancer or promoter sequence) via their DNA-binding domains. Binding of promoter sequences can stimulate or repress transcription of the target gene (Singh, 1998; Spitz & Furlong, 2012). Among the proteins identified via Y2H were 3 transcription factors, AKIN10, MYB3, and BZIP61.

In silico analysis of CPR5 protein sequence conducted via Phyre2 (Kelley, Mezulis, Yates, Wass, & Sternberg, 2015) proposed CPR5 as an RNA/DNA binding protein and predicted several potential RNA/DNA binding domains at 123-156aa and at 107-131aa (Kelley & Sternberg, 2009). The presence of a predicted bipartite nuclear localization signal and the predicted RNA/DNA binding domains support CPR5 as a nuclear protein and indicate a potential involvement in gene regulation (Faisal, 2015). CPR5 is annotated to have 4 regions that contain putative coiled-coil domains a proposed crucial motif required for action of RNA/DNA binding proteins, supporting CPR5 involvement in transcriptional regulation via DNA binding (Faisal, 2015). The results of *in silico* analysis of CPR5 suggest that CPR5 has the potential to be a TF, or may participate in multi-protein complexes to regulate the transcription of target genes (Faisal, 2015). Transcription factors are generally regulators of multiple gene targets in various processes (Singh, 1998; Spitz & Furlong, 2012). CPR5 interaction with TFs provides a model mechanism by which CPR5 influences multiple regulatory processes through a single protein interaction.

It is difficult to ascertain the potential of CPR5 interaction with MYB3 and BZIP61 as little is known about their specific functions despite being part of large TF protein families (Dubos et al., 2008; Jakoby et al., 2002; Shen, Cao, & Wang, 2007; Zhou et al., 2015; Zimmermann, Heim, Weisshaar, & Uhrig, 2004). BZIP61 is categorized with one other similarly coded protein BZIP34, but their functions have not yet been identified (Jakoby, et al., 2002; Shen, et al., 2007). MYB3 is one of 4 closely related proteins from the R2R3-MYB

subgroup 4, and has been suggested to interact with BHLH proteins that control the expression of flavonoid structural genes (Dubos, et al., 2008; Zimmermann, et al., 2004). However, as TF families generally consist of proteins with overlapping functions (Singh, 1998), it is difficult to predict the effect of CPR5 interaction with MYB3, BZIP61, and AKIN10.

In order to assess the role of CPR5 interaction with AKIN10 and BZIP61, double mutant lines were analyzed to determine any phenotypic alternations to *cpr5-2* mutant phenotypes caused by the abolishment of these transcription factors. No MYB3 double mutant line was created, and no analysis of the single mutant was possible due to the lack of a SALK TDNA insertion line available from TAIR. Consistent with the notion that BZIP61 and AKIN10 (Baena-González, et al., 2007; Tsai & Gazzarrini, 2012) play redundant roles, is the lack of noticeable phenotype differences when abolished in Col-*0* wild-type plants (Figure 3.8). Additionally, abolishing the TFs in a *cpr5-2* mutant background did not rescue any of the *cpr5-2* mutant phenotypes suggesting that the interaction occurs upstream of CPR5 or that these TFs play redundant roles in the regulation of transcription.

Analysis of a *myb3 and cpr5-2 myb3* mutant could yield new insights on the potential interaction between CPR5 and MYB3 and the subsequent effect on downstream processes. Although no alterations to normal growth or drought tolerance was observed in the *cpr5-2* akin10 and *cpr5-2 bzip61* mutant lines, there is evidence of akin10 and *bzip61* involvement in *cpr5-2* hypersensitivity as measured by the observed alterations to *cpr5-2* phenotypes under both dark and sucrose treatments. However, further analysis is required to uncouple the mechanisms by which CPR5 interacts with AKIN10 and BZIP61, and the exact mechanism by which they both regulate CPR5 sensitivity to dark and sucrose treatments. Although interaction was not identified via BiFC, this may be due to a limitation in the BiFC system to detect low levels of nuclear interaction. Further study should be conducted on these 3 proteins to assess the viability of CPR5 interaction with these proteins in the nucleus.

4.4 CPR5-The Grand Scheme of Things

4.4.1 CPR5 Upstream Regulation of Downstream Targets

There has been a lot of speculation of CPR5 regulation of plant processes (Bao & Hua, 2014; Boch, et al., 1998; Bowling, et al., 1997; Faisal, 2015; Gao, et al., 2011; H.-C. Jing & Dijkwel, 2008; Kirik, et al., 2001; Yoshida, et al., 2002); however the upstream interaction and regulation of CPR5 has not been closely examined despite lack of information available about CPR5 upstream signalling and regulation. As mentioned previously, DNAJ is a heat shock chaperone protein involved in abiotic stress tolerance (Qiu, et al., 2006; Zhao, et al., 2010). However, DNAJ is also known to hold proteins in an unfolded state (Qiu, et al., 2006), which may provide the first look at an upstream element of CPR5 regulation. As heatshock proteins are well documented to help cells regulate the harmful effects of abiotic stresses such as NaCl, heat, and drought through proper protein folding and activation of regulatory pathways, DNAJ may regulate drought tolerance by binding and inactivating CPR5 during times of stress (Whitley, Goldberg, & Jordan, 1999). This theory is consistent with *cpr5* enhanced tolerance to drought due to the lack of a functional CPR5 protein. Additionally, *dnaj* single mutant plants exhibited wild-type like growth (data not shown), but no drought tolerance assays were performed to determine the effects abolishing DNAJ on drought tolerance.

In silico analysis using Dispred and DisMeta web interfaces reveals that the C-terminal region of CPR5 is a predicted intrinsically disordered region (Faisal, 2015). The intrinsically disordered region of proteins remains as a flexibly mobile region in their functional form and do not adopt a native fixed structure (Dunker, 2004; Dunker & Obradovic, 2001). Disordered proteins have been identified in plants in many stress-response pathways, and also have been annotated to act as protein chaperones or in protecting other cellular components and structures. Intrinsically disordered proteins have been observed to be some of the most important proteins in the plant proteome as mutation of these proteins have been observed to cause lethality or disease in mammals. In mammals, half of the highly studied protein p53 has been annotated as intrinsically disordered, and p53 has been annotated to interact with more than a hundred different known partners (Oldfield et al., 2008). There is no plant homolog for p53, however, CPR5 has been compared to mammalian p53 due to the similar misregulation of the host system exhibited when CPR5 function is abolished (H.-C. Jing, et al., 2007) as well as the conserved nature of the protein across multiple plant species.

If CPR5 is a plant equivalent of mammalian p53, it is highly likely that there are proteins that act as regulators of CPR5 protein structure which help direct CPR5 downstream interactions. p53 has also been observed to interact with heat shock chaperone proteins via co-precipitation assays (Whitesell, Sutphin, Pulcini, Martinez, & Cook, 1998), providing corroborating evidence that CPR5 may be able to interact with DNAJ and perhaps other chaperone proteins in a similar capacity. It is possible also that DNAJ is the first identified upstream interaction of CPR5 and a direct regulator of CPR5 function.

4.4.2 CPR5 Functionality in and Outside of the Nucleus

Proteins are complex molecules whose expression, modification, localization and interactions are unique to each molecule. Many proteins are not limited to one interacting partner or localization within the cell (Baena-González, et al., 2007; Garcia et al., 2010). For instance, enhanced disease susceptibility 1 protein (EDS1) was identified in Y2H to have the potential to dimerize and interact with protein PAD4 (Feys, et al., 2001). Localization studies have identified EDS1 as a nucleo-cytoplasmic protein that is important in the regulation of transcriptional reprogramming by allowing the activation and repression of specific defense-related genes during an immune response. EDS1 nuclear function in transcriptional reprogramming is contingent on the nuclear accumulation of EDS1 and the enhanced export from inside the nucleus compromises resistance. However, cytoplasmic EDS1 is required for complete resistance to bacterial and oomycete pathogens, and its levels are maintained during infections (Feys, et al., 2001).

Although studies have been conducted to identify the localization pattern of CPR5, these studies have not provided conclusive evidence and indeed have supplied conflicting conclusions (Gao, et al., 2011; D. Perazza et al., 2011; S. Wang, et al., 2014). A recent study (Daniel Perazza, et al., 2011) supports the hypothesis that CPR5 is a nuclear protein via localization of a CPR5 N-terminus GFP fusion protein (GFP-CPR5). GFP is known to auto-localize to the nucleus and thus may affect CPR5 native localization (Chytilova, Macas, & Galbraith, 1999). Additionally, coiled-coil regions of protein structures have also been associated with RNA/DNA binding, and the putative identification of 4 of these structures asserts that CPR5 may also play a function via interaction with RNA or DNA (Mason & Arndt, 2004; Meissner, Koppen-Rung, Dittmer, Lapp, & Bogner, 2011; Xie, Ren, Zhang, & Yu, 2012). However, the GFP-CPR5 fusion construct was able to rescue the *cpr5-2* background and thus supports nuclear localization as native to CPR5. Conversely, another

study (Gao, et al., 2011) used a CPR5 C-terminus EGFP fusion protein (CPR5-EGFP) that localized predominantly to the cytoplasm to rescue the *cpr5-1* mutant. Upon close inspection of figure 11 from Gao, et al., (2011), there appears to be some low level localization of EGFP-CPR5 localized in the nucleus. This nuclear localization, albeit at a low level, could have been sufficient to induce the rescued phenotype as it is still unclear how much protein is required for the rescue of *cpr5* phenotypes. The visualized nuclear EGFP signal in the second study (Gao, et al., 2011) could also be explained by cleaved EGFP auto-localization to the nucleus. Alternatively, the complementation observed in the first study (Daniel Perazza, et al., 2011) could be demonstrative of a pre-nuclear-localized or cleavage-freed CPR5 cytoplasmic functionality. Additionally, both fusion constructs were fused to a 35S promoter, resulting in constitutive expression of the constructs (Gao, et al., 2011; Daniel Perazza, et al., 2011). The overexpression of these constructs could also have led to altered localization due to the high levels of fusion constructs present.

Y2H analysis revealed that several proteins that exhibited interaction with CPR5 within the system. The identity and localization pattern of these identified proteins suggest that CPR5 participates in interactions that are not in agreement with a role solely as a nuclear membrane bound protein. For example, CRK4 is a calcium dependent protein kinase-like protein that is annotated to be membrane bound in the cytosol which may be why no interaction was observed in the full length protein Y2H transformation assay (Du, et al., 2005; Harmon, 2003; Hrabak, 2003). Studies suggest that CPR5 is a nuclear-localized and membrane bound protein (Gao, et al., 2011; Daniel Perazza, et al., 2011; S. Wang, et al., 2014). Although one study shows that CPR5 may be cleaved of its transmembrane domain, it is unclear whether this truncated protein is real and if it's localized to the nucleus or elsewhere in the cell (Daniel Perazza, et al., 2011). BiFC analysis suggests however that CRK4 interacts with the CPR5 outside of the nucleus as indicated by the fluorescence observed around the cell periphery (Figure 3.6B). Interestingly, CRK4 interacted with CPR5-cYFP indicating that the interaction most likely occurs proximally to C-terminal end of the CPR5 protein. Analysis of CPR5 protein sequence indicates that CPR5 has several predicted phosphorylation sites (Figure 4.1). The idea that CPR5 may interact with CRK4 in the cytosol, perhaps through phosphorylation via kinase activity, is supported by the confirmed BiFC assay that exhibited fluorescence indicative of physical interaction with CPR5.

4.4.3 CPR5 Post-Translational Modification

The importance of protein-protein interactions in modulating enzyme activity, facilitation of signal transduction and transcriptional regulation has been strongly established. Generally protein-protein interactions are thought to be restricted by colocalization of interacting partners (Getzoff, 1986; Hrabak, 2003; S. Jones & Thornton, 1996; Keskin, Gursoy, Ma, & Nussinov, 2008; Whitley, et al., 1999).

Recently however, complex mechanisms of regulation have been unravelled; including protein cleavage followed by translocation of the truncated terminal to interact with proteins in other organelles, which serves as an elegant way of bypassing the localization restriction. A protein exploiting this mechanism is EIN2, whose phosphorylation and subsequent proteolytic cleavage triggers translocation of the processed protein from the endoplasmic reticulum (ER) to the nucleus (Cooper, 2013; Wen et al., 2012).

Another novel C-terminal proteolytic processing mechanism was identified to occur to cytosolic pyruvate kinase ($PyrKin_c$) (Tang, Hardin, Dewey, & Huber, 2003). This truncated protein not only exhibited pyruvate kinase activity but also activation by aspartate (Tang, et al., 2003). Alternatively, $PyrKin_c$ has also been observed to be ubiquitinated in a phosphorylation dependent manner and subsequently targeted to the 26S proteasome for degradation.

Although expression of truncated CPR5 lacking all putative transmembrane domain regions did not rescue *cpr5-2* phenotype (Daniel Perazza, et al., 2011), expression of full length CPR5 did result in rescue of *cpr5-2* phenotypes. Detection of CPR5 protein expression via western blot analysis revealed the low expression of a protein that corresponded in molecular weight to a protein similar in size to that of the truncated CPR5 protein lacking in the C-terminal membrane domain regions (Daniel Perazza, et al., 2011).

The presence of this lowly detected protein by Perazza, et al, (2011) suggests that full length CPR5 may work in a cleavage dependent manner that gives rise to a transmembrane domain truncated version of CPR5 *in vivo*. Analysis of CPR5 sequence identified several predicted phosphorylation site that partially match the consensus sequence recognized by CDPKs and SnRK1 kinases in plants similar to cytosolic pyruvate kinase (Figure 4.1). Among the proteins identified via Y2H were two kinases (Figure 3.2). More specifically AKIN10, an isoform of SnRK1, and CRK4, a calcium dependent protein kinase (CDPK) related protein. CRK4 is a cytosol membrane bound protein, and AKIN10 is has been reported to function in a variety of pathways within the nucleus, cytoplasm, and

chloroplasts (Figure 3.2) (Baena-González, et al., 2007; Coello, et al., 2011; Du, et al., 2005; Harmon, 2003; Hrabak, 2003; Tsai & Gazzarrini, 2012).

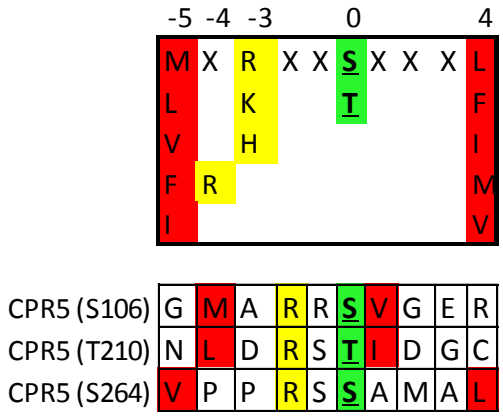

Figure 4.1: CPR5 predicted phosphorylation sites
Predicted SnRK1 (Akin10) consensus sequence (top) and putative SnRK1 target phosphorylation sites within the CPR5 sequence (bottom). Phosphorylated serines (S) and threonines (T) are in bold and underlined. Basic amino acids (R, K, H) are in yellow, hydrophobic amino acids (M,V,L,I,F) are in red.

Interestingly, the predicted phosphorylation sites on PyrKin$_c$ match the consensus sequence recognized by calcium-dependent protein kinases (CDPKs) and SnRK1 (SNF1 related) kinases in plants and is also phosphorylated by SnRK1 within the nucleus (Tang, et al., 2003). SnRK1 has the potential to phosphorylate target sites that only partially match the SnRK1/CDPKs consensus sequences, suggesting that CPR5 could also be targeted in a similar manner (Tsai & Gazzarrini, 2012). As SnRK1 or CDPKs are responsible for the phosphorylation of PyrKin$_c$ and subsequent truncation or targeting for degradation, CPR5 may also be cleaved and/or targeted to specific locations.

Protein-protein studies indicate that AKIN10 not only also acts as a kinase, able to phosphorylate FUSCA3, PyrKin$_c$ and other protein partners within the nucleus but also exhibits phosphorylation-dependent transcriptional regulatory roles (Tang, et al., 2003; Tsai & Gazzarrini, 2012). Phosphorylation of AKIN10 by specific BZIP transcription factors allows for the activation of AKIN10 as a transcriptional regulator that can inhibit or facilitate transcription of certain genes (Baena-González, et al., 2007).

SnRK1 is a homolog of mammalian AMPK and yeast SNF1, all of which have the same target site (Dale, Wilson, Edelman, & Hardie, 1995). The shared target site of these homologs suggests that commercially available AMPK could be used to target CPR5 to conduct pull-down or co-immunoprecipitation assays. Alternatively Phostag gel electrophoresis could also be used to determine if CPR5 is phosphorylated, giving insight on the likelihood that CPR5 is targeted by AKIN10 or CRK4. Site-directed mutagenesis of

putative SNKR1 serine or threonine in CPR5 may reveal the importance of phosphorylation in function of CPR5.

Given that post-translational modifications can lead to modification of protein localization and function, CPR5 may be processed similarly. The identification of both nuclear and cytoplasmic localized proteins via Y2H and BiFC suggest that CPR5 is localized to and may function in more than one location. However, more extensive research must be conducted to determine whether any post-translational modifications occur, and the purpose that any of these modifications serve.

4.5 Summary of Discussion

The main objective of this thesis was to characterize the functionality of CPR5 within the plant system by determining potential direct protein partners of CPR5 via protein-protein interaction assays. The secondary objective of this thesis was to determine the viability of the identified putative protein-interactions via plant morphological studies and the quantification of the expression of key genes in *cpr5-2* double knock out mutants. This study has provided enough evidence to support the hypothesis that CPR5 is a multifunctional protein involved in interactions with multiple proteins localized to various locations within the cell.

This study has also highlighted for the first time, CPR5 potential exonuclear action rather than sole nuclear localization and interactions, via the identification of several potential protein partners that not only localize outside of the nuclear envelope, but also through *in planta* interaction assay that indicate the location of observed interaction to be cytoplasmic. Morphological studies also suggest an uncoupling of CPR5 regulation skotomorphogenic early seedling development and sugar-mediated root and hypocotyl elongation.

A total of ten genes were identified and direct interaction was observed via BiFC as well as individual Y2H protein pair assays and various alterations to *cpr5-2* mutant phenotypes were observed in several of the double mutant lines produced.

Based on the results described in this thesis, a tentative model of CPR5 direct interactions and the regulatory pathways they are associated with has been proposed (Figure 4.2). The interactions proposed in the CPR5 genetic map may well be involved in other processes or pathways to regulate CPR5 involvement in the plant system.

Identification of 3 transcription factors, MYB3, BZIP61, and AKIN10 suggests CPR5 function as a transcriptional regulator influencing various pathways through single interactions as interaction with a TF would result in the downstream regulation of multiple genes. BiFC analysis identified several interactions that localize outside of the proposed model CPR5 nuclear localized interactions and suggests that CPR5 is capable of interacting with proteins in various cell locations.

As CPR5 is a proposed regulator of ROS, CPR5 interaction with FSD1 suggests this interaction as a potential interaction mechanism involved in ROS regulation. Alternatively, FSD1 and DNAJ, both parts of families of proteins that have known regulators of abiotic stress, may direct CPR5 negative regulation of abiotic stress tolerance consistent with the constitutive abiotic stress tolerance conferred through the abolishment of CPR5.

Although no alterations were observed in double mutant lines under normal growth conditions, alterations to growth conditions and genetic alterations indicate that CPR5 interaction with PATL3 plays an important role in the regulation of resistance and defense as highlighted by the differential expression of *PR1* and *PDF1.2* suggesting PI signalling as a regulatory mechanism of resistance.

Potential upstream regulatory mechanism of CPR5 have been identified and research suggesting that post-translational modification may play a role in the localization of CPR5. These modifications may also regulate CPR5 interactions with varying partners as is supported by the intrinsically disordered region of CPR5; a domain characteristically capable of interacting with numerous protein partners depending on the adopted conformation.

The proposed interactions and modes of regulation remain speculative and still need to be further characterized to determine the validity of the proposed models of direct interaction and subsequent action on the specified pathways. However, the work presented in this thesis provides a solid basis for refining current hypotheses and future research.

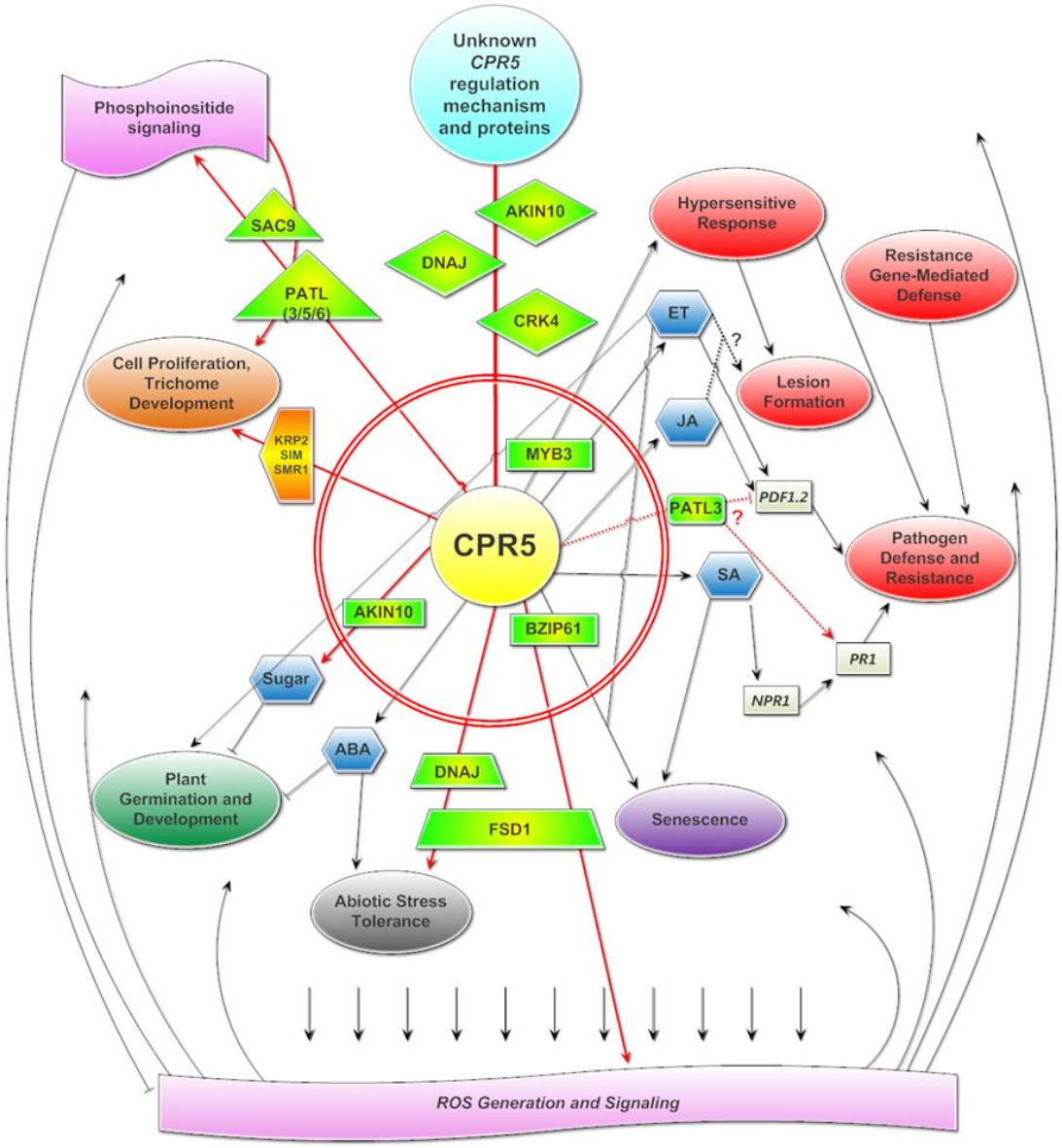

Figure 4.2: Proposed Model of CPR5 Dependent Regulation of Plant Processes via Putative Direct Interaction with Identified Proteins

Predicted CPR5 protein interactions (GREEN/YELLOW GRADIENT) and previously reported CPR5 protein interactions (ORANGE/YELLOW GRADIENT) and their proposed pathways of involvement and regulation (RED LINES). Transcription factors (RECTANGLES) encircled (RED, DOUBLE CIRCLE) indicate that proposed TF interaction with CPR5 regulates numerous unspecified plant regulatory pathways. Predicted CPR5 protein interactions involved in CPR5 upstream regulation mechanisms (DIAMONDS), downstream involvement in PI signalling (TRIANGLES), and stress and ROS regulation (TRAPEZOIDS) are noted. CPR5 interaction with PATL3 and the proposed involvement in PR1 and PDF1.2 expression regulation is noted (RED, DOTTED LINE/?) Plant regulatory pathways and signalling involving hormones and sugar (DARK BLUE) induced plant processes related to Pathogen defense (RED), Senescence (PURPLE), Abiotic Stresses (GREY), Plant Development (GREEN), and Cell Proliferation and trichome development (ORANGE). Genes known to be involved in particular mechanisms are mentioned to provide specific characterization pertaining to that pathway (RECTANGLES). ROS generation and signalling (PINK RIBBON) is shown as a general signalling and response mechanism involved in all major plant processes. Indicated also are known CPR5-independent pathways and putative CPR5-dependent pathway interactions

Appendices

Appendix 1. *CPR5* Coding Sequences

CPR5:

ATGGAAGCCCTCCTCCTCCCTCCTTCGCCGGAACCCCAAAATCAAATCACCAATCCGGCGAATTCAAAGCC
AAATCATCAATCTGGTGACGTACATAAAGATGAGACGATGATGATGAAGAAGAAGAAGGATACGAATCC
ATCGAATTTGGAAAAGAGAAAACTCAAGGGAAAGAAGAAAGAGATTATGGACAACGACGAAGCTTCTTC
GTCCTATTGTTCTACATCTTCTACCTCTAATTCAAATTCTACTAAAAGGGTTACGAGAGTGGTTCATAGA
TTACGAAACCCTATGCGGTTAGGTATGGCTCGACGAAGCGTTGGTGAACGACAAGCTGAAAAATTGGCGA
AGCCTCTGGGCTTTTCACTTGCCGCTTTTGCTAATATGGTTATTGCGAGAAAGAATGCCGCAGGTCAGAAT
GTTTATGTTGATGATCTTGTTGAGATCTTTGCTACTCTTGTCGAAGAATCATTAGCCAATGTTTATGGTA
ATAAGCTTGGTTCCTTTGCGACCAACTTTGAGCAAACATTCAGCAGTACTCTAAAGATCCTTAAATTGACC
AATGAATGTGCAAATCCACATCAGTCAAACAATAATGATGGTGGGAGTTGTAATTTAGATCGCTCTACCA
TAGACGGATGCTCAGACACCGAGCTATTTGAGAGGGAGACTTCATCTGCTACGTCTGCTTATGAAGTGAT
GCAAGGCAGTGCAACAGCAACCTCTTTGATGAATGAGCTTGCCCTTTTCGAAGAGACTCTACAACTCTCTT
GTGTCCCTCCTAGAAGTTCAGCAATGGCTTTGACCACAGACGAAAGGTTTTTAAAAGAGCAAACACGAGC
AAACGACCTAAAGACCGTGGAGATTGGTCTTCAAATAAGAGAGTTAAGGTGCAAAGAGACGGCGCTAGGA
TTAAAATTTGAATCAAACAACCTGGGGAAAGCGGCGCTAGAGTTGGATGTTTCGAAAGCTGCATTCAGAG
CGGAGAAATTCAAAACCGAATTAGAAGATACAAGAAAAGAAGAGATGGTCACAAGAATCATGGATTGGC
TCCTCGTAAGTGTCTTCAGCATGTTGGCTTCTATGGTACTTGGCGTTTACAATTTTTCAATAAAGAGAATC
GAGGATGCTACCTCAGTATGCGACCAATCCGAGGAGAAAAGTTCGTCGTGGTGGGTTCCTAAACAAGTTT
CATCGATTAACTCAGGCTTCAACACCTTCATCTGCCGGGTTCGAGTTTGGGTGCAGATATTTTTCGGTGTG
TTAATGATCATTGTCTTCACTTACTTTCTAAACAAACGATCATCAGGTACGAAGCAGACAATGCCGATAA
GTTTCATCGTTCTTTTCCTCGGTATATTTTGCGGTGTATCGGGTAAATTGTGTGTGGACACATTGGGCGGT
GATGGCAAACTCTGGCTAATAGTTTGGGAAGTGTTTTGCCTTTTGCAATTCGTTGCAAATGTCTTCACAT
TGGCTTTGTATGGTCTAATGTTCGGTCCTATAAACGTGACTCAAGAGACCAGATCGAACCGTTGTAACAG
TATGTTTCCATATTGGGCAAGGCGCAGTGTCGTGTATGTGGTGATTCTGTTTGTTCTTCCAGTCATAAACG
GTCTTTTGCCATTTGCAACATTTGGTGAATGGAGAGACTTCGCTATGTATCACCTTCATGGTGGGTCTGAC
TATGCTTGA

CPR5TM0:

ATGGAAGCCCTCCTCCTCCCTCCTTCGCCGGAACCCCAAAATCAAATCACCAATCCGGCGAATTCAAAGCC
AAATCATCAATCTGGTGACGTACATAAAGATGAGACGATGATGATGAAGAAGAAGAAGGATACGAATCC
ATCGAATTTGGAAAAGAGAAAACTCAAGGGAAAGAAGAAAGAGATTATGGACAACGACGAAGCTTCTTC
GTCCTATTGTTCTACATCTTCTACCTCTAATTCAAATTCTACTAAAAGGGTTACGAGAGTGGTTCATAGA
TTACGAAACCCTATGCGGTTAGGTATGGCTCGACGAAGCGTTGGTGAACGACAAGCTGAAAAATTGGCGA
AGCCTCTGGGCTTTTCACTTGCCGCTTTTGCTAATATGGTTATTGCGAGAAAGAATGCCGCAGGTCAGAAT
GTTTATGTTGATGATCTTGTTGAGATCTTTGCTACTCTTGTCGAAGAATCATTAGCCAATGTTTATGGTA
ATAAGCTTGGTTCCTTTGCGACCAACTTTGAGCAAACATTCAGCAGTACTCTAAAGATCCTTAAATTGACC
AATGAATGTGCAAATCCACATCAGTCAAACAATAATGATGGTGGGAGTTGTAATTTAGATCGCTCTACCA
TAGACGGATGCTCAGACACCGAGCTATTTGAGAGGGAGACTTCATCTGCTACGTCTGCTTATGAAGTGAT
GCAAGGCAGTGCAACAGCAACCTCTTTGATGAATGAGCTTGCCCTTTTCGAAGAGACTCTACAACTCTCTT
GTGTCCCTCCTAGAAGTTCAGCAATGGCTTTGACCACAGACGAAAGGTTTTTAAAAGAGCAAACACGAGC
AAACGACCTAAAGACCGTGGAGATTGGTCTTCAAATAAGAGAGTTAAGGTGCAAAGAGACGGCGCTAGGA
TTAAAATTTGAATCAAACAACCTGGGGAAAGCGGCGCTAGAGTTGGATGTTTCGAAAGCT

CPR5TM1:

ATGGAAGCCCTCCTCCTCCCTCCTTCGCCGGAACCCCAAAATCAAATCACCAATCCGGCGAATTCAAAGCC
AAATCATCAATCTGGTGACGTACATAAAGATGAGACGATGATGATGAAGAAGAAGAAGGATACGAATCC
ATCGAATTTGGAAAAGAGAAAACTCAAGGGAAAGAAGAAAGAGATTATGGACAACGACGAAGCTTCTTC
GTCCTATTGTTCTACATCTTCTACCTCTAATTCAAATTCTACTAAAAGGGTTACGAGAGTGGTTCATAGA
TTACGAAACCCTATGCGGTTAGGTATGGCTCGACGAAGCGTTGGTGAACGACAAGCTGAAAAATTGGCGA
AGCCTCTGGGCTTTTCACTTGCCGCTTTTGCTAATATGGTTATTGCGAGAAAGAATGCCGCAGGTCAGAAT
GTTTATGTTGATGATCTTGTTGAGATCTTTGCTACTCTTGTCGAAGAATCATTAGCCAATGTTTATGGTA
ATAAGCTTGGTTCCTTTGCGACCAACTTTGAGCAAACATTCAGCAGTACTCTAAAGATCCTTAAATTGACC
AATGAATGTGCAAATCCACATCAGTCAAACAATAATGATGGTGGGAGTTGTAATTTAGATCGCTCTACCA
TAGACGGATGCTCAGACACCGAGCTATTTGAGAGGGAGACTTCATCTGCTACGTCTGCTTATGAAGTGAT
GCAAGGCAGTGCAACAGCAACCTCTTTGATGAATGAGCTTGCCCTTTTCGAAGAGACTCTACAACTCTCTT
GTGTCCCTCCTAGAAGTTCAGCAATGGCTTTGACCACAGACGAAAGGTTTTTAAAAGAGCAAACACGAGC
AAACGACCTAAAGACCGTGGAGATTGGTCTTCAAATAAGAGAGTTAAGGTGCAAAGAGACGGCGCTAGGA
TTAAAATTTGAATCAAACAACCTGGGGAAAGCGGCGCTAGAGTTGGATGTTTCGAAAGCTGCATTCAGAG
CGGAGAAATTCAAAACCGAATTAGAAGATACAAGAAAAGAAGAGATGGTCACAAGAATCATGGATTGGC
TCCTCGTAAGTGTCTTCAGCATGTTGGCTTCTATGGTACTTGGCGTTTACAATTTTTCAATAAAGAGAATC
GAGGATGCTACCTCAGTATGCGACCAATCCGAGGAGAAAAGTTCGTCGTGGTGGGTTCCTAAACAAGTTT
CATCGATTAACTCAGGC

Appendix 2. Plasmid Vector maps for Y2H Cloning

A) pGBKT7

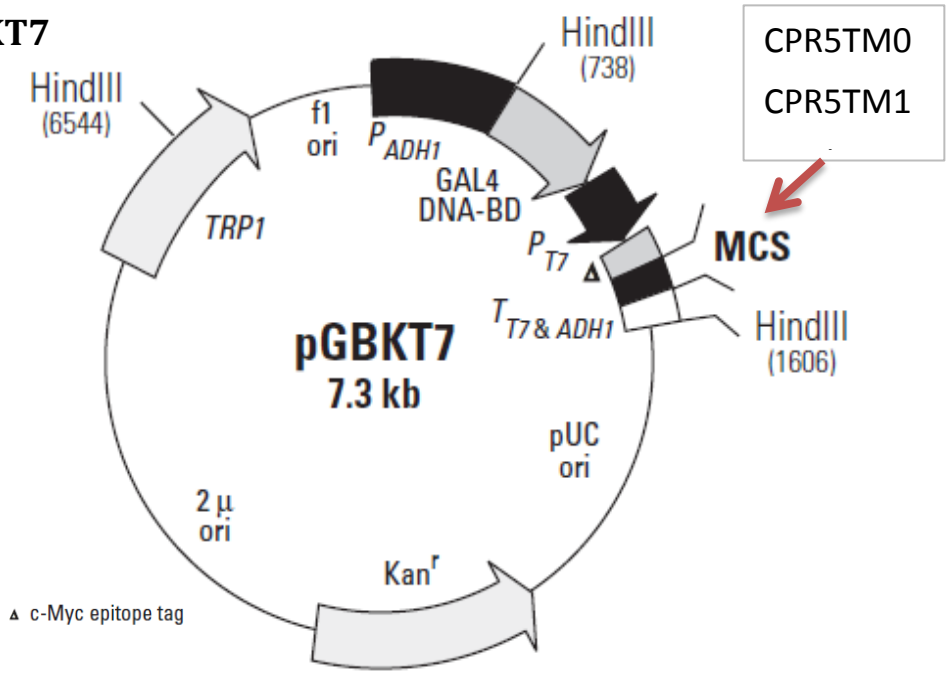

CPR5TM0

CPR5TM1

GAL4-BD fusions

B) pGADT7-RecAB

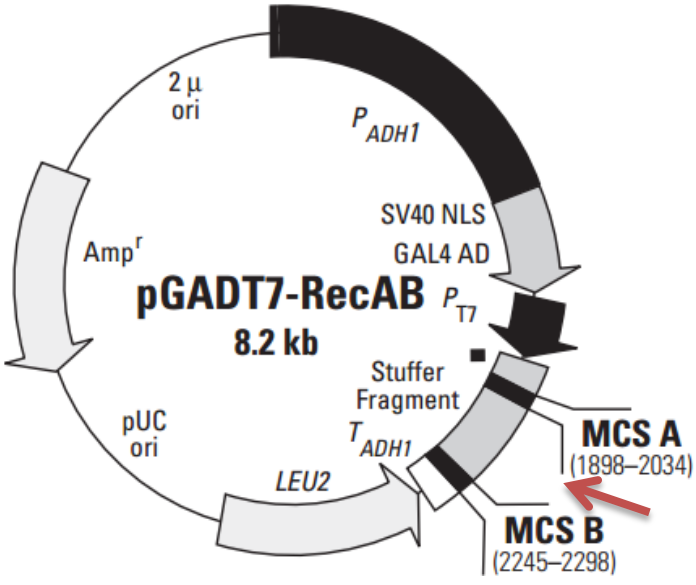

Universal Arabidopsis (Normalized) transcriptome

GAL4-AD "Mate and Plate" Library

C) pGADT7

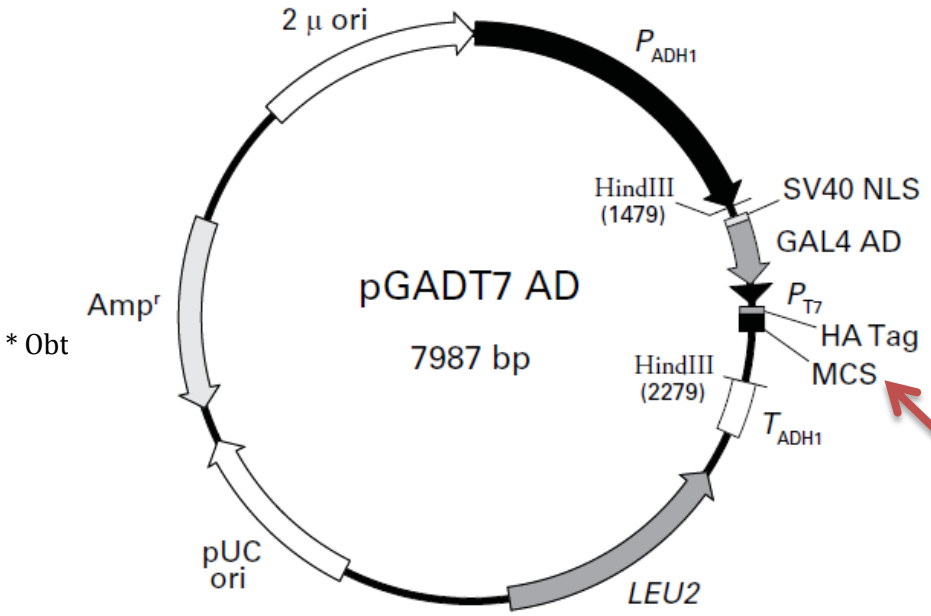

* Obt

GAL4-AD fusions

AKIN10
FSD1
MYB3
PATL3
BZIP61
CRPK4
DNAJ
SAC9
PATL5
PATL6
KRP2
SIM
SMR1

Appendix 3. Restriction Sites used for Y2H

Gene	Restriction Enzyme 1	Restriction Enzyme 2
CPR5TM0	NdeI	BamHI
CPR5TM1	NdeI	BamHI
AKIN10	Xmal	SacI
FSD1	Xmal	SacI
MYB3	NdeI	XmaI
PATL3	NdeI	XmaI
DNAJ	XmaI	SacI
SAC9	NdeI	Xmal
BZIP61	NdeI	XmaI
CRK4	Xmal	SacI
PATL5	NdeI	XmaI
PATL6	NdeI	XmaI
KRP2	NdeI	XmaI
SIM	NdeI	XmaI
SMR1	NdeI	XmaI

Appendix 4. YFP Coding Sequences

nYFP

ATGGTGAGCAAGGGCGAGGAGCTGTTCACCGGGGTGGTGCCCATCCTGGTCGAGCTGGACGGCG
ACGTAAACGGCCACAAGTTCAGCGTGTCCGGCGAGGGCGAGGGCGATGCCACCTACGGCAAGCT
GACCCTGAAGCTGATCTGCACCACCGGCAAGCTGCCCGTGCCCTGGCCCACCCTCGTGACCACCC
TGGGCTACGGCCTGCAGTGCTTCGCCCGCTACCCCGACCACATGAAGCAGCACGACTTCTTCAAG
TCCGCCATGCCCGAAGGCTACGTCCAGGAGCGCACCATCTTCTTCAAGGACGACGGCAACTACA
AGACCCGCGCCGAGGTGAAGTTCGAGGGCGACACCCTGGTGAACCGCATCGAGCTGAAGGGCAT
CGACTTCAAGGAGGACGGCAACATCCTGGGGCACAAGCTGGAGTACAACTACAACAGCCACAAC
GTCTATATCATGGCC

cYFP

ATGGACAAGCAGAAGAACGGCATCAAGGCCAACTTCAAGATCCGCCACAACATCGAGGACGGCG
GCGTGCAGCTCGCCGACCACTACCAGCAGAACACCCCCATCGGCGACGGCCCCGTGCTGCTGCCC
GACAACCACTACCTGAGCTACCAGTCCGCCCTGAGCAAAGACCCCAACGAGAAGCGCGATCACA
TGGTCCTGCTGGAGTTCGTGACCGCCGCCGGGATCACTCTCGGCATGGACGAGCTGTACAAG
(TGA)

Appendix 5 pGreenII 0029 62 SK plasmid vector map for BiFC cloning and pSOUP helper plasmid

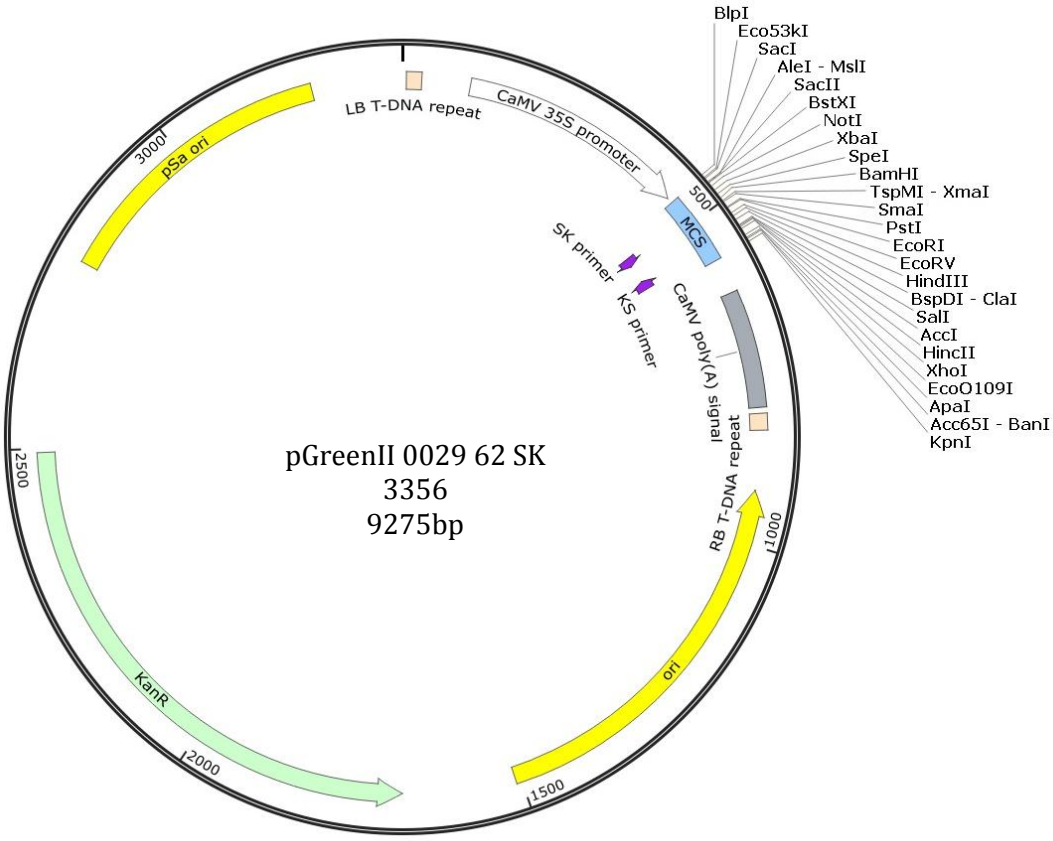

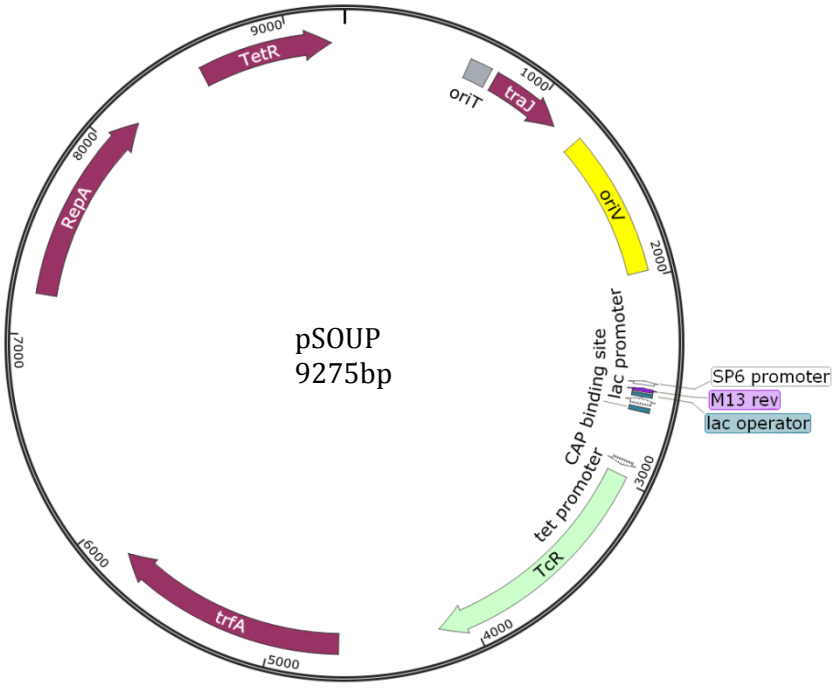

Appendix 6 Primers and Cloning Restriction Sites for BiFC Cloning

6A: Primers for BiFC Cloning of p(HA:;cYFP), p(cYFP::HA) and p(nYFP::HA)

Note: Plasmids are highlighted in bold. * indicates construct was not successfully constructed

Final pGreenII 0229 62 SK Plasmid Construct	**Gene**	**Primer**	**Sequence**
p(HA::cYFP)	NdeI-cYFP	cYFP_F_NdeI	CAGCAT**ATG**GCGGCTATTAGATCAATGGAC
	cYFP-XhoI	cYFP_R_XhoI	GACCTCGAGTCACTTGTACAGCTCGTCC
	PstI-HA	HA_F_PstI	CAGCTGCAGATGGAGTACCCATACGACG
	HA-MCS-AD	HA_R_MCS AD	AGATGGTGCACGATGCACAG
p(cYFP::HA)	SacI-cYFP	cYFP_F_SacI	GGAGAGCTCGCGGCTATTAGATCAATGGAC
	cYFP-SpeI	cYFP_R_SpeI	GGAACTAGTCTTGTACAGCTCGTCCATG
	SpeI-HA	HA_F_SpeI	GGAACTAGTATGGAGTACCCATACGACGTA
	HA-MCS-AD	HA_R_MSC AD	AGATGGTGCACGATGCACAG
p(nYFP::HA)	SacI-nYFP	nYFP_FSacI	GACGAGCTC**ATG**GTGAGCAAGGGCGAG
	nYFP-SpeI	nYFP_RSpeI	GGAACTAGTGGCCATGATATAGACGTTGTG
	SpeI-HA	HA_FSpeI	GGAACTAGTATGGAGTACCCATACGACGTA
	HA-MCS-AD	HA_R-AD	AGATGGTGCACGATGCACAG

6B: Primers for BiFC Cloning of plasmids p(cYFP::HA::GOI-X), p(GOI-X::HA::cYFP), and (p(nYFP::HA::GOI-Y)

Construct	Gene	Primer	Sequence
p(GOI-X::HA::cYFP)	SacI-CPR5	CPR5_F_SacI	GGAGAGCTCCATATGGAAGCCCTCCTC
	CPR5-PstI	CPR5_R_PstI	GACCTGCAGAGCATAGTCAGACCCACCA
	SpeI-EDS1	EDS1_F_SpeI	GGAACTAGTATGGCGTTTGAAGCTCTTA
	EDS1-PstI	EDS1_R_PstI	GACCTGCAGGGTATCTGTTATTTCATCCA
p(cYFP::HA::GOI-X)	NdeI-CPR5	CPR5-F_NdeI	CAT**ATG**GAAGCCCTCCTCCTC
	CPR5-XhoI	CPR5-R_XhoI	GGACTCGAGTCAAGCATAGTCAGACCCAC
	NdeI-EDS1	EDS1_F_NdeI	CAGCAT**ATG**GCGTTTGAAGCTCTTA
	EDS1-XhoI	EDS1_R_XhoI	GGACTCGAGCACCACCTAAGGTTCAG
p(nYFP::HA::GOI-X)	NdeI-EDS1	EDS1_F_NdeI	CAGCAT**ATG**GCGTTTGAAGCTCTTA
	EDS1-XhoI	EDS1_R_XhoI	GGACTCGAGCACCACCTAAGGTTCAG

6C: Restriction enzymes for BiFC Cloning of p(HA:;cYFP), p(cYFP::HA) and p(nYFP::HA)

Final pGreenII 0229 62 SK Plasmid Construct	Coding Region or Plasmid	Restriction Enzyme 1	Restriction Enzyme 2
p(HA::cYFP)	**pGreenII 0229 62 SK**	PstI	XhoI
	HA	PstI	NdeI
p(cYFP::HA)	**pGreenII 0229 62 SK**	SacI	XhoI
	cYFP	SacI	SpeI
	HA	SpeI	XhoI
p(nYFP::HA)	**pGreenII 0229 62 SK**	SacI	XhoI
	nYFP	SacI	SpeI
	HA	SpeI	XhoI

6D: Restriction enzymes for BiFC Cloning of p(cYFP::HA::GOI-X), p(GOI-X::HA::cYFP), and (p(nYFP::HA::GOI-Y)

pGreenII 0229 62 SK Plasmid Construct	Coding Region or Plasmid	Restriction Enzyme 1	Restriction Enzyme 2
p(CPR5-X::HA::cYFP)	**pHA::cYFP**	SacI	PstI
	CPR5	SacI	PstI
p(EDS1-X::HA::cYFP)	**pHA::cYFP**	SpeI	PstI
	EDS1	SpeI	PstI
p(cYFP::HA::CPR5)	**pHA::cYFP**	NdeI	XhoI
	CPR5	NdeI	XhoI
p(cYFP::HA::EDS1)	**pHA::cYFP**	NdeI	XhoI
	EDS1	NdeI	XhoI
p(nYFP::HA::GOI-Y)	**p(nYFP::HA)**	NdeI	XhoI
(NdeI/XhoI)	EDS1	NdeI	XhoI
	CRPK4	Xmal	PstI
	PATL5	NdeI	XhoI
	PATL6	NdeI	XhoI
	KRP2	NdeI	XhoI
	SIM	NdeI	XhoI
	SMR1	NdeI	XhoI
	BZIP61	NdeI	XhoI
	MYB3	NdeI	XhoI
	PATL3	NdeI	XhoI
p(nYFP::HA::GOI-Y)	**p(nYFP::HA)**	XmaI	XhoI
(XmaI/XhoI)	AKIN10	XmaI	XhoI
	FSD1	Xmal	XhoI
p(nYFP::HA::GOI-Y)	**p(nYFP::HA)**	Xmal	PstI
(XmaI/PstI)	DNAJ	Xmal	PstI
p(nYFP::HA::GOI-Y)	**p(nYFP::HA)**	NdeI	Xmal
(NdeI/XmaI)	SAC9*	NdeI	Xmal

Appendix 7 TAIR Ascension and obtained SALK lines

Gene	TAIR Ascension	SALK line
AKIN10	AT3G01090	SALK_127939
FSD1	AT4G25100	SALK_036006C
MYB3	AT1G22640	
PATL3	AT1G72160	SALK_093994C
DNAJ	AT2G22360	SALK_031700
SAC9	AT3G59770	SALK_041090
BZIP61	AT3G58120	SALK_138883
CRK4	AT5G24430	SALK_009503C
PATL5	AT4G09160	SALK_124448
PATL6	AT3G51670	SALK_099089

References

Abdel-Ghany, S. E., Muller-Moule, P., Niyogi, K. K., Pilon, M., & Shikanai, T. (2005). Two p-type ATPases are required for copper delivery in Arabidopsis thaliana chloroplasts. *Plant Cell, 17*(4), 1233-1251. doi: 10.1105/tpc.104.030452

Aki, T., Konishi, M., Kikuchi, T., Fujimori, T., Yoneyama, T., & Yanagisawa, S. (2007). Distinct modulations of the hexokinase1-mediated glucose response and hexokinase1-independent processes by HYS1/CPR5 in Arabidopsis. *Journal of Experimental Botany, 58*(12), 3239-3248. doi: 10.1093/jxb/erm169

Alonso, J. M., Hirayama, T., Roman, G., Nourizadeh, S., & Ecker, J. R. (1999). EIN2, a bifunctional transducer of ethylene and stress responses in Arabidopsis. [Article]. *Science, 284*(5423), 2148-2152. doi: 10.1126/science.284.5423.2148

Apel, K., & Hirt, H. (2004). Reactive oxygen species: Metabolism, oxidative stress, and signal transduction. *Annual Review of Plant Biology, 55*, 373-399. doi: 10.1146/annurev.arplant.55.031903.141701

Ausubel, F. M. (2005). Are innate immune signaling pathways in plants and animals conserved? *Nature Immunology, 6*(10), 973-979.

Baena-González, E., Rolland, F., Thevelein, J. M., & Sheen, J. (2007). A central integrator of transcription networks in plant stress and energy signalling. *Nature, 448*(7156), 938-942. doi: 10.1038/nature06069

Balla, T. (2013). Phosphoinositides: Tiny Lipids With Giant Impact on Cell Regulation. *Physiological Reviews, 93*(3), 1019-1137. doi: 10.1152/physrev.00028.2012

Bankaitis, V. A., Malehorn, D. E., Emr, S. D., & Greene, R. (1989). The Saccharomyces cerevisiae SEC14 gene encodes a cytosolic factor that is required for transport of secretory proteins from the yeast Golgi complex. *Journal of Cell Biology, 108*(4), 1271-1281. doi: 10.1083/jcb.108.4.1271

Bao, Z., & Hua, J. (2014). Interaction of CPR5 with Cell Cycle Regulators UVI4 and OSD1 in Arabidopsis. *PLoS ONE, 9*(6). doi: 10.1371/journal.pone.0100347

Baxter, A., Mittler, R., & Suzuki, N. (2014). ROS as key players in plant stress signalling. *Journal of Experimental Botany, 65*(5), 1229-1240. doi: 10.1093/jxb/ert375

Boch, J., Verbsky, M. L., Robertson, T. L., Larkin, J. C., & Kunkel, B. N. (1998). Analysis of resistance gene-mediated defense responses in Arabidopsis thaliana plants carrying a mutation in CPR5. [Article]. *Molecular Plant-Microbe Interactions, 11*(12), 1196-1206. doi: 10.1094/mpmi.1998.11.12.1196

Borghi, M., Rus, A., & Salt, D. E. (2011). Loss-of-Function of Constitutive Expresser of Pathogenesis Related Genes5 Affects Potassium Homeostasis in

Arabidopsis thaliana. *PLoS ONE, 6*(10). doi: e26360, 10.1371/journal.pone.0026360

Bowling, S. A., Clarke, J. D., Liu, Y. D., Klessig, D. F., & Dong, X. N. (1997). The cpr5 mutant of Arabidopsis expresses both NPR1-dependent and NPR1-independent resistance. *Plant Cell, 9*(9), 1573-1584. doi: 10.2307/3870444

Brininstool, G., Kasili, R., Simmons, L. A., Kirik, V., Hulskamp, M., & Larkin, J. C. (2008). Constitutive Expressor of Pathogenesis-Related Genes5 affects cell wall biogenesis and trichome development. *BMC Plant Biology, 8*(58), (16 May 2008)-(2016 May 2008).

Brueckner, A., Polge, C., Lentze, N., Auerbach, D., & Schlattner, U. (2009). Yeast Two-Hybrid, a Powerful Tool for Systems Biology. *International journal of molecular sciences, 10*(6), 2763-2788. doi: 10.3390/ijms10062763

Buchanan-Wollaston, V. (1997). The molecular biology of leaf senescence. [Review]. *Journal of Experimental Botany, 48*(307), 181-199. doi: 10.1093/jxb/48.2.181

Buchanan-Wollaston, V., Page, T., Harrison, E., Breeze, E., Lim, P. O., Nam, H. G., . . . Leaver, C. J. (2005). Comparative transcriptome analysis reveals significant differences in gene expression and signalling pathways between developmental and dark/starvation-induced senescence in Arabidopsis. *Plant Journal, 42*(4), 567-585. doi: 10.1111/j.1365-313X.2005.02399.x

BuchananWollaston, V. (1997). The molecular biology of leaf senescence. [Review]. *Journal of Experimental Botany, 48*(307), 181-199. doi: 10.1093/jxb/48.2.181

Chen, Z. Y., Kloek, A. P., Boch, J., Katagiri, F., & Kunkel, B. N. (2000). The Pseudomonas syringae avrRpt2 gene product promotes pathogen virulence from inside plant cells. *Molecular Plant-Microbe Interactions, 13*(12), 1312-1321. doi: 10.1094/mpmi.2000.13.12.1312

Chytilova, E., Macas, J., & Galbraith, D. W. (1999). Green fluorescent protein targeted to the nucleus, a transgenic phenotype useful for studies in plant biology. *Annals of Botany, 83*(6), 645-654. doi: 10.1006/anbo.1999.0866

Clarke, J. D., Volko, S. M., Ledford, H., Ausubel, F. M., & Dong, X. N. (2000). Roles of salicylic acid, jasmonic acid, and ethylene in cpr-induced resistance in Arabidopsis. *Plant Cell, 12*(11), 2175-2190. doi: 10.2307/3871113

Clontech Laboratories, I. (2009). Yeast Protocol Handbook.

Clontech Laboratories, I. (2013). Matchmaker Gold Yeast Two-Hybrid System User Manual (PT4084-1).

Clontech Laboratories, I. (2015). SMART cDNA Library Construction Kit User Manual (PT3000-1).

Coello, P., Hey, S. J., & Halford, N. G. (2011). The sucrose non-fermenting-1-related (SnRK) family of protein kinases: potential for manipulation to improve stress tolerance and increase yield. *Journal of Experimental Botany, 62*(3), 883-893. doi: 10.1093/jxb/erq331

Collazo, C., Chacón, O., & Borrás, O. (2006). Programmed cell death in plants resembles apoptosis of animals. *Biotecnologia Aplicada, 23*(1), 1-10.

Cooper, B. (2013). Separation anxiety: an analysis of ethylene-induced cleavage of EIN2. *Plant signaling & behavior, 8*(7), e24721-e24721. doi: 10.4161/psb.24721

Czechowski, T., Stitt, M., Altmann, T., Udvardi, M. K., & Scheible, W. R. (2005). Genome-wide identification and testing of superior reference genes for transcript normalization in Arabidopsis. *Plant Physiology, 139*(1), 5-17. doi: 10.1104/pp.105.063743

Dale, S., Wilson, W. A., Edelman, A. M., & Hardie, D. G. (1995). Similar substrate recognition motifs for mammalian AMP-activated protein-kinase, higher-plant HMG-COA reductase kinase-A, yeast SNF1, and mammalian calmodulin-dependent protein-kinase- I. *Febs Letters, 361*(2-3), 191-195. doi: 10.1016/0014-5793(95)00172-6

De Veylder, L., Beeckman, T., & Inze, D. (2007). The ins and outs of the plant cell cycle. [Review]. *Nature Reviews Molecular Cell Biology, 8*(8), 655-665. doi: 10.1038/nrm2227

De Vleesschauwer, D., Xu, J., & Höfte, M. (2014). Making sense of hormone-mediated defense networking: from rice to Arabidopsis. *Frontiers in Plant Science, 5*. doi: 10.3389/fpls.2014.00611

DeGrado-Warren, J., Dufford, M., Chen, J., Bartel, P. L., Shattuck, D., & Frech, G. C. (2008). Construction and characterization of a normalized yeast two-hybrid library derived from a human protein-coding clone collection. *Biotechniques, 44*(2), 265-273. doi: 10.2144/000112674

Dekkers, B. J. W., & Bentsink, L. (2015). Regulation of seed dormancy by abscisic acid and DELAY OF GERMINATION 1. *Seed Science Research, 25*(02), 82-98. doi: 10.1017/s0960258514000415

Dekkers, B. J. W., Schuurmans, J. A. M. J., & Smeekens, S. C. M. (2008). Interaction between sugar and abscisic acid signalling during early seedling development in Arabidopsis. *Plant Molecular Biology, 67*(1-2), 151-167. doi: 10.1007/s11103-008-9308-6

Desrivieres, S., Cooke, F. T., Morales-Johansson, H., Parker, P. J., & Hall, M. N. (2002). Calmodulin controls organization of the actin cytoskeleton via regulation of phosphatidylinositol (4,5)-bisphosphate synthesis in Saccharomyces cerevisiae. *Biochemical Journal, 366*, 945-951. doi: 10.1042/bj20020429

Dijkwel, P. P., Kock, P. A. M., Bezemer, R., Weisbeek, P. J., & Smeekens, S. C. M. (1996). Sucrose represses the developmentally controlled transient activation of the plastocyanin gene in Arabidopsis thaliana seedlings. *Plant Physiology, 110*(2), 455-463.

Du, W., Wang, Y., Liang, S. P., & Lu, Y. T. (2005). Biochemical and expression analysis of an Arabidopsis calcium-dependent protein kinase-related kinase. *Plant Science, 168*(5), 1181-1192. doi: 10.1016/j.plantsci.2004.12.019

Dubos, C., Le Gourrierec, J., Baudry, A., Huep, G., Lanet, E., Debeaujon, I., . . . Lepiniec, L. (2008). MYBL2 is a new regulator of flavonoid biosynthesis in Arabidopsis thaliana. *Plant Journal, 55*(6), 940-953. doi: 10.1111/j.1365-313X.2008.03564.x

Dunker, A. K. (2004). Instrinsically disordered protein and cell signaling. *Biophysical Journal, 86*(1), 354A-355A.

Dunker, A. K., & Obradovic, Z. (2001). The protein trinity - linking function and disorder. *Nature Biotechnology, 19*(9), 805-806. doi: 10.1038/nbt0901-805

Faisal, M. (2015). The Role of CPR5 in the Regulation of Programmed Cell Death in A. Thaliana (Doctoral dissertation) (In preparation).

Fang, Y., & Spector, D. L. (2010). BiFC imaging assay for plant protein-protein interactions. *Cold Spring Harbor protocols, 2010*(2), pdb.prot5380-pdb.prot5380. doi: 10.1101/pdb.prot5380

Fesik, S. W. (2000). Insights into programmed cell through structural biology. *Cell, 103*(2), 273-282.

Feys, B. J., Moisan, L. J., Newman, M. A., & Parker, J. E. (2001). Direct interaction between the Arabidopsis disease resistance signaling proteins, EDS1 and PAD4. *Embo Journal, 20*(19), 5400-5411. doi: 10.1093/emboj/20.19.5400

Finkelstein, R. R., & Gibson, S. I. (2001). ABA and sugar interactions regulating development: cross-talk or voices in a crowd? *Current Opinion in Plant Biology, 5*, 26–32.

Fragoso, S., Espindola, L., Paez-Valencia, J., Gamboa, A., Camacho, Y., Martinez-Barajas, E., & Coello, P. (2009). SnRK1 Isoforms AKIN10 and AKIN11 Are Differentially Regulated in Arabidopsis Plants under Phosphate Starvation. *Plant Physiology, 149*(4), 1906-1916. doi: 10.1104/pp.108.133298

Fujiki, Y., Nakagawa, Y., Furumoto, T., Yoshida, S., Biswal, B., Ito, M., . . . Nishida, I. (2005). Response to darkness of late-responsive dark-inducible genes is positively regulated by leaf age and negatively regulated by calmodulin-antagonist-sensitive signalling in Arabidopsis thaliana. *Plant and Cell Physiology, 46*(10), 1741-1746. doi: 10.1093/pcp/pci174

Gao, G., Zhang, S., Wang, C., Yang, X., Wang, Y., Su, X., . . . Yang, C. (2011). Arabidopsis CPR5 Independently Regulates Seed Germination and Postgermination Arrest of Development through LOX Pathway and ABA Signaling. *PLoS ONE, 6*(4), e19406-e19406. doi: 10.1371/journal.pone.0019406

Garcia, A. V., Blanvillain-Baufume, S., Huibers, R. P., Wiermer, M., Li, G., Gobbato, E., . . . Parker, J. E. (2010). Balanced Nuclear and Cytoplasmic Activities of EDS1 Are Required for a Complete Plant Innate Immune Response. *PLoS Pathogens, 6*(7). doi: 0.1371/journal.ppat.1000970

Getzoff, E. D. (1986). Principles of protein-protein recognition and interaction. *Abstracts of Papers of the American Chemical Society, 192*, 2-PHYS.

Ghassemian, M., Nambara, E., Cutler, S., Kawaide, H., Kamiya, Y., & McCourt, P. (2000). Regulation of abscisic acid signaling by the ethylene response

pathway in arabidopsis. *Plant Cell, 12*(7), 1117-1126. doi: 10.1105/tpc.12.7.1117

Gilchrist, D. G. (1998) Programmed cell death in plant disease: The purpose and promise of cellular suicide. *Vol. 36* (pp. 393-414): Annu. Rev. Phytopathol.

Gookin, T. E., & Assmann, S. M. (2014). Significant reduction of BiFC non-specific assembly facilitates in planta assessment of heterotrimeric G-protein interactors. *Plant Journal, 80*(3), 553-567. doi: 10.1111/tpj.12639

Gururani, M. A., Mohanta, T. K., & Bae, H. (2015). Current Understanding of the Interplay between Phytohormones and Photosynthesis under Environmental Stress. [; Research Support, Non-U.S. Gov't; Review]. *International journal of molecular sciences, 16*(8), 19055-19085. doi: 10.3390/ijms160819055

Harmon, A. C. (2003). Calcium-regulated protein kinases of plants. *Gravitational and space biology bulletin : publication of the American Society for Gravitational and Space Biology, 16*(2), 83-90.

Hasegawa, P. M., Bressan, R. A., Zhu, J. K., & Bohnert, H. J. (2000). Plant cellular and molecular responses to high salinity. *Annual Review of Plant Physiology and Plant Molecular Biology, 51*, 463-499. doi: 10.1146/annurev.arplant.51.1.463

Heath, M. C. (2000). Hypersensitive response-related death. *Plant Molecular Biology, 44*(3), 321-334. doi: 10.1023/a:1026592509060

Hebeler, R., Oeljeklaus, S., Reidegeld, K. E., Eisenacher, M., Stephan, C., Sitek, B., . . . Warscheid, B. (2008). Study of early leaf senescence in Arabidopsis thaliana by quantitative proteomics using reciprocal N-14/N-15 Labeling and difference gel electrophoresis. *Molecular & Cellular Proteomics, 7*(1), 108-120. doi: 10.1074/mcp.M700340-MCP200

Heidel, A. J., Clarke, J. D., Antonovics, J., & Dong, X. N. (2004). Fitness costs of mutations affecting the systemic acquired resistance pathway in Arabidopsis thaliana. *Genetics, 168*(4), 2197-2206. doi: 10.1534/genetics.104.032193

Hofmann, K., & Stoffel, W. (1993). TMbase - A database of membrane spanning proteins segments. *Biol. Chem. Hoppe-Seyler 374*, 166.

Horstman, A., Tonaco, I. A. N., Boutilier, K., & Immink, R. G. H. (2014). A Cautionary Note on the Use of Split-YFP/BiFC in Plant Protein-Protein Interaction Studies. *International journal of molecular sciences, 15*(6), 9628-9643. doi: 10.3390/ijms15069628

Hrabak, E. M. (2003). The Arabidopsis CDPK-SnRK Superfamily of Protein Kinases. *Plant Physiology, 132*(2), 666-680. doi: 10.1104/pp.102.011999

Hu, C.-D., Grinberg, A. V., & Kerppola, T. K. (2006). Visualization of protein interactions in living cells using bimolecular fluorescence complementation (BiFC) analysis. *Current protocols in cell biology / editorial board, Juan S. Bonifacino ... [et al.], Chapter 21*, Unit 21.23. doi: 10.1002/0471143030.cb2103s29

Hu, C. D., Chinenov, Y., & Kerppola, T. K. (2002). Visualization of interactions among bZip and Rel family proteins in living cells using bimolecular fluorescence complementation. *Molecular Cell, 9*(4), 789-798. doi: 10.1016/s1097-2765(02)00496-3

Huang, H., & Bader, J. S. (2009). Precision and recall estimates for two-hybrid screens. [Article]. *Bioinformatics, 25*(3), 372-378. doi: 10.1093/bioinformatics/btn640

Inze, D., & De Veylder, L. (2006). Cell cycle regulation in plant development *Annual Review of Genetics* (Vol. 40, pp. 77-105).

Iqbal, N., Trivellini, A., Masood, A., Ferrante, A., & Khan, N. A. (2013). Current understanding on ethylene signaling in plants: The influence of nutrient availability. *Plant Physiology and Biochemistry, 73*, 128-138. doi: 10.1016/j.plaphy.2013.09.011

Jakoby, M., B.Weisshaar, Dröge-Laser, W., Vicente-Carbajosa, J., Tiedemann, J., Kroj, T., . . . Group, b. R. (2002). bZIP transcription factors in Arabidopsis. *TRENDS in Plant Science, 7*(3).

Jeong, E.-Y., Seo, P. J., Woo, J. C., & Park, C.-M. (2015). AKIN10 delays flowering by inactivating IDD8 transcription factor through protein phosphorylation in Arabidopsis. *BMC Plant Biology, 15*. doi: 110 10.1186/s12870-015-0503-8

Jing, H.-C., Anderson, L., Sturre, M. J. G., Hille, J., & Dijkwel, P. P. (2007). Arabidopsis CPR5 is a senescence-regulatory gene with pleiotropic functions as predicted by the evolutionary theory of senescence. *Journal of Experimental Botany, 58*(14), 3885-3894. doi: 10.1093/jxb/erm237

Jing, H.-C., & Dijkwel, P. P. (2008). CPR5: A Jack of all trades in plants. *Plant signaling & behavior, 3*(8), 562-563.

Jing, H. C., Hebeler, R., Oeljeklaus, S., Sitek, B., Stuehler, K., Meyer, H. E., . . . Dijkwel, P. P. (2008). Early leaf senescence is associated with an altered cellular redox balance in Arabidopsis cpr5/old1 mutants. *Plant Biology, 10*, 85-98. doi: 10.1111/j.1438-8677.2008.00087.x

Jing, H. C., Schippers, J. H. M., Hille, J., & Dijkwei, P. P. (2005). Ethylene-induced leaf senescence depends on age-related changes and OLD genes in Arabidopsis. *Journal of Experimental Botany, 56*(421), 2915-2923. doi: 10.1093/jxb/eri287

Jing, H. C., Sturre, M. J. G., Hille, J., & Dijkwel, P. P. (2002). Arabidopsis onset of leaf death mutants identify a regulatory pathway controlling leaf senescence. *Plant Journal, 32*(1), 51-63. doi: 10.1046/j.1365-313X.2002.01400.x

Jones, J. D. G., & Dangl, J. L. (2006). The plant immune system. *Nature, 444*(7117), 323-329. doi: 10.1105/tpc.105.037648;

Jones, S., & Thornton, J. M. (1996). Principles of protein-protein interactions. *Proceedings of the National Academy of Sciences of the United States of America, 93*(1), 13-20. doi: 10.1073/pnas.93.1.13

Josse, E.-M., & Halliday, K. J. (2008). Skotomorphogenesis: The Dark Side of Light Signalling. *Current Biology, 18*(24), R1144-R1146. doi: 10.1016/j.cub.2008.10.034

Kelley, L. A., Mezulis, S., Yates, C. M., Wass, M. N., & Sternberg, M. J. E. (2015). The Phyre2 web portal for protein modeling, prediction and analysis. *Nature protocols, 10*(6), 845-858. doi: 10.1038/nprot.2015.053

Kelley, L. A., & Sternberg, M. J. E. (2009). Protein structure prediction on the Web: a case study using the Phyre server. *Nature Protocols, 4*(3), 363-371. doi: 10.1038/nprot.2009.2

Kepczynski, J., & Kepczynska, E. (1997). Ethylene in seed dormancy and germination. [Article]. *Physiologia Plantarum, 101*(4), 720-726. doi: 10.1034/j.1399-3054.1997.1010407.x

Kerppola, T. K. (2006). Design and Implementation of Bimolecular Fluorescence Complementation (BiFC) Assays for the Visualization of Protein Interactions in Living Cells. *Nature protocols, 1*, 1278-1286.

Keskin, O., Gursoy, A., Ma, B., & Nussinov, R. (2008). Principles of protein-protein interactions: What are the preferred ways for proteins to interact? *Chemical Reviews, 108*(4), 1225-1244. doi: 10.1021/cr040409x

Khan, M., Rozhon, W., & Poppenberger, B. (2014). The Role of Hormones in the Aging of Plants - A Mini-Review. *Gerontology, 60*(1), 49-55. doi: 10.1159/000354334

Khurana, S. M. P., Pandey, S. K., Sarkar, D., & Chanemougasoundharam, A. (2005). Apoptosis in plant disease response: A close encounter of the pathogen kind. *Current Science, 88*(5), 740-752.

Kim, J., Chang, C., & Tucker, M. L. (2015). To grow old: regulatory role of ethylene and jasmonic acid in senescence. *Frontiers in Plant Science, 6*. doi: 10.3389/fpls.2015.00020

Kirik, V., Bouyer, D., Schobinger, U., Bechtold, N., Herzog, M., Bonneville, J. M., & Hulskamp, M. (2001). CPR5 is involved in cell proliferation and cell death control and encodes a novel transmembrane protein. *Current Biology, 11*(23), 1891-1895. doi: 10.1016/s0960-9822(01)00590-5

Kliebenstein, D. J., Monde, R.-A., & Last, R. L. (1998). Superoxide Dismutase in Arabidopsis: An Eclectic Enzyme

Family with Disparate Regulation and Protein Localization. *Plant Physiology, 118*, 637–650.

Koegl, M., & Uetz, P. (2007). Improving yeast two-hybrid screening systems. *Briefings in functional genomics & proteomics, 6*(4), 302-312. doi: 10.1093/bfgp/elm035

Kucera, B., Cohn, M. A., & Leubner-Metzger, G. (2005). Plant hormone interactions during seed dormancy release and germination. *Seed Science Research, 15*(4), 281-307. doi: 10.1079/ssr2005218

Larkins, B. A., Dilkes, B. P., Dante, R. A., Coelho, C. M., Woo, Y. M., & Liu, Y. (2001). Investigating the hows and whys of DNA endoreduplication. *Journal of Experimental Botany, 52*(355), 183-192. doi: 10.1093/jexbot/52.355.183

Larrieu, A., & Vernoux, T. (2015). Comparison of plant hormone signalling systems. *Essays In Biochemistry, 58*(0), 165-181. doi: 10.1042/bse0580165

Maier, R. H., Maier, C. J., & Onder, K. (2011). Construction of improved Yeast Two-Hybrid libraries. *Methods in molecular biology (Clifton, N.J.), 729*, 71-84. doi: 10.1007/978-1-61779-065-2_5

Mason, J. M., & Arndt, K. M. (2004). Coiled coil domains: Stability, specificity, and biological implications. *Chembiochem, 5*(2), 170-176. doi: 10.1002/cbic.200300781

McSteen, P., & Zhao, Y. (2008). Plant hormones and signaling: Common themes and new developments. [Article]. *Developmental Cell, 14*(4), 467-473. doi: 10.1016/j.devcel.2008.03.013

Meijer, H. J. G., & Munnik, T. (2003). Phospholipid-based signaling in plants. *Annual Review of Plant Biology, 54*, 265-306. doi: 10.1146/annurev.arplant.54.031902.134748

Meissner, C. S., Koppen-Rung, P., Dittmer, A., Lapp, S., & Bogner, E. (2011). A "coiled-coil" motif is important for oligomerization and DNA binding properties of human cytomegalovirus protein UL77. *Plos One, 6*(10), e25115. doi: 10.1371/journal.pone.0025115

Mittler, R., Vanderauwera, S., Suzuki, N., Miller, G., Tognetti, V. B., Vandepoele, K., . . . Van Breusegem, F. (2011). ROS signaling: the new wave? [Review]. *TRENDS in Plant Science, 16*(6), 300-309. doi: 10.1016/j.tplants.2011.03.007

Myouga, F., Hosoda, C., Umezawa, T., Iizumi, H., Kuromori, T., Motohashi, R., . . . Shinozaki, K. (2008). A Heterocomplex of Iron Superoxide Dismutases Defends Chloroplast Nucleoids against Oxidative Stress and Is Essential for Chloroplast Development in Arabidopsis. [Article]. *Plant Cell, 20*(11), 3148-3162. doi: 10.1105/tpc.108.061341

Nanda, A. K., Andrio, E., Marino, D., Pauly, N., & Dunand, C. (2010). Reactive Oxygen Species during Plant-microorganism Early Interactions. *Journal of Integrative Plant Biology, 52*(2), 195-204. doi: 10.1111/j.1744-7909.2010.00933.x

Neill, S., Desikan, R., & Hancock, J. (2002). Hydrogen peroxide signalling. *Current Opinion in Plant Biology, 5*(5), 388-395. doi: 10.1016/S1369-5266(02)00282-0

Niu, X. M., Bressan, R. A., Hasegawa, P. M., & Pardo, J. M. (1995). Ion Homeostasis in NaCl Stress Environments. *Plant Physiology, 109*(3), 735-742.

Ohad, N., Shichrur, K., & Yalovsky, S. (2007). The analysis of protein-protein interactions in plants by bimolecular fluorescence complementation. *Plant Physiology, 145*(4), 1090-1099. doi: 10.1104/pp.107.107284

Oldfield, C. J., Meng, J., Yang, J. Y., Yang, M. Q., Uversky, V. N., & Dunker, A. K. (2008). Flexible nets: disorder and induced fit in the associations of p53 and 14-3-3 with their partners. *Bmc Genomics, 9*. doi: S1 10.1186/1471-2164-9-s1-s1

Pallavi, S., Jha, A. B., Dubey, R. S., & Pessarakli, M. (2012). Reactive oxygen species, oxidative damage, and antioxidative defense mechanism in plants under stressful conditions. *Journal of Botany, 2012*, 217037-Article ID 217037.

Parker, J. E. (2014). Co-opting the Cell-Cycle Machinery for Plant Immunity. *Cell Host & Microbe, 16*(6), 707-709. doi: 10.1016/j.chom.2014.11.015

Penninckx, I., Eggermont, K., Terras, F. R. G., Thomma, B., DeSamblanx, G. W., Buchala, A., . . . Broekaert, W. F. (1996). Pathogen-induced systemic activation of a plant defensin gene in Arabidopsis follows a salicylic acid-independent pathway. *Plant Cell, 8*(12), 2309-2323. doi: 10.1105/tpc.8.12.2309

Perazza, D., Laporte, F., Balague, C., Chevalier, F., Remo, S., Bourge, M., . . . Vachon, G. (2011). GeBP/GPL Transcription Factors Regulate a Subset of CPR5-Dependent Processes. *Plant Physiology, 157*(3), 1232-1242. doi: 10.1104/pp.111.179804

Perazza, D., Laporte, F., Balagué, C., Chevalier, F., Remo, S., Bourge, M., . . . Vachon, G. (2011). GeBP/GPL transcription factors regulate a subset of CPR5-dependent processes. *Plant Physiology, 157*(3), 1232-1242.

Peterman, T. K. (2004). Patellin1, a Novel Sec14-Like Protein, Localizes to the Cell Plate and Binds Phosphoinositides. *Plant Physiology, 136*(2), 3080-3094. doi: 10.1104/pp.104.045369

Qiu, X. B., Shao, Y. M., Miao, S., & Wang, L. (2006). The diversity of the DnaJ/Hsp40 family, the crucial partners for Hsp70 chaperones. *Cellular and Molecular Life Sciences, 63*(22), 2560-2570. doi: 10.1007/s00018-006-6192-6

Robert-Seilaniantz, A., Grant, M., & Jones, J. D. G. (2011). Hormone Crosstalk in Plant Disease and Defense: More Than Just JASMONATE-SALICYLATE Antagonism. In N. K. VanAlfen, G. Bruening & J. E. Leach (Eds.), *Annual Review of Phytopathology, Vol 49* (Vol. 49, pp. 317-343).

Rodriguez-Gacio, M. d. C., Matilla-Vazquez, M. A., & Matilla, A. J. (2009). Seed dormancy and ABA signaling: the breakthrough goes on. *Plant signaling & behavior, 4*(11), 1035-1049.

Shen, H., Cao, K., & Wang, X. (2007). A conserved proline residue in the leucine zipper region of AtbZIP34 and AtbZIP61 in Arabidopsis thaliana interferes with the formation of homodimer. *Biochemical and Biophysical Research Communications, 362*(2), 425-430. doi: 10.1016/j.bbrc.2007.08.026

Singh, K. B. (1998). Transcriptional regulation in plants: The importance of combinatorial control. *Plant Physiology, 118*(4), 1111-1120. doi: 10.1104/pp.118.4.1111

Spitz, F., & Furlong, E. E. M. (2012). Transcription factors: from enhancer binding to developmental control. *Nature Reviews Genetics, 13*(9), 613-626. doi: 10.1038/nrg3207

Stocker, A., & Baumann, U. (2003). Supernatant protein factor in complex with RRR-alpha-tocopherylquinone: A link between oxidized vitamin E and cholesterol biosynthesis. *Journal of Molecular Biology, 332*(4), 759-765. doi: 10.1016/s0022-2836(03)00924-0

Swamy, P. M., & Smith, B. N. (1999). Role of abscisic acid in plant stress tolerance. [Review]. *Current Science, 76*(9), 1220-1227.

Tall, E. G., Spector, I., Pentyala, S. N., Bitter, I., & Rebecchi, M. J. (2000). Dynamics of phosphatidylinositol 4,5-bisphosphate in actin-rich structures. *Current Biology, 10*(12), 743-746. doi: 10.1016/s0960-9822(00)00541-8

Tang, G. Q., Hardin, S. C., Dewey, R., & Huber, S. C. (2003). A novel C-terminal proteolytic processing of cytosolic pyruvate kinase, its phosphorylation and degradation by the proteasome in developing soybean seeds. *Plant Journal, 34*(1), 77-93. doi: 10.1046/j.1365-313X.2003.01711.x

Torres, M. A., Jones, J. D. G., & Dangl, J. L. (2006). Reactive oxygen species signaling in response to pathogens. *Plant Physiology, 141*(2), 373-378. doi: 10.1104/pp.106.079467

Tripathy, B. C., & Oelmüller, R. (2014). Reactive oxygen species generation and signaling in plants. *Plant signaling & behavior, 7*(12), 1621-1633. doi: 10.4161/psb.22455

Tsai, A. Y.-L., & Gazzarrini, S. (2012). AKIN10 and FUSCA3 interact to control lateral organ development and phase transitions in Arabidopsis. *The Plant Journal, 69*(5), 809-821. doi: 10.1111/j.1365-313X.2011.04832.x

Vellosillo, T., Vicente, J., Kulasekaran, S., Hamberg, M., & Castresana, C. (2010). Emerging Complexity in Reactive Oxygen Species Production and Signaling during the Response of Plants to Pathogens. *Plant Physiology, 154*(2), 444-448. doi: 10.1104/pp.110.161273

Vollmer, A. H., Youssef, N. N., & DeWald, D. B. (2011). Unique cell wall abnormalities in the putative phosphoinositide phosphatase mutant AtSAC9. *Planta, 234*(5), 993-1005. doi: 10.1007/s00425-011-1454-4

Waadt, R., Schmidt, L. K., Lohse, M., Hashimoto, K., Bock, R., & Kudla, J. (2008). Multicolor bimolecular fluorescence complementation reveals simultaneous formation of alternative CBL/CIPK complexes in planta. *Plant Journal, 56*(3), 505-516. doi: 10.1111/j.1365-313X.2008.03612.x

Walter, M., Chaban, C., Schutze, K., Batistic, O., Weckermann, K., Nake, C., . . . Kudla, J. (2004). Visualization of protein interactions in living plant cells using bimolecular fluorescence complementation. *Plant Journal, 40*(3), 428-438. doi: 10.1111/j.1365-313X.2004.02219.x

Wang, C., Feng, C., Song, K., Wang, F., Zhao, Y., Yang, L., & Yang, L. (2012). Construction of a bimolecular fluorescence complementation (BiFC) platform for protein interaction assays in plants. *African Journal of Biotechnology, 11*(62), 12522-12528. doi: 10.5897/ajb12.588

Wang, S., Gu, Y., Zebell, S. G., Anderson, L. K., Wang, W., Mohan, R., & Dong, X. (2014). A Noncanonical Role for the CKI-RB-E2F Cell-Cycle Signaling

Pathway in Plant Effector-Triggered Immunity. *Cell Host & Microbe, 16*(6), 787-794. doi: 10.1016/j.chom.2014.10.005

Wang, X. M. (2002). Phospholipase D in hormonal and stress signaling. *Current Opinion in Plant Biology, 5*(5), 408-414. doi: 10.1016/s1369-5266(02)00283-2

Weinthal, D., & Tzfira, T. (2009). Imaging protein-protein interactions in plant cells by bimolecular fluorescence complementation assay. *TRENDS in Plant Science, 14*(2), 59-63. doi: 10.1016/j.tplants.2008.11.002

Wen, X., Zhang, C., Ji, Y., Zhao, Q., He, W., An, F., . . . Guo, H. (2012). Activation of ethylene signaling is mediated by nuclear translocation of the cleaved EIN2 carboxyl terminus. *Cell Research, 22*(11), 1613-1616. doi: 10.1038/cr.2012.145

Whitesell, L., Sutphin, P. D., Pulcini, E. J., Martinez, J. D., & Cook, P. H. (1998). The physical association of multiple molecular chaperone proteins with mutant p53 is altered by Geldanamycin, an hsp90-binding agent. *Molecular and Cellular Biology, 18*(3), 1517-1524.

Whitley, D., Goldberg, S. P., & Jordan, W. D. (1999). Heat shock proteins: A review of the molecular chaperones. *Journal of Vascular Surgery, 29*(4), 748-751. doi: 10.1016/s0741-5214(99)70329-0

Williams, M. E. (2005). Mutations in the Arabidopsis Phosphoinositide Phosphatase Gene SAC9 Lead to Overaccumulation of PtdIns(4,5)P2 and Constitutive Expression of the Stress-Response Pathway. *Plant Physiology, 138*(2), 686-700. doi: 10.1104/pp.105.061317

Wilson, A. K., Pickett, F. B., Turner, J. C., & Estelle, M. (1990). A DOMA dominant mutation in arabidopsis confers resistance to auxin, ethylene and abscisic-acid. [Article]. *Molecular & General Genetics, 222*(2-3), 377-383. doi: 10.1007/bf00633843

Xie, M., Ren, G., Zhang, C., & Yu, B. (2012). The DNA- and RNA-binding protein FACTOR of DNA METHYLATION 1 requires XH domain-mediated complex formation for its function in RNA-directed DNA methylation. *Plant J, 72*(3), 491-500. doi: 10.1111/j.1365-313X.2012.05092.x

Yan, J., Tsuichihara, N., Etoh, T., & Iwai, S. (2007). Reactive oxygen species and nitric oxide are involved in ABA inhibition of stomatal opening. *Plant, Cell & Environment, 30*(10), 1320-1325. doi: 10.1111/j.1365-3040.2007.01711.x

Yin, H. L., & Janmey, P. A. (2003). Phosphoinositide regulation of the actin cytoskeleton. [Review]. *Annual Review of Physiology, 65*, 761-789. doi: 10.1146/annurev.physiol.65.092101.142517

Yoshida, S., Ito, M., Nishida, I., & Watanabe, A. (2002). Identification of a novel gene HYS1/CPR5 that has a repressive role in the induction of leaf senescence and pathogen-defence responses in Arabidopsis thaliana. *Plant Journal, 29*(4), 427-437. doi: 10.1046/j.0960-7412.2001.01228.x

Yu, S. M. (1999). Cellular and genetic responses of plants to sugar starvation. *Plant Physiology, 121*(3), 687-693. doi: 10.1104/pp.121.3.687

Zhao, Z., Zhang, W., Yan, J., Zhang, J., Liu, Z. L. X. L. Z., & Yi, Y. (2010). Over-expression of Arabidopsis DnaJ (Hsp40) contributes to NaCl-stress tolerance. *African Journal of Biotechnology, 9*(7), 972-978.

Zhou, M., Sun, Z., Wang, C., Zhang, X., Tang, Y., Zhu, X., . . . Wu, Y. (2015). Changing a conserved amino acid in R2R3-MYB transcription repressors results in cytoplasmic accumulation and abolishes their repressive activity inArabidopsis. *The Plant Journal, 84*(2), 395-403. doi: 10.1111/tpj.13008

Zimmermann, I. M., Heim, M. A., Weisshaar, B., & Uhrig, J. F. (2004). Comprehensive identification of Arabidopsis thaliana MYB transcription factors interacting with R/B-like BHLH proteins. [Article]. *Plant Journal, 40*(1), 22-34. doi: 10.1111/j.1365-313X.2004.02183.x